MicroBooNE results and BSM program

and a review of short-baseline anomalies

Giuseppe Cerati (Fermilab)
on behalf of the MicroBooNE Collaboration

FPCP Conference

May 25, 2022

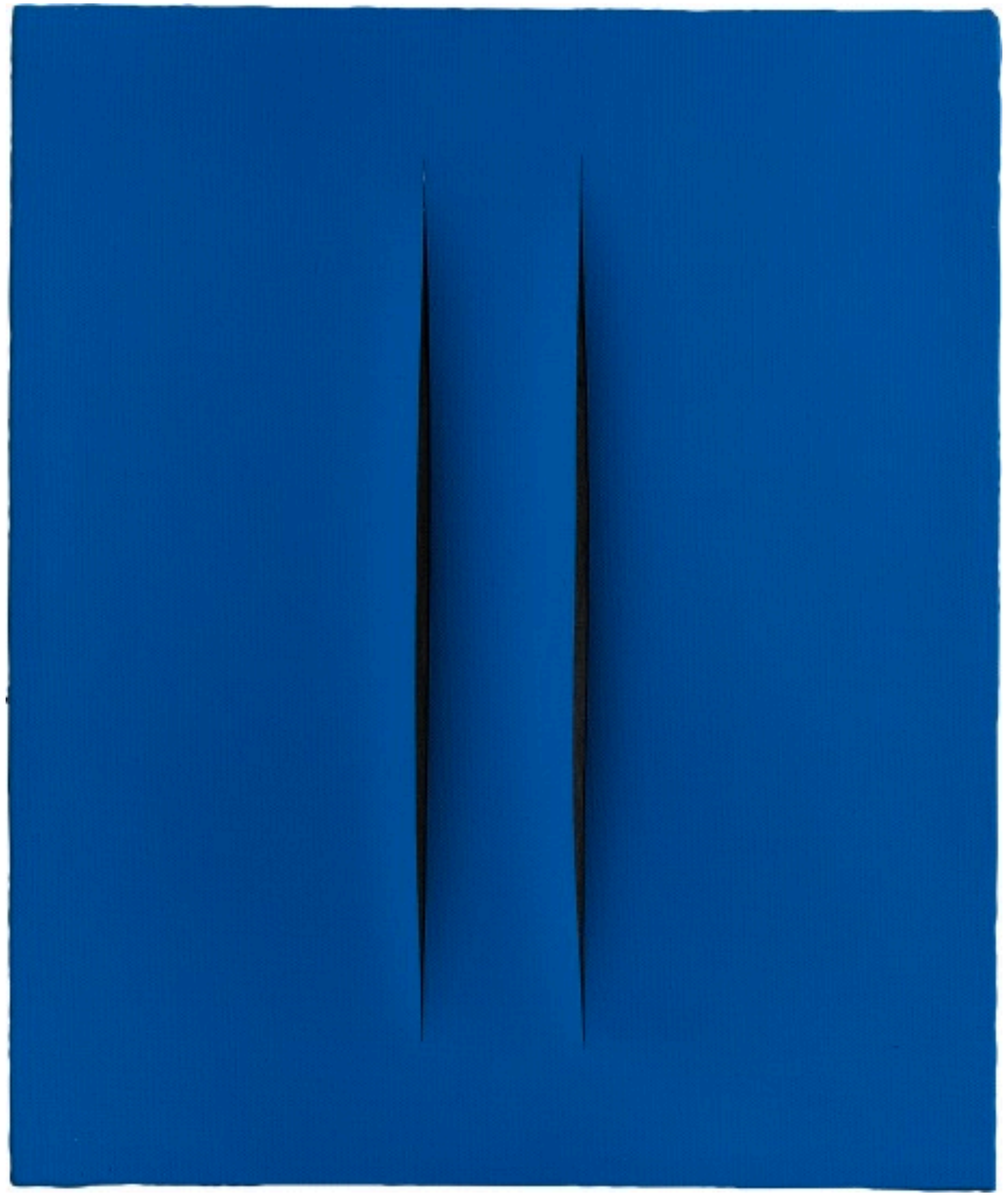

LUCIO FONTANA,
Concetto spaziale, Attese [Spatial Concept, Expectations]
Waterpaint on canvas, 1968

Neutrinos in the Standard Model

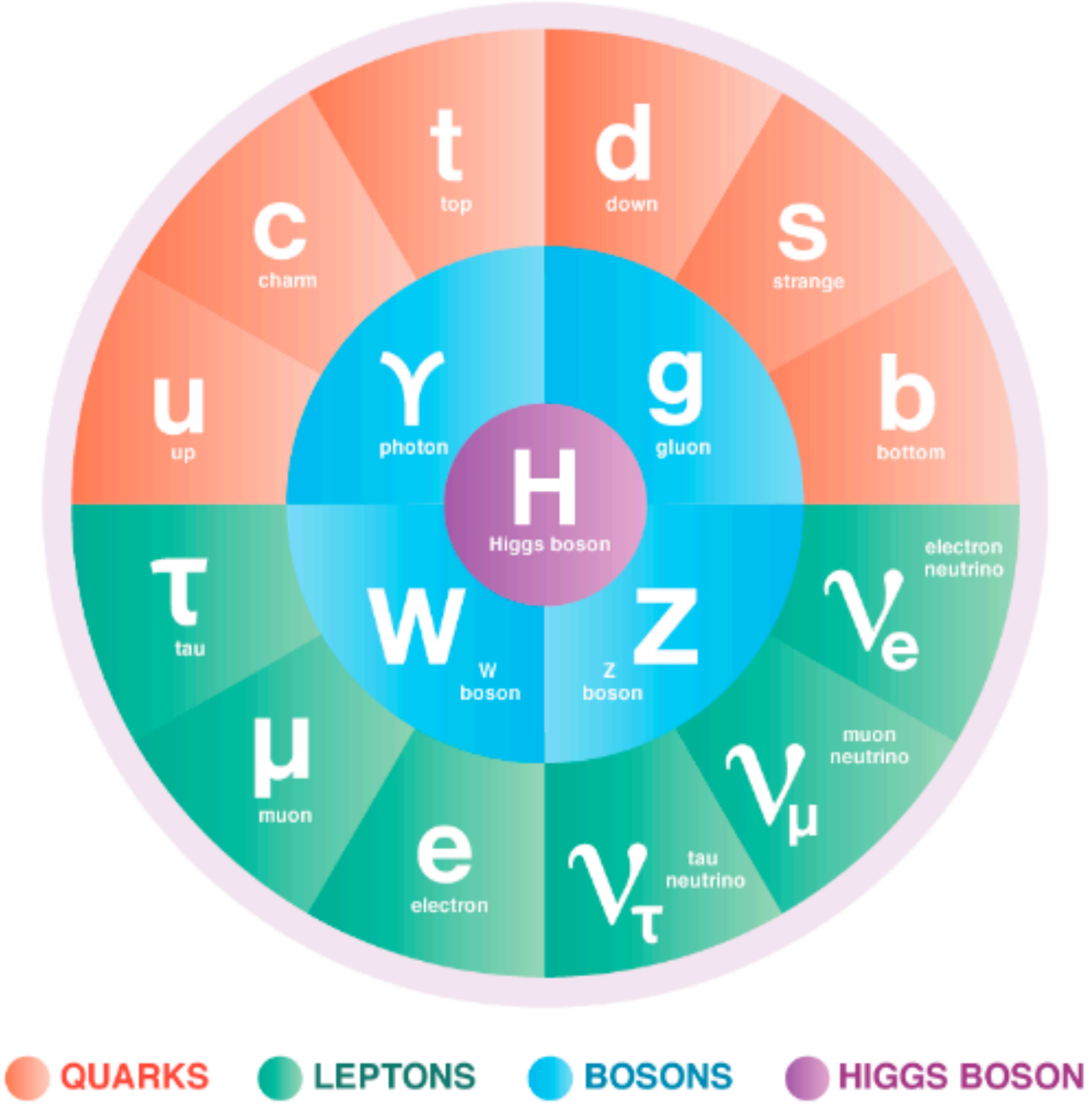

Image courtesy of Symmetry magazine, a joint Fermilab/SLAC publication. Artwork by Sandbox Studio, Chicago.

- Neutrinos fit nicely in the SM
  - massless, neutral leptons
  - 3 flavors, mirroring the charged leptons

Neutrinos in the Standard Model

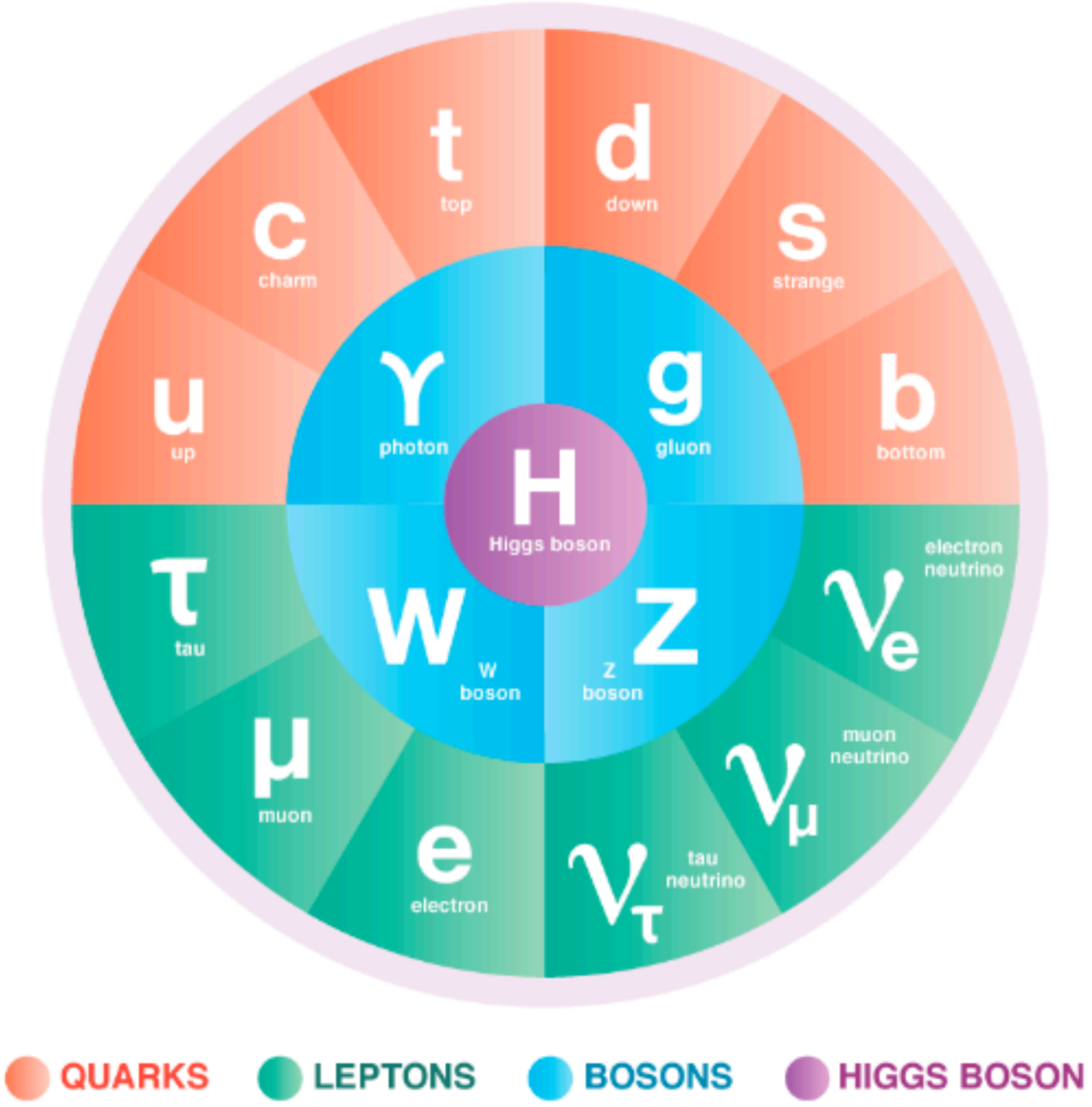

Image courtesy of Symmetry magazine, a joint Fermilab/SLAC publication. Artwork by Sandbox Studio, Chicago.

- Neutrinos fit nicely in the SM
  - massless, neutral leptons
  - 3 flavors, mirroring the charged leptons
- Except that we know they have mass!
  - are there also >3 flavors?

3-flavor neutrino oscillations

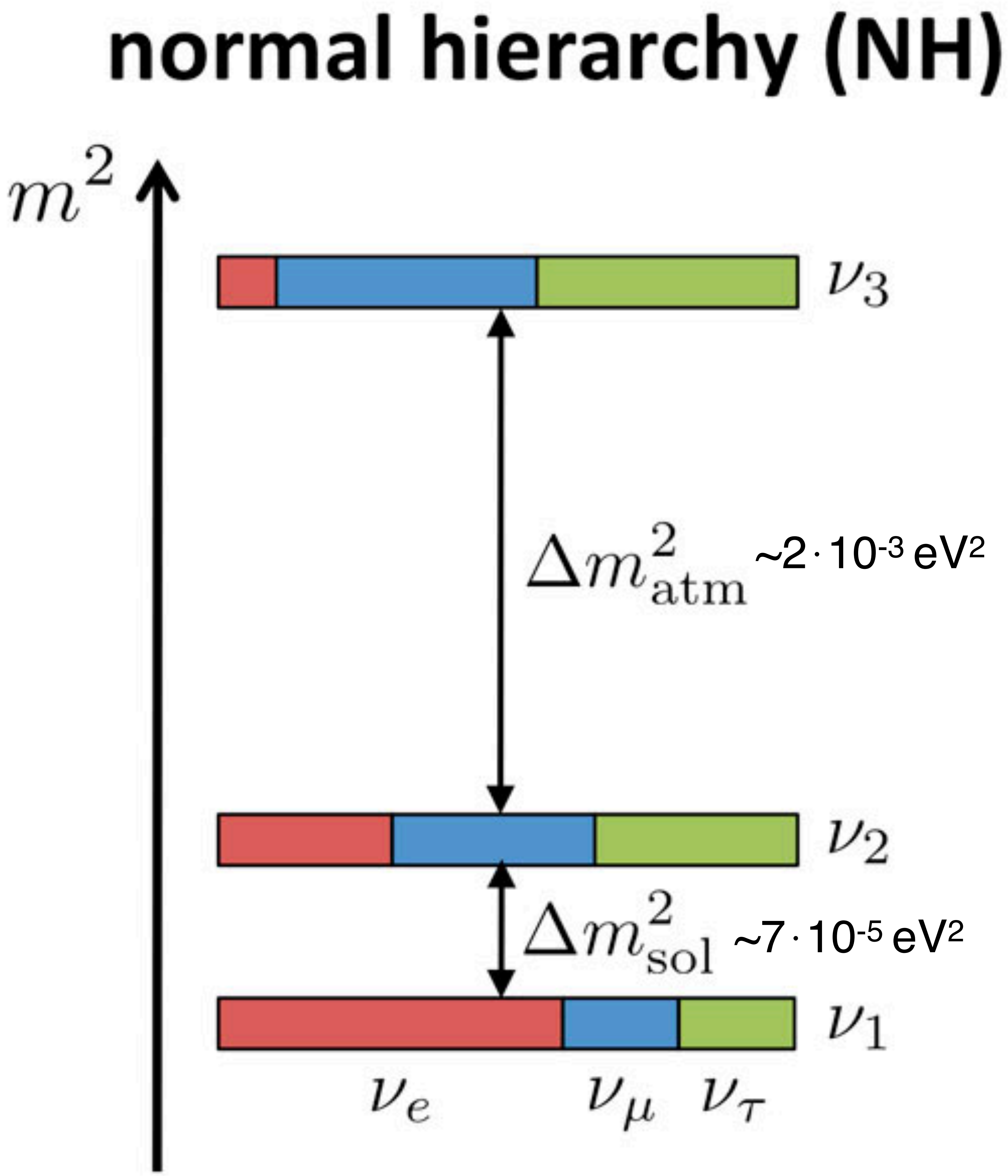

- We know neutrinos have mass because of neutrino oscillations: they have a mass state that differs from the interaction state

$$\begin{pmatrix}\nu_e\\ \nu_\mu\\ \nu_\tau\end{pmatrix} = \left(\text{PMNS matrix} \right) \begin{pmatrix}\nu_1\\ \nu_2\\ \nu_3\end{pmatrix}$$

- Two main oscillations patterns between 2 mass states: solar and atmospheric

$$P(\nu_\alpha \rightarrow \nu_\beta) = sin^2(2\theta)sin^2(1.27\Delta m^2 \frac{L(km)}{E(GeV)})$$

  - mixing angle $\sin^2(2\theta)$ determines amplitude (size of effect)
  - L/E determines oscillation frequency, allowing to extract Δm^2

- PMNS matrix formalism works extremely well
  - except for short-baseline anomalies!

More about neutrino oscillations in R. Patterson's talk later in this session

Short-baseline Neutrino Anomalies

credit: G. Karagiorgi

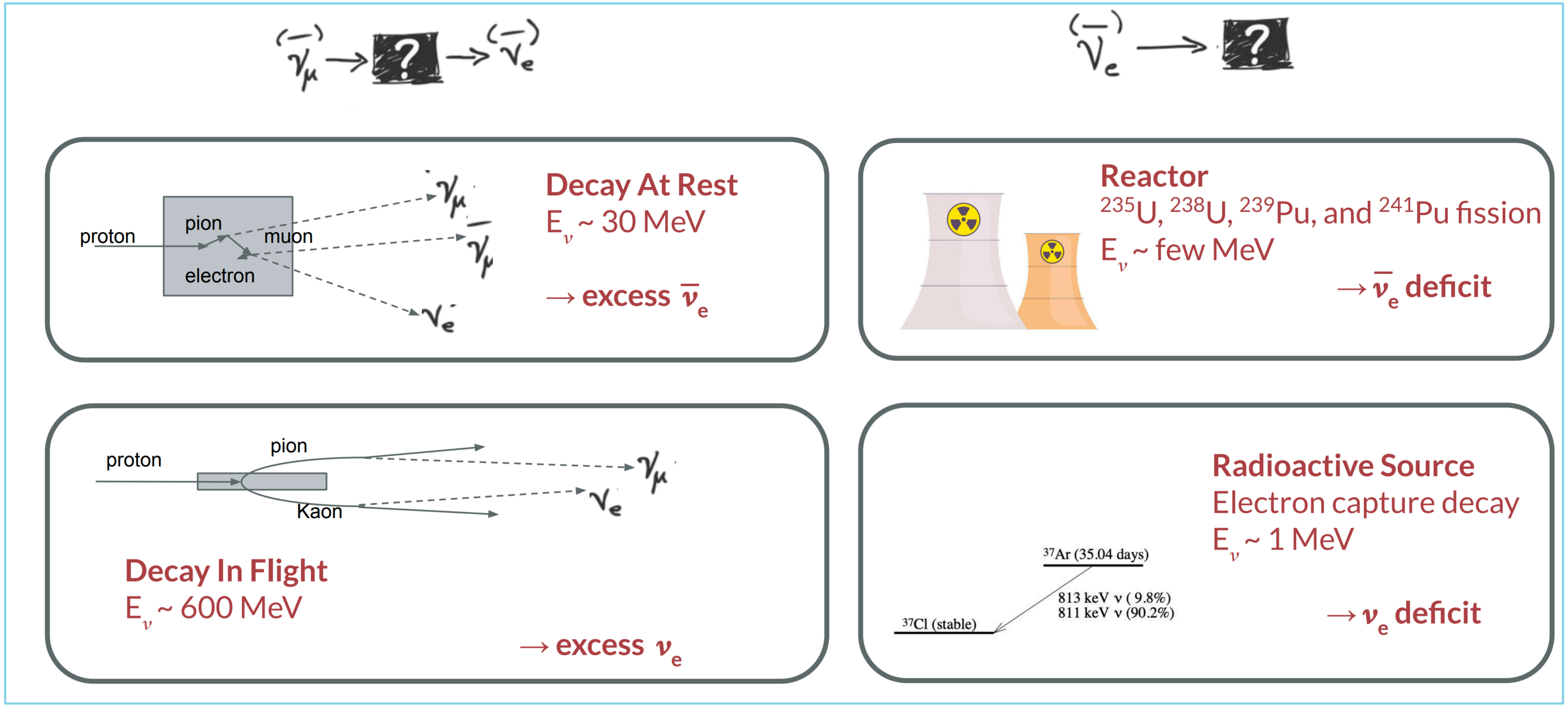

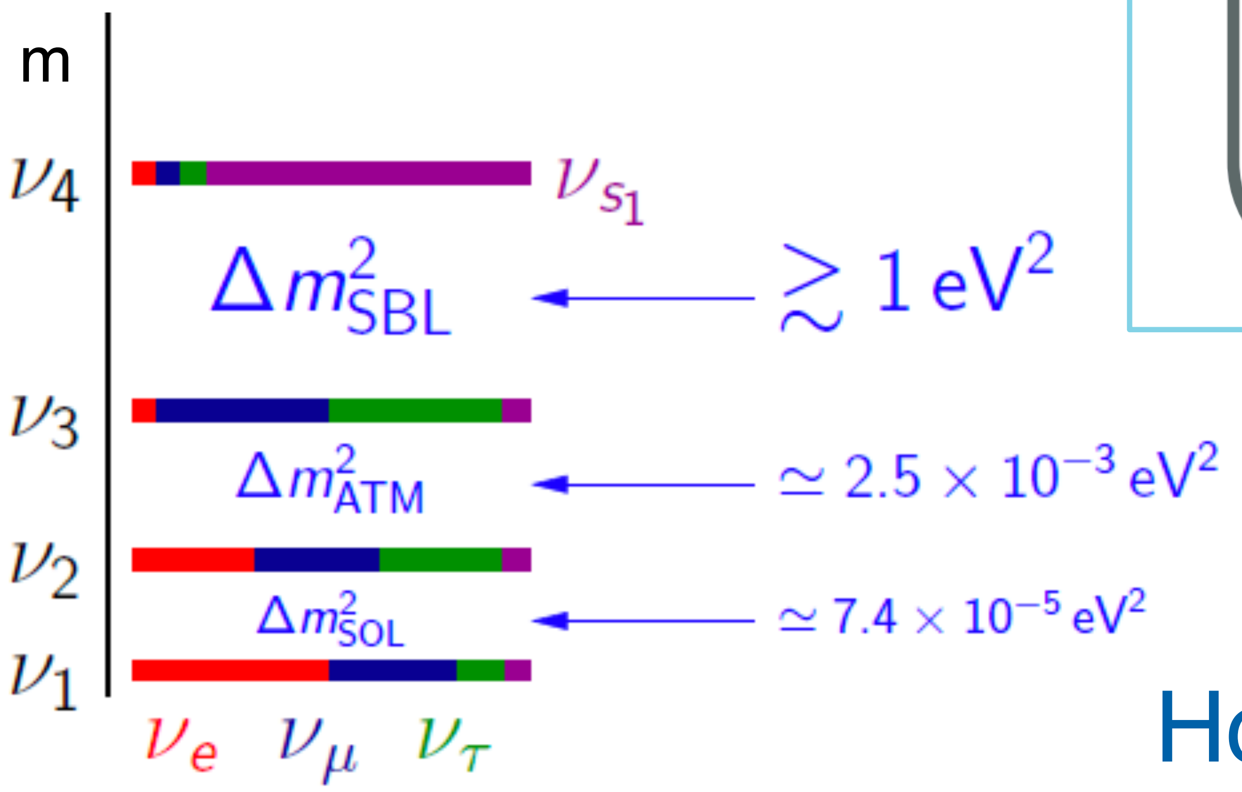

Interpreted as oscillations beyond PMNS paradigm.

All independently compatible with a sterile neutrino (3+1) with $\Delta m^2 \sim O(1\ \text{eV}^2)$.

However, their result is in tension with other experiments: no evidence ν_μ disappearance

For more complete reviews see e.g. Snowmass whitepaper (arXiv:2203.07323) and Giunti/Lasserre (arXiv:1901.08330)

Radioactive anomalies - E~1 MeV

- SAGE/GALLEX experiments used ^{51}Cr and ^{37}Ar radioactive sources (producing ν_e) for calibration of their Gallium detectors
  - results show deficit compared to prediction at ~3σ
  - cross-section uncertainties are being re-evaluated, likely to reduce but not remove significance

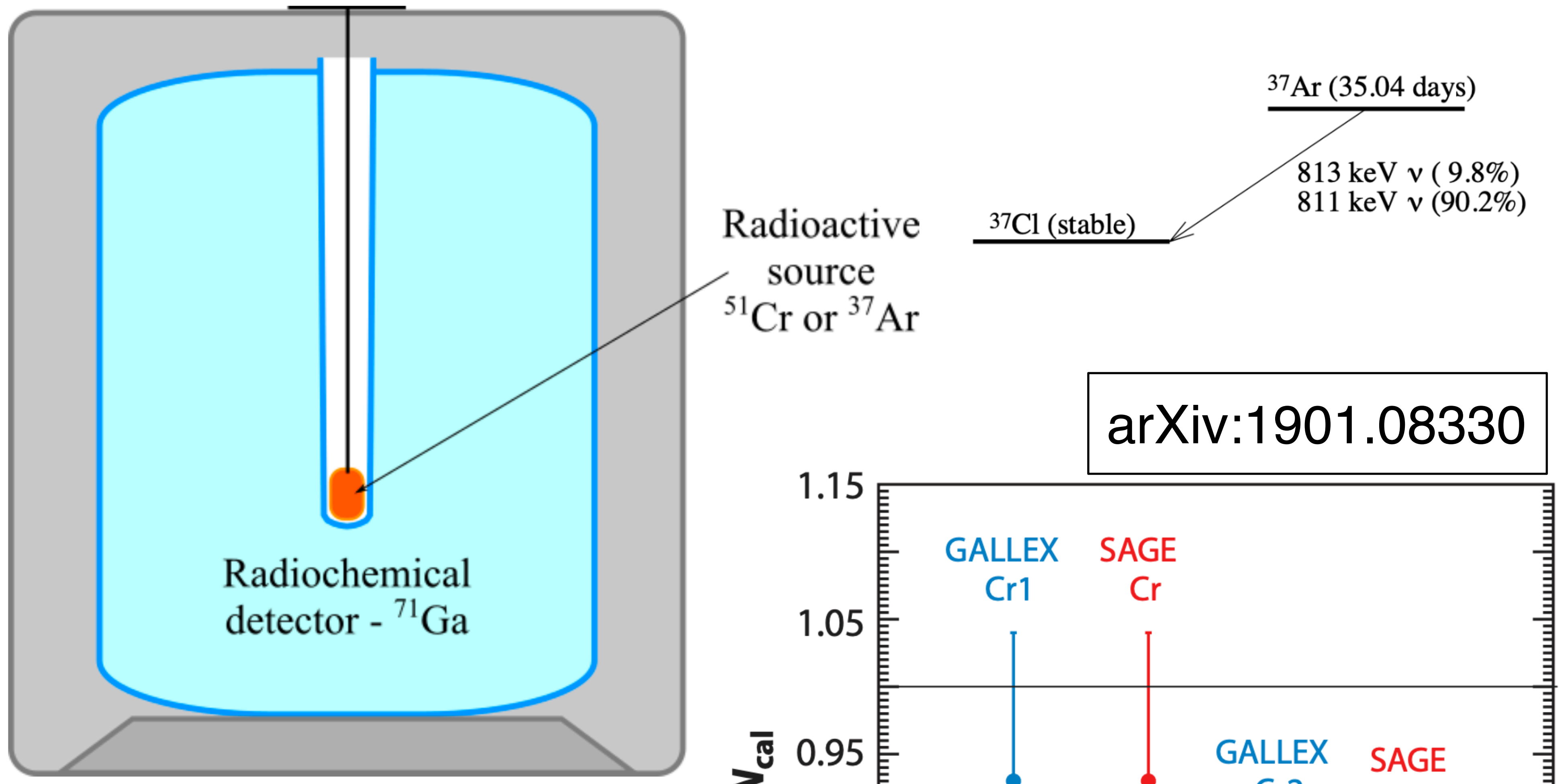

$$\nu_e + {}^{71}\mathrm{Ga} \rightarrow {}^{71}\mathrm{Ge} + e^-$$

arXiv:1901.08330

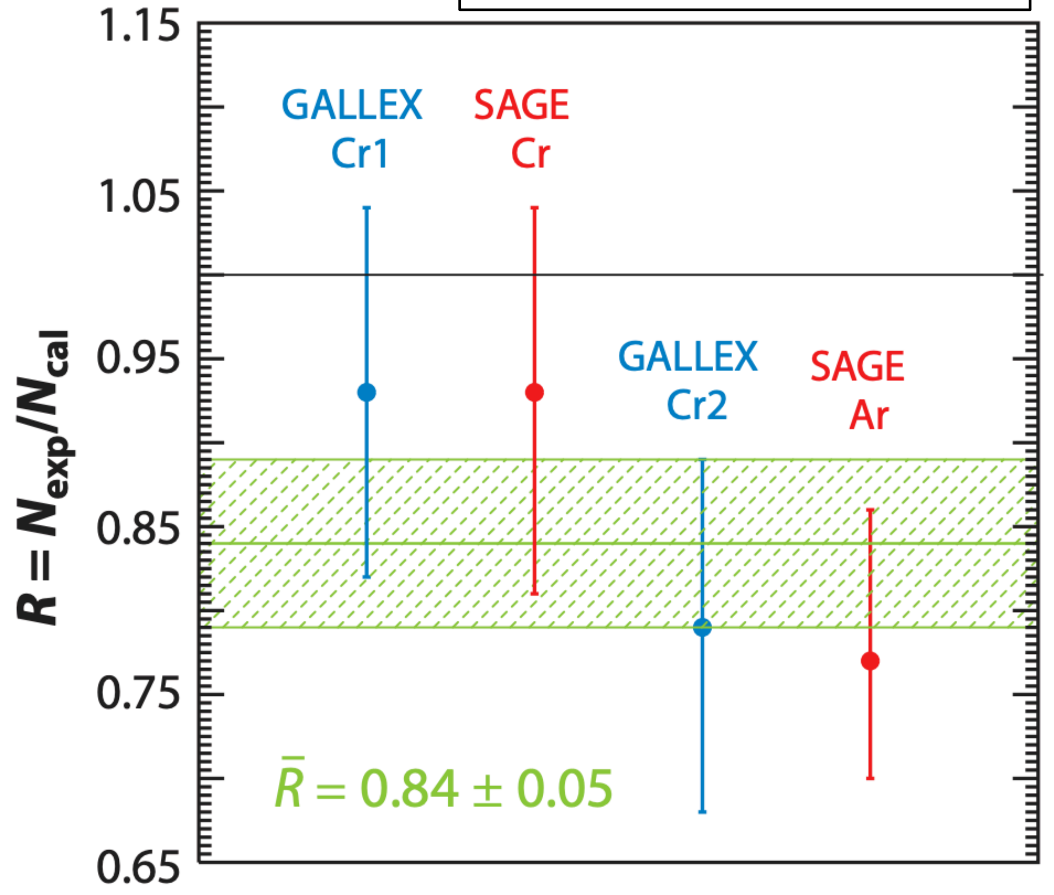

Fermilab

Radioactive anomalies - E~1 MeV

- SAGE/GALLEX experiments used ^{51}Cr and ^{37}Ar radioactive sources (producing ν_e) for calibration of their Gallium detectors
  - results show deficit compared to prediction at ~3σ
  - cross-section uncertainties are being re-evaluated, likely to reduce but not remove significance

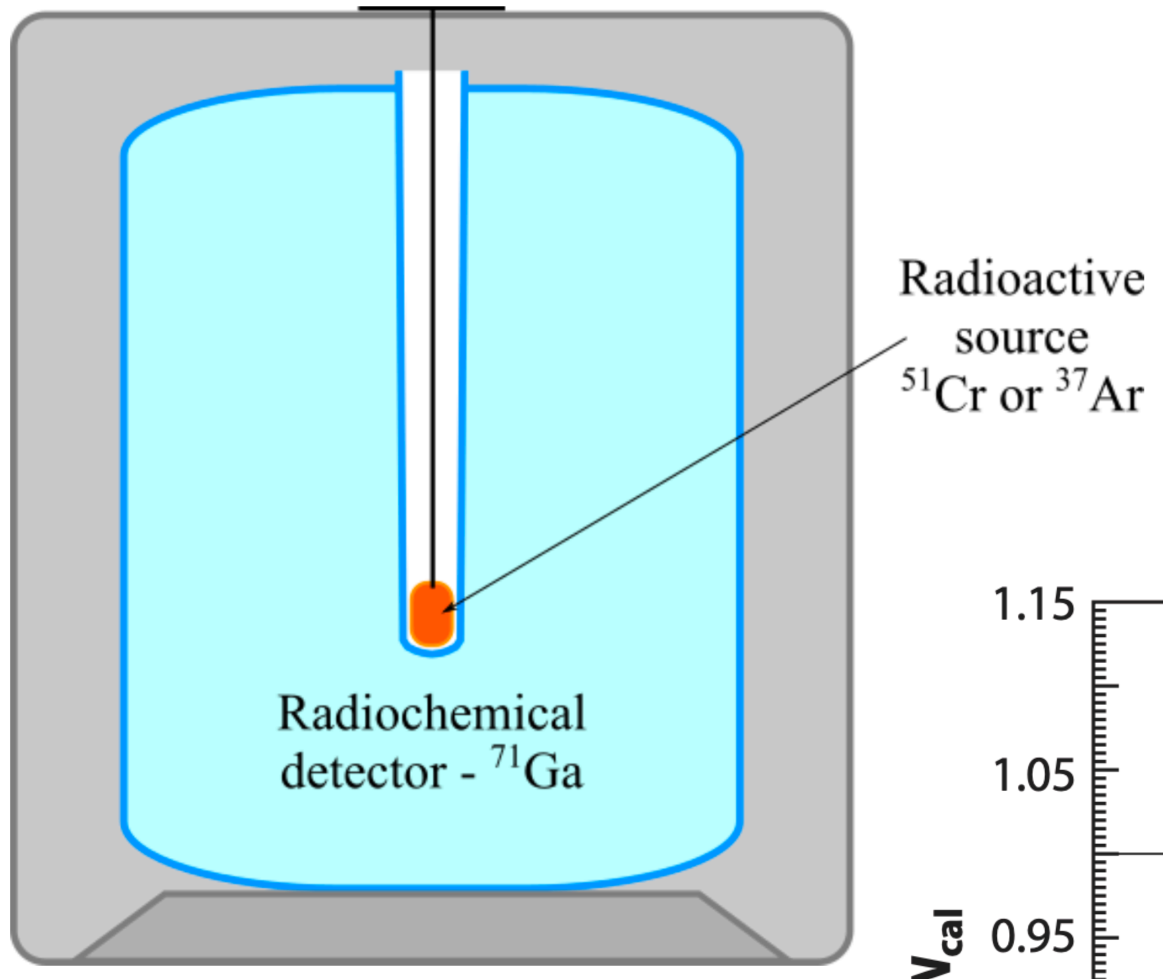

$$\nu_e + {}^{71}\mathrm{Ga} \rightarrow {}^{71}\mathrm{Ge} + e^-$$

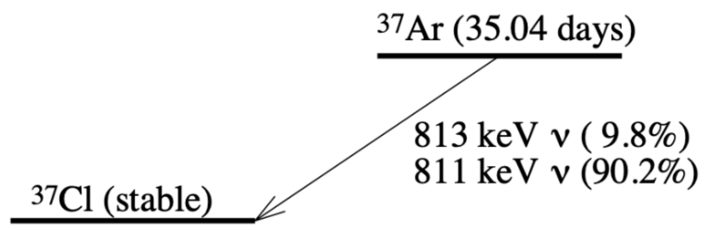

arXiv:1901.08330

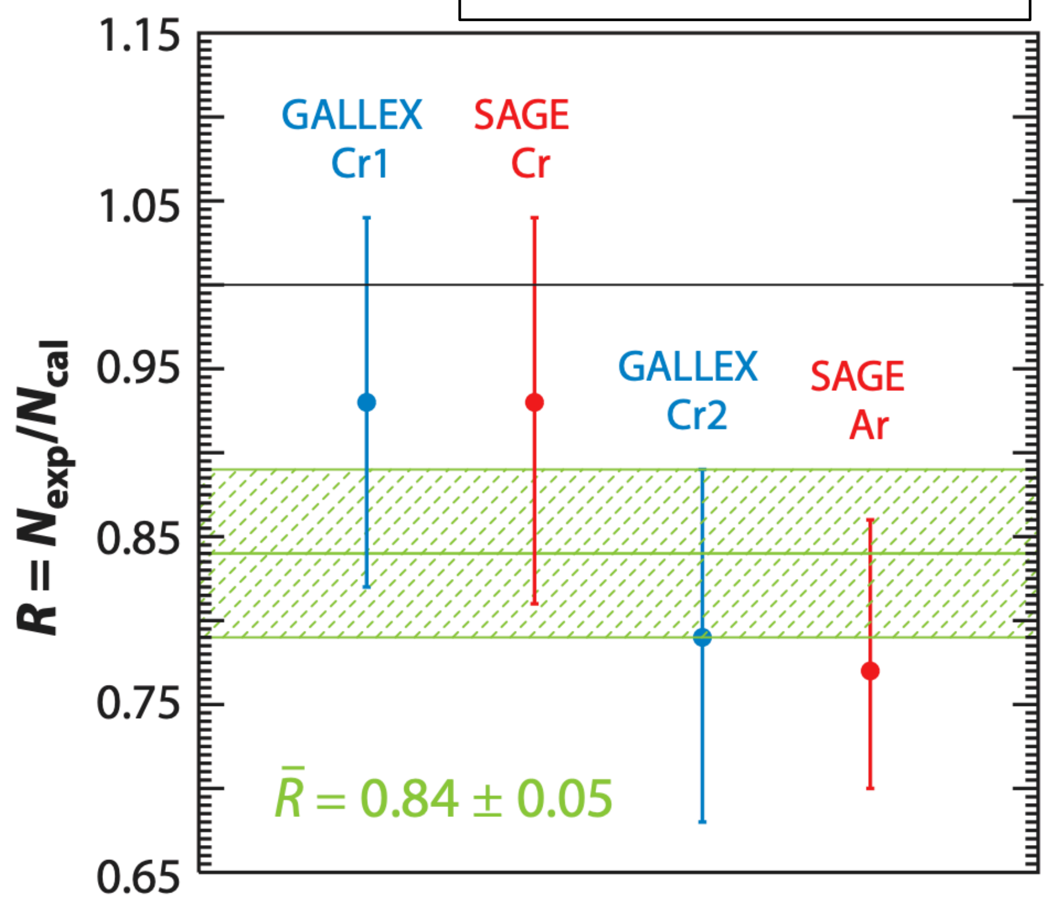

- BEST experiment recently confirmed deficit
  - Gallium detector with a two-target (inner/outer) setup
  - larger (>4σ) deficit compared to prediction
  - no significant rate difference between targets
  - fitted as $\Delta m^2 = 3.3$ eV^2 and $\sin^2(2\theta) = 0.42$

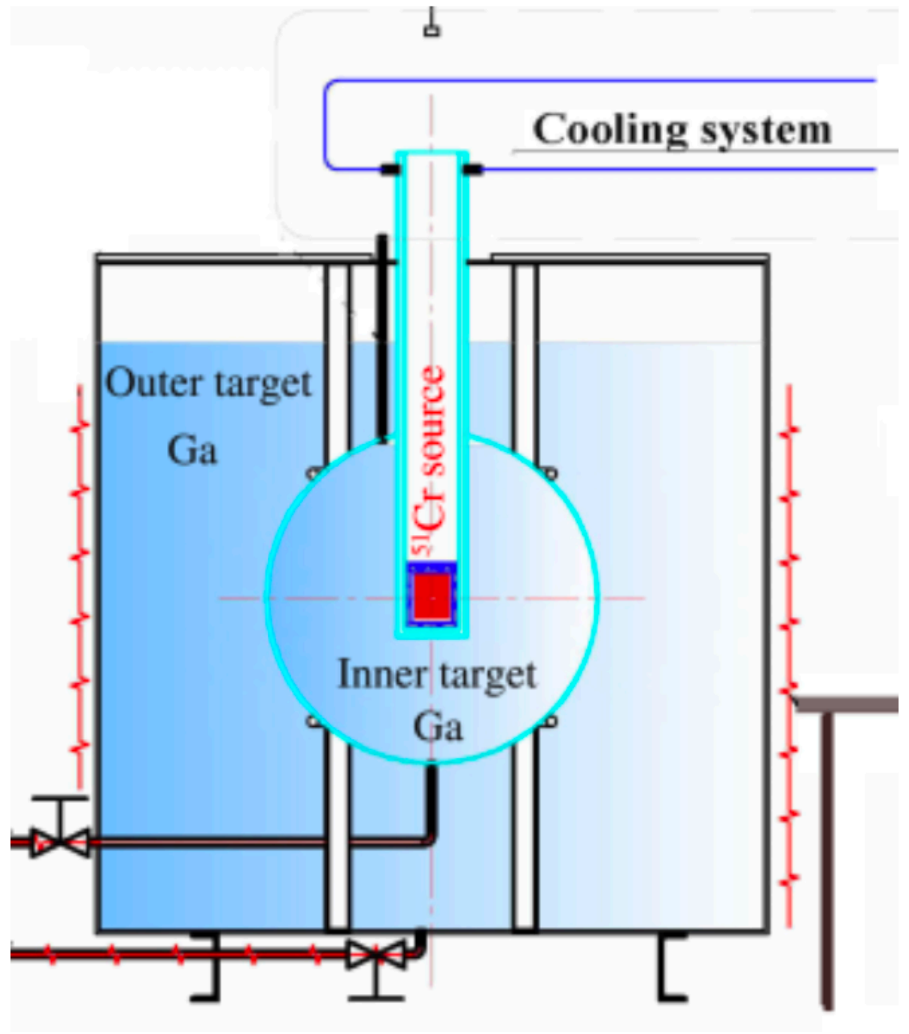

Obs/Pred

Inner	Outer
0.79 ± 0.05	0.77 ± 0.05

arXiv:2109.11482

Reactor anomalies - E~few MeV

PLB 829 (2022) 137054

- $\bar{\nu}_e$ produced by reactors are measured by experiments via inverse beta decays:
  - large range of technologies used, results are overall consistent: ~6% deficit compared to flux predictions from Huber and Mueller et al. (HM)
  - no L/E dependence observed; leading interpretation is now that deficit is likely from deficiencies of HM flux prediction

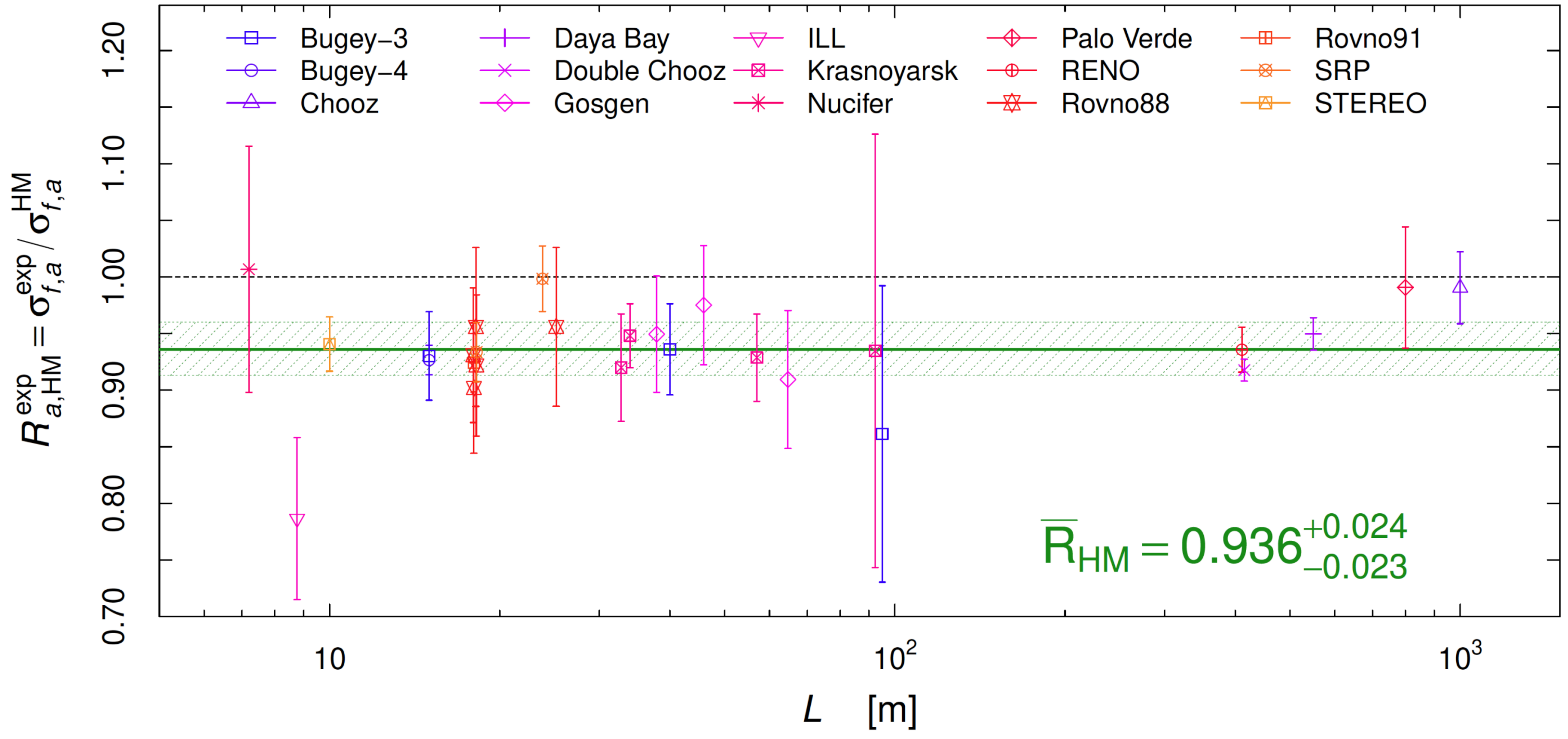

Fermilab

Reactor anomalies - E~few MeV

- $\bar{\nu}_e$ produced by reactors are measured by experiments via inverse beta decays:
  - large range of technologies used, results are overall consistent: ~6% deficit compared to flux predictions from Huber and Mueller et al. (HM)
  - no L/E dependence observed; leading interpretation is now that deficit is likely from deficiencies of HM flux prediction

- Neutrino4 experiment recently reported an L/E dependence, with >3σ significance
  - movable detector with L ranging 6-12 m
  - best fit point $\Delta m^2 \sim 7$ eV^2 and $\sin^2(2\theta) = 0.36$
  - strong tension with results from PROSPECT

PLB 829 (2022) 137054

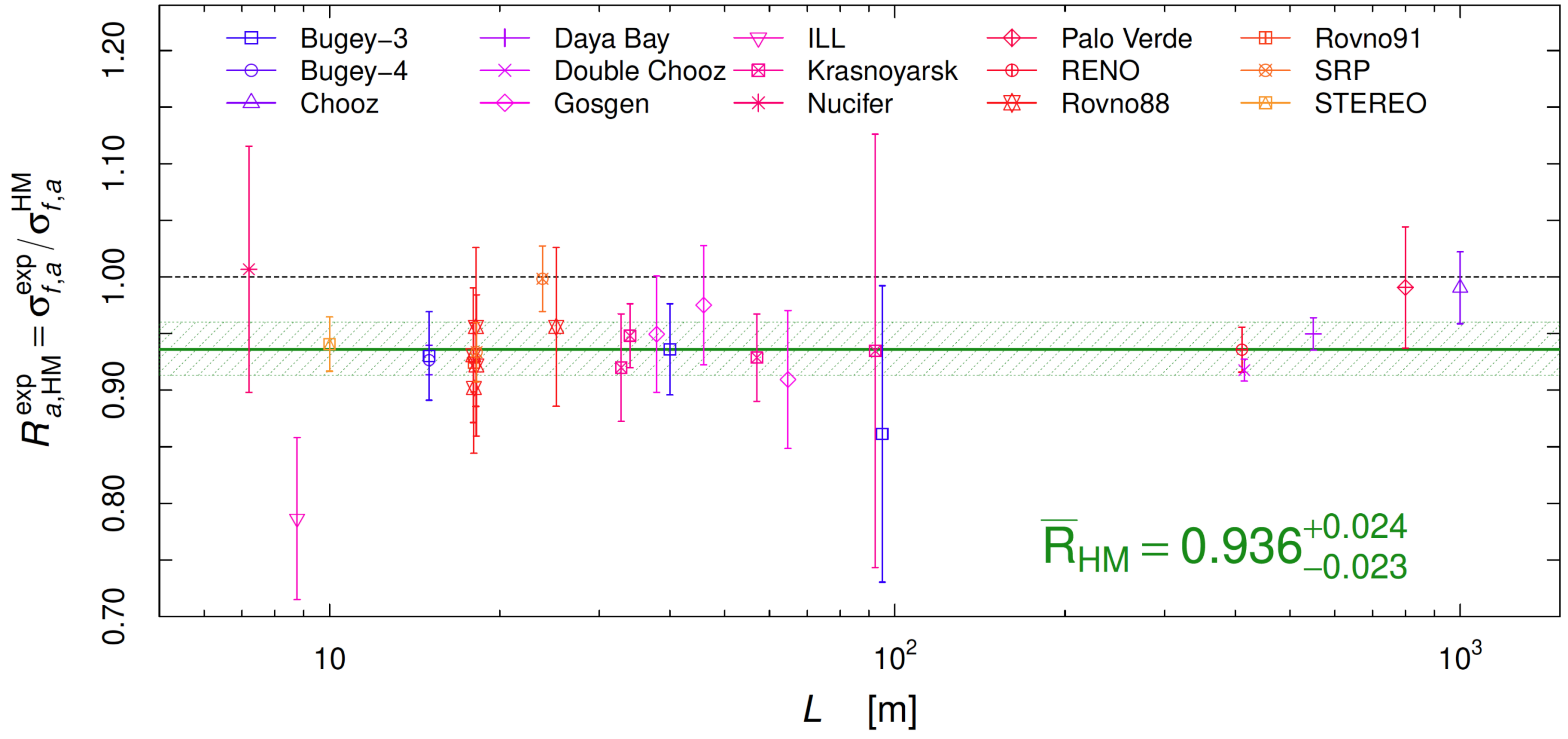

PRD 104 (2021) 3, 032003

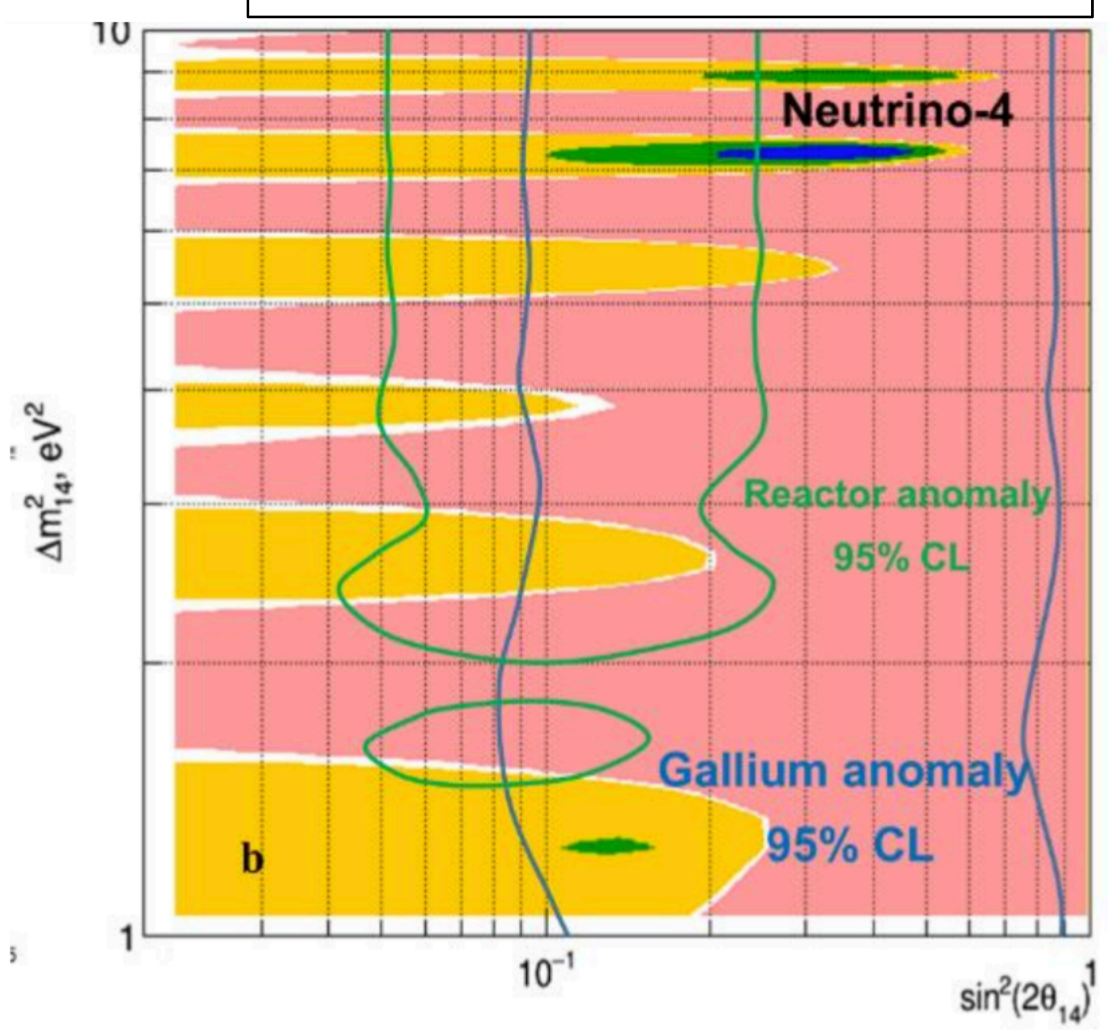

PRD 103 (2021) 3, 032001

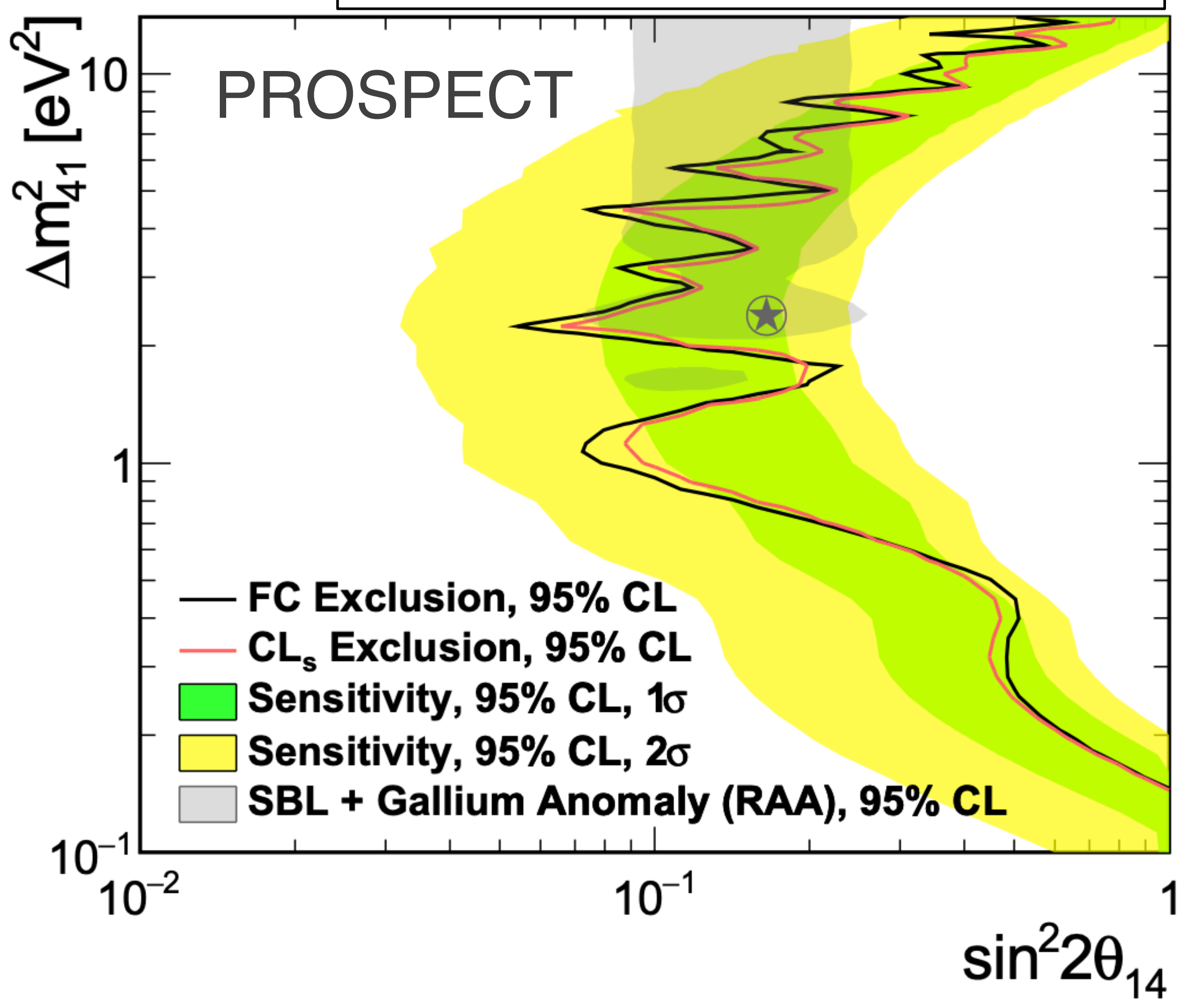

Fermilab

Meson decay anomalies: E~30-600 MeV

- LSND looked for oscillations of anti-ν_μ produced by decay chain of pions at rest at L=30 m
  - relative beam content of anti-ν_e is < 10^{-3}
  - excess of anti-ν_e events over prediction at 3.8σ significance
  - interpreted as oscillation signal with $\Delta m^2 \sim 1$ eV^2 $(\sin^2 2\theta, \Delta m^2)_{best-fit} = (0.003, 1.2\mathrm{eV}^2)$
  - KARMEN (lower sensitivity) did not see an excess

PRD 64 (2001) 112007

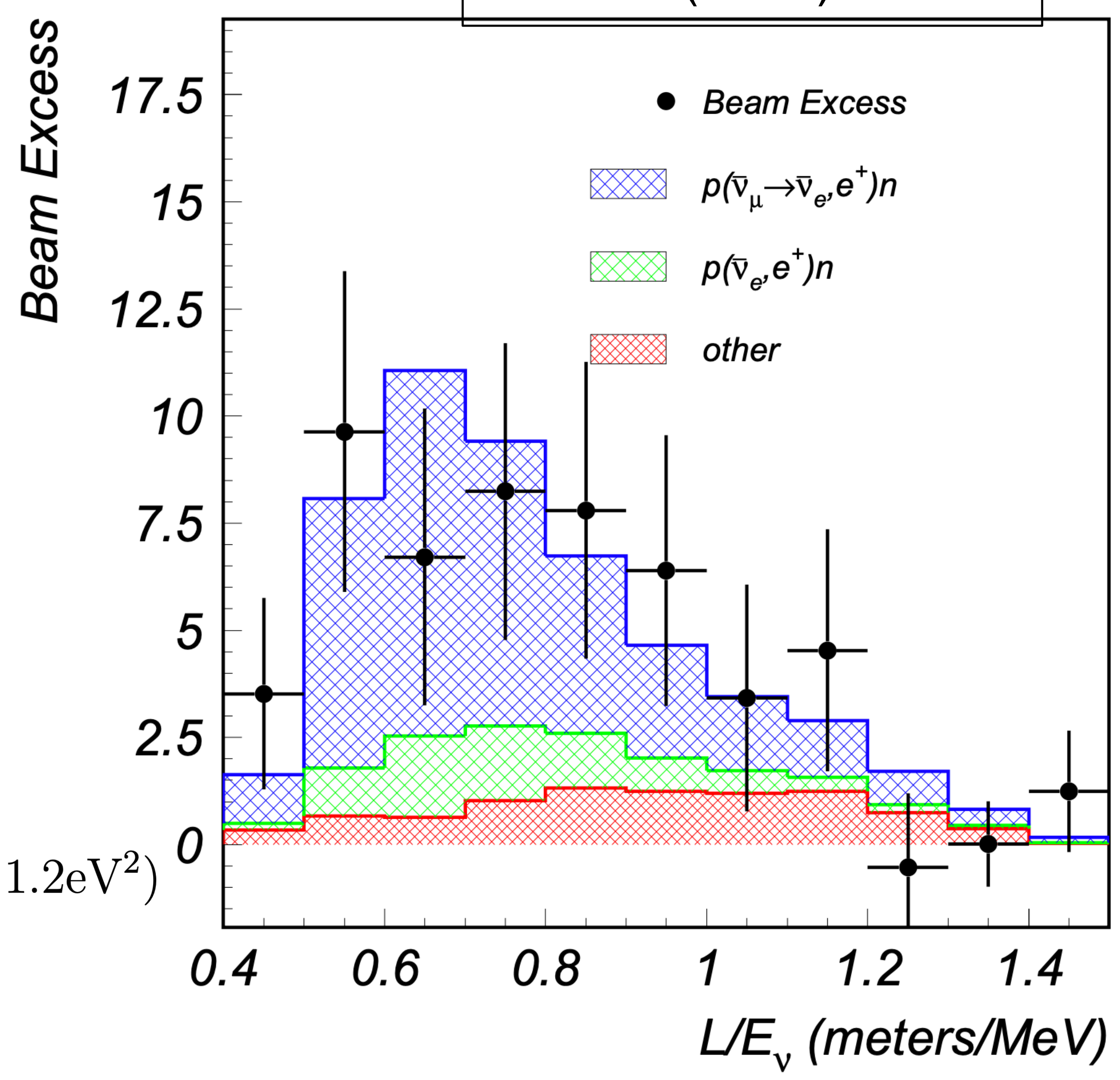

Fermilab

Meson decay anomalies: E~30-600 MeV

- LSND looked for oscillations of anti-ν_μ produced by decay chain of pions at rest at L=30 m
  - relative beam content of anti-ν_e is < 10^{-3}
  - excess of anti-ν_e events over prediction at 3.8σ significance
  - interpreted as oscillation signal with $\Delta m^2 \sim 1$ eV^2 $(\sin^2 2\theta, \Delta m^2)_{best-fit} = (0.003, 1.2\text{eV}^2)$
  - KARMEN (lower sensitivity) did not see an excess

PRD 64 (2001) 112007

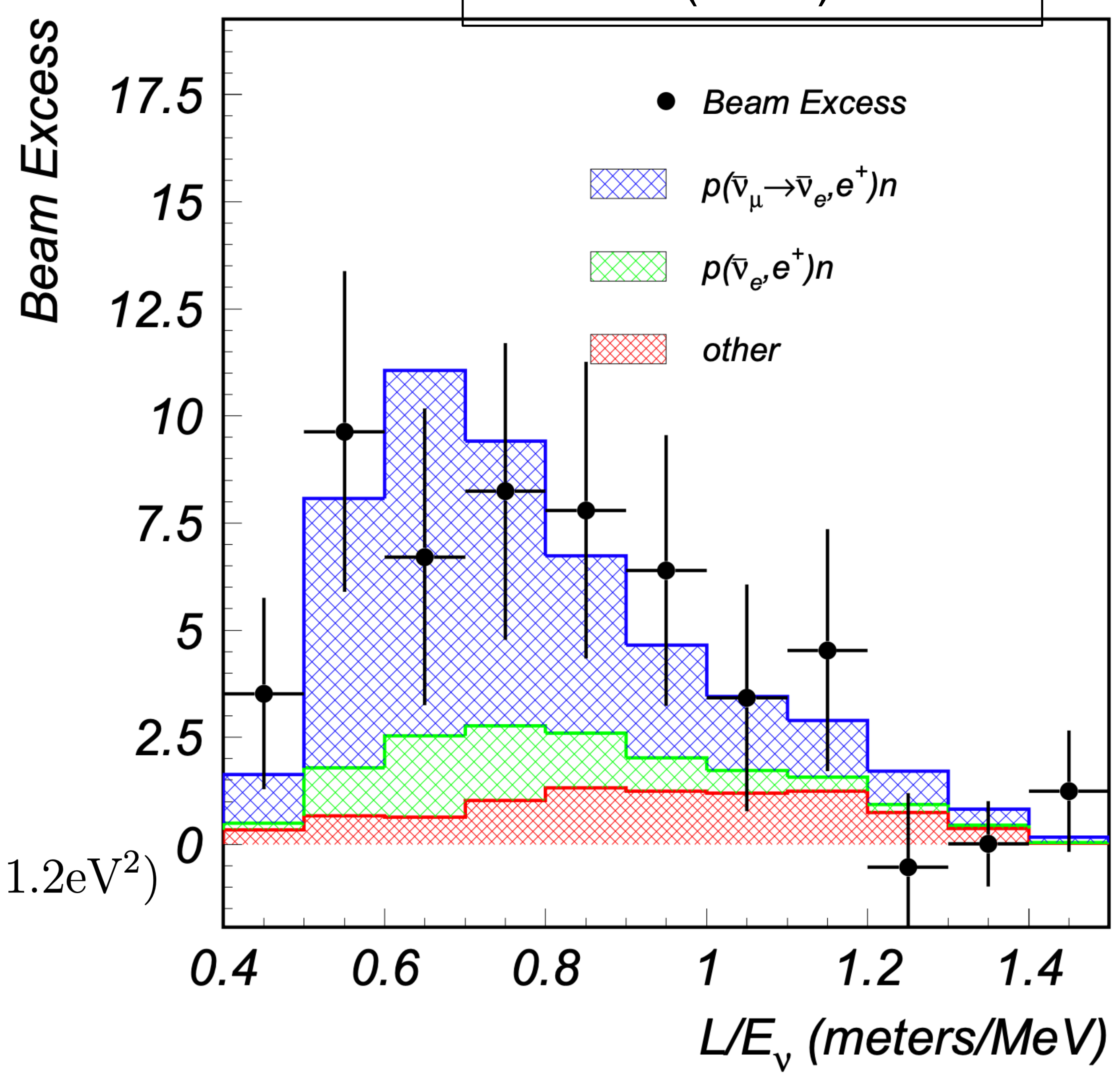

- MiniBooNE investigated the LSND result using a beam of 99.5% ν_μ from meson decays in flight (BNB)
  - L=540 m, same L/E as LSND to test oscillation hypothesis
  - tested both neutrino and antineutrino beam
  - E_ν reconstruction based on E_{lep} assuming CCQE process
  - excess of ν_e-like events at 4.8σ significance, mostly low-energy

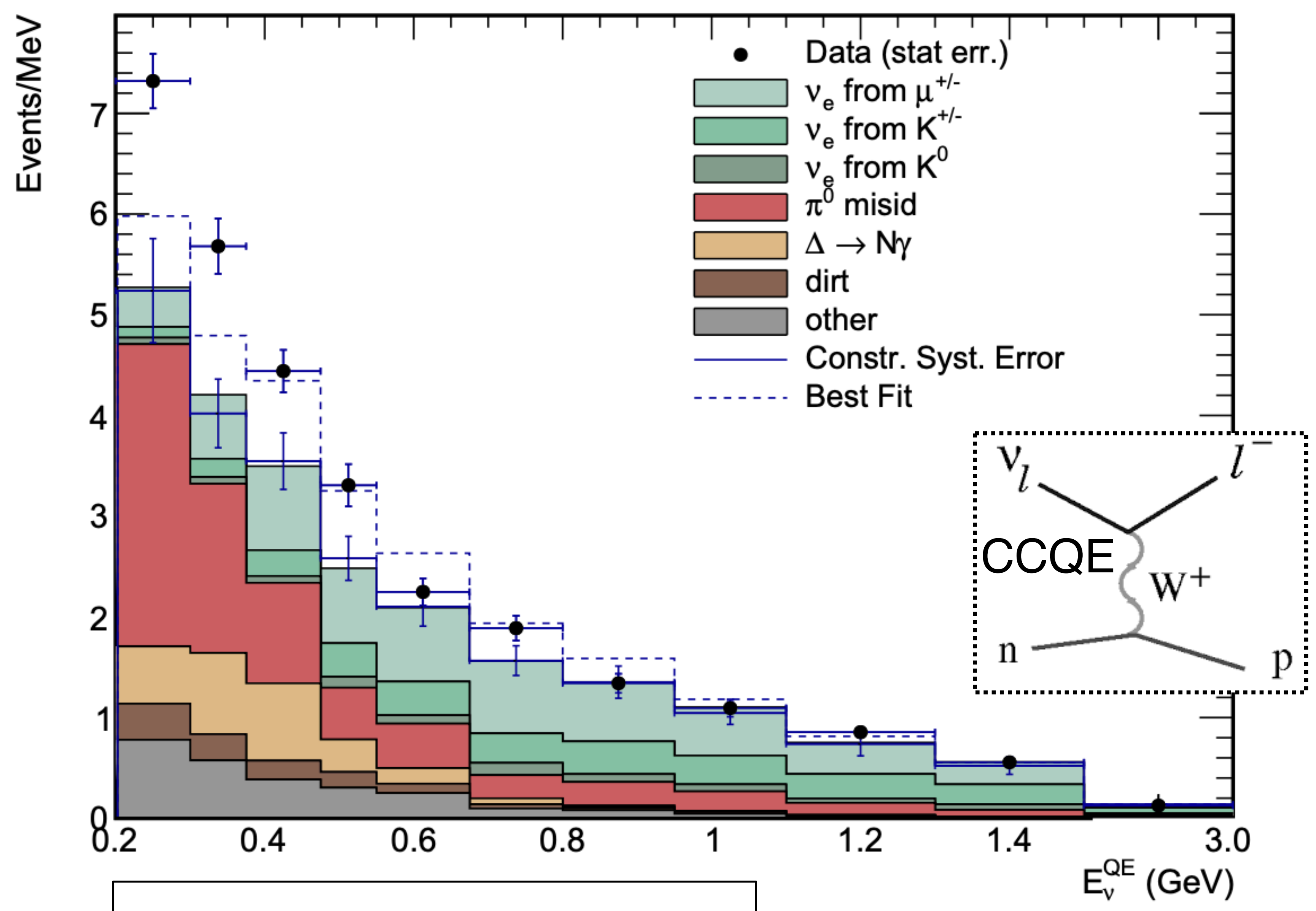

PRD 103 (2021) 5, 052002

More on the MiniBooNE anomaly

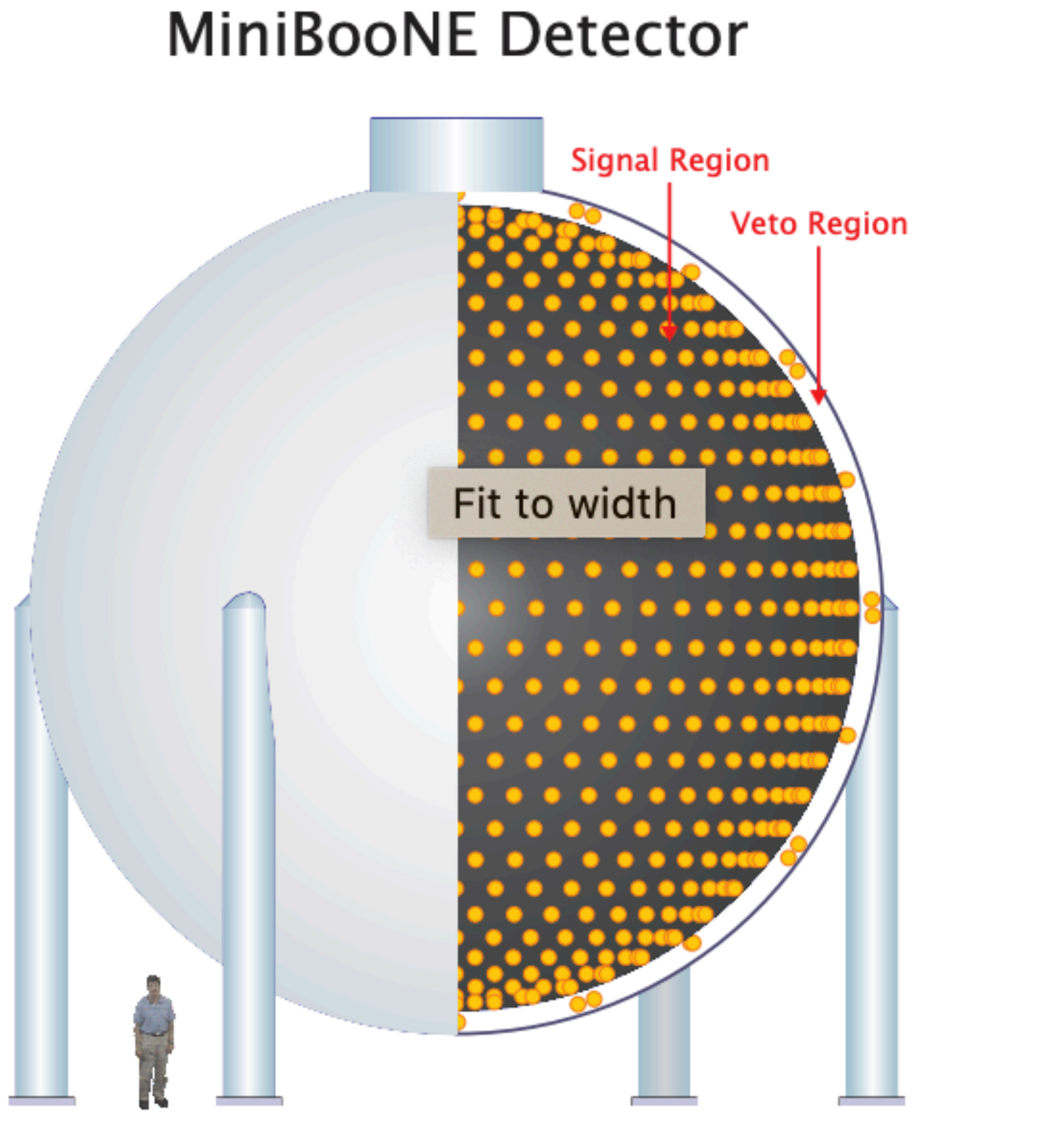

Figure 31. A schematic drawing of the MiniBooNE detector.

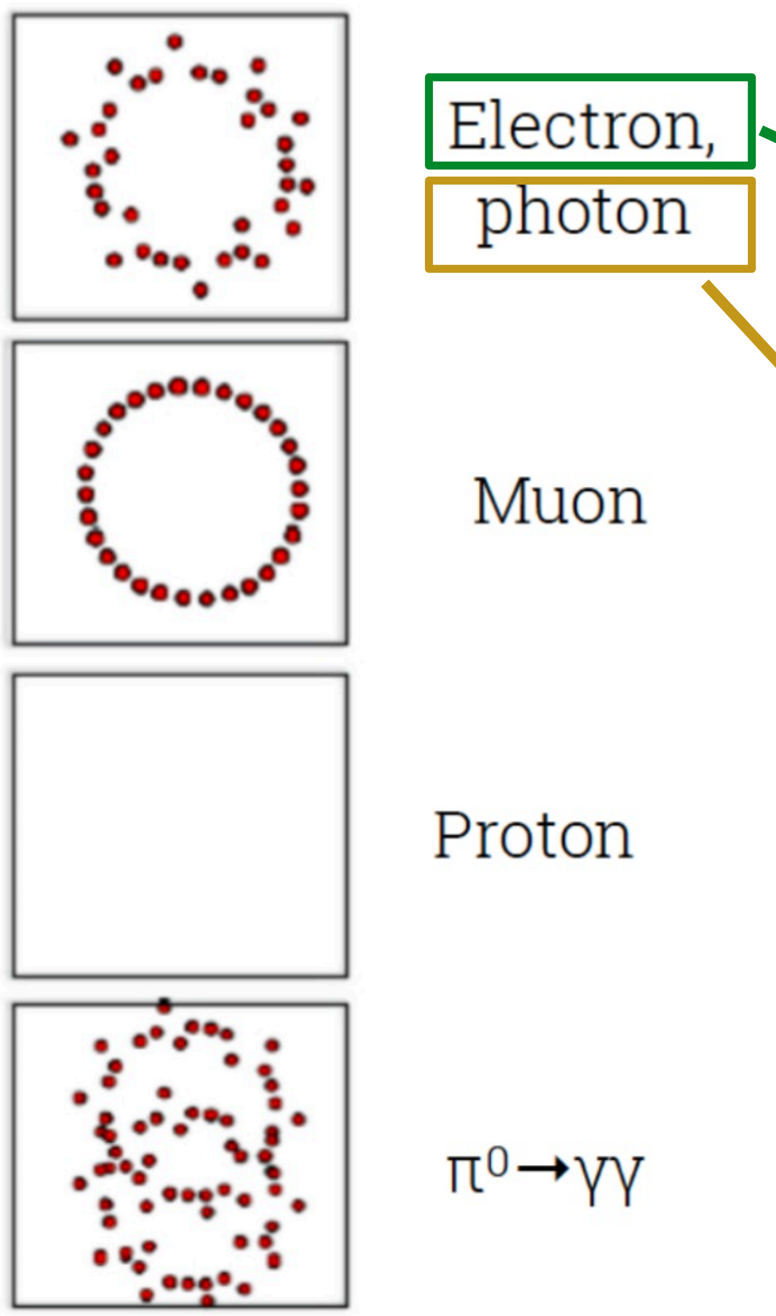

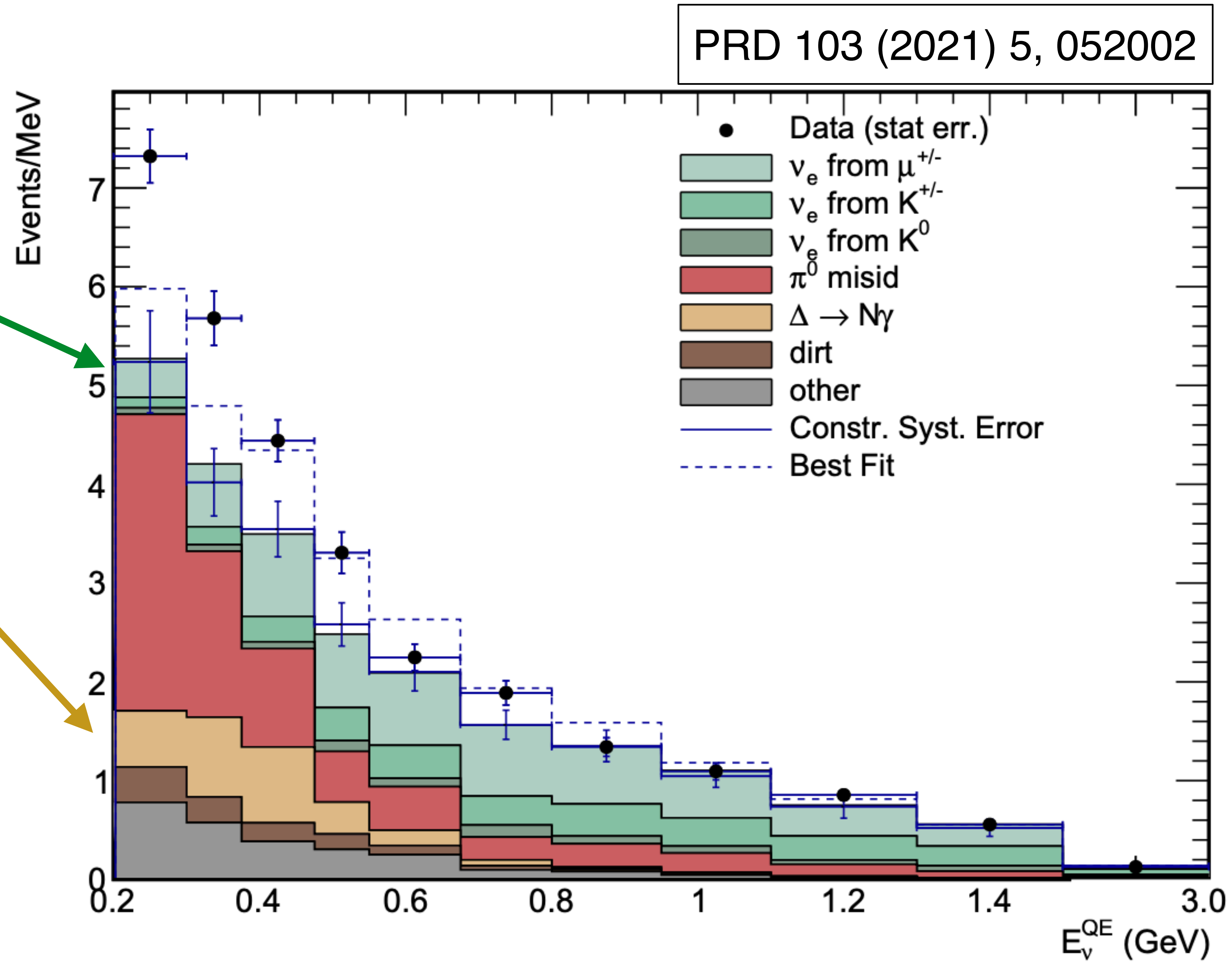

- Cherenkov detector cannot distinguish rings from *e* vs single γ
  - nor it cannot observe the proton activity, mostly below Cherenkov threshold
- Two alternative mainstream hypotheses have been proposed as reason for the excess: ν_e events (oscillations) or $\Delta\rightarrow N\gamma$ (unconstrained background)
  - other possible interpretations are however emerging (we'll discuss them later)

arXiv:1503.01520

Enter MicroBooNE

- Designed to test the MiniBooNE low-energy excess (LEE)
  - same neutrino beam (BNB)
  - similar distance from source
  - analyzed about 1/2 data
- But experimental program goes well beyond the LEE
  - nu-Ar cross sections
  - BSM physics searches
  - LArTPC development
  - also off-axis to NuMI beam
- Part of broader SBN program to test short-baseline oscillations

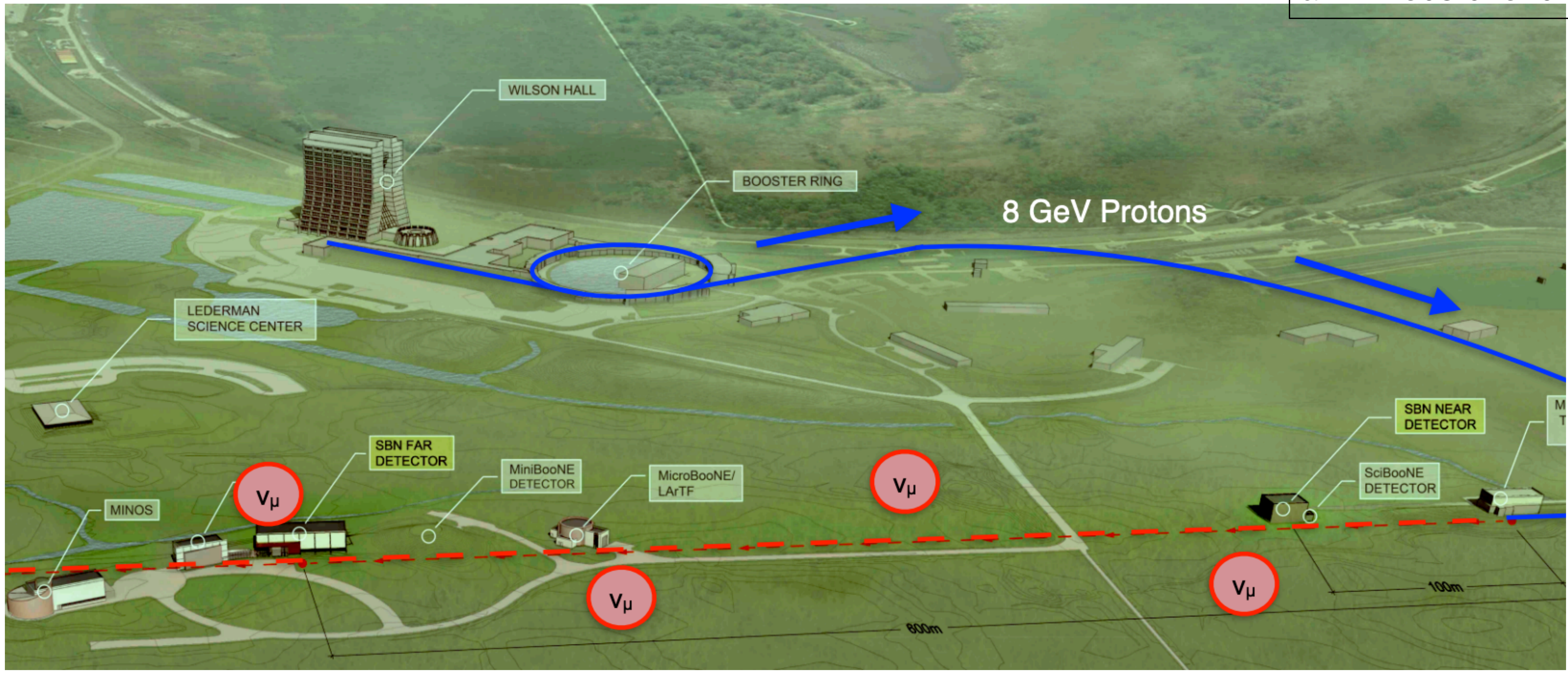

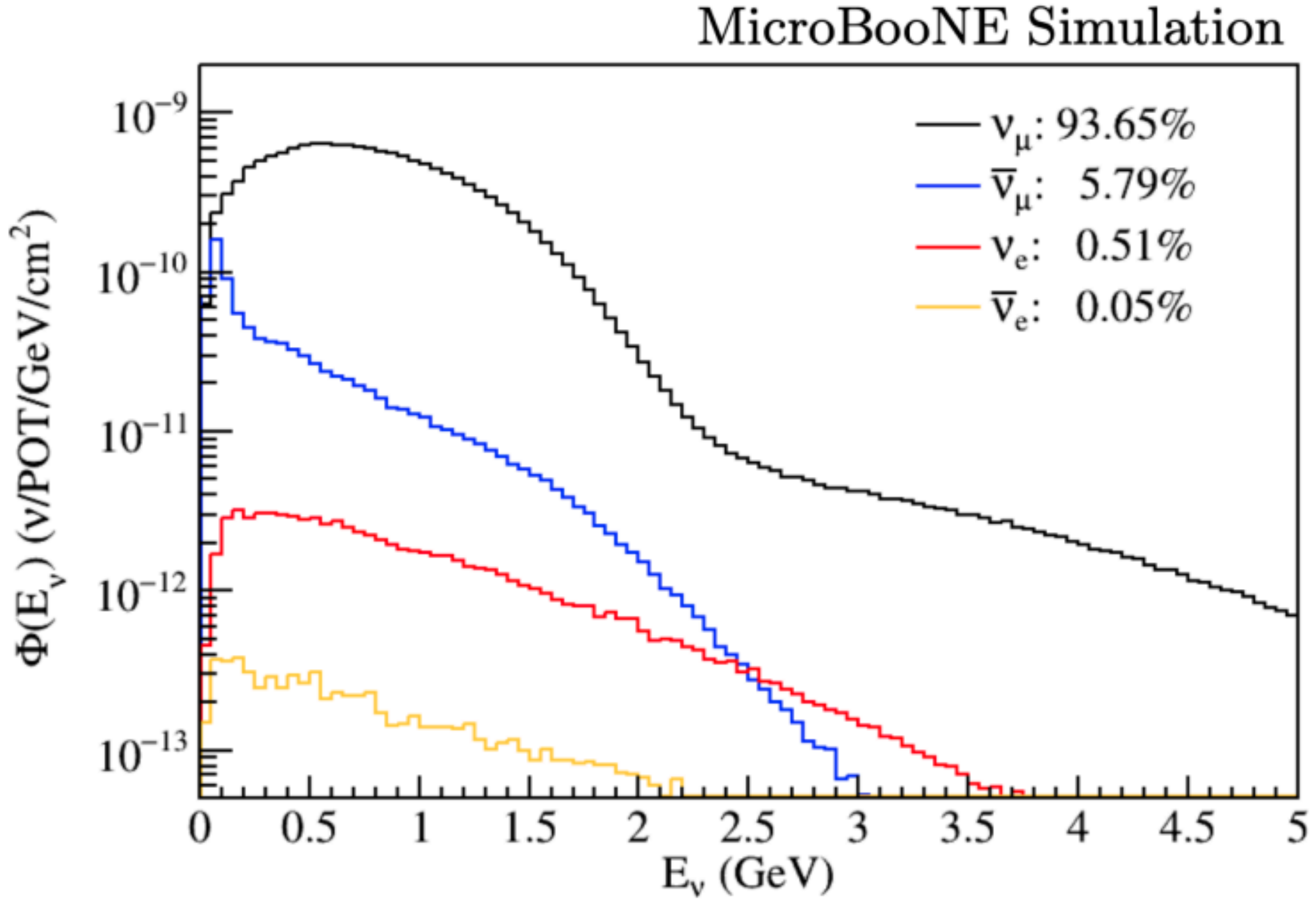

MICROBOONE-NOTE-1031

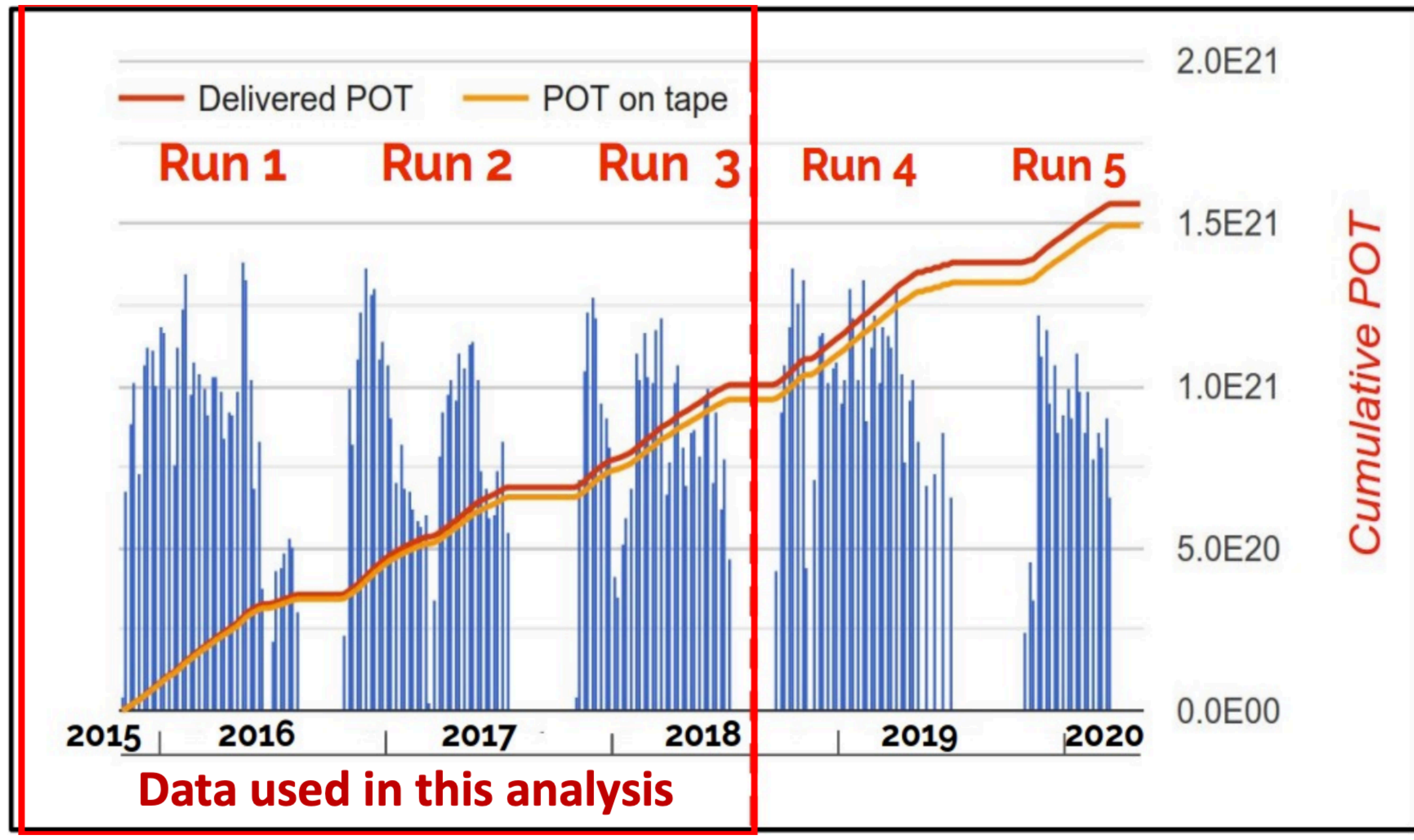

Fermilab

MicroBooNE detector

JINST 12, P02017 (2017)

- Charged particles produced in neutrino interactions ionize the argon, ionization electrons drift in electric field towards anode planes
- Sense wires detect the incoming charge, producing beautiful detector data images

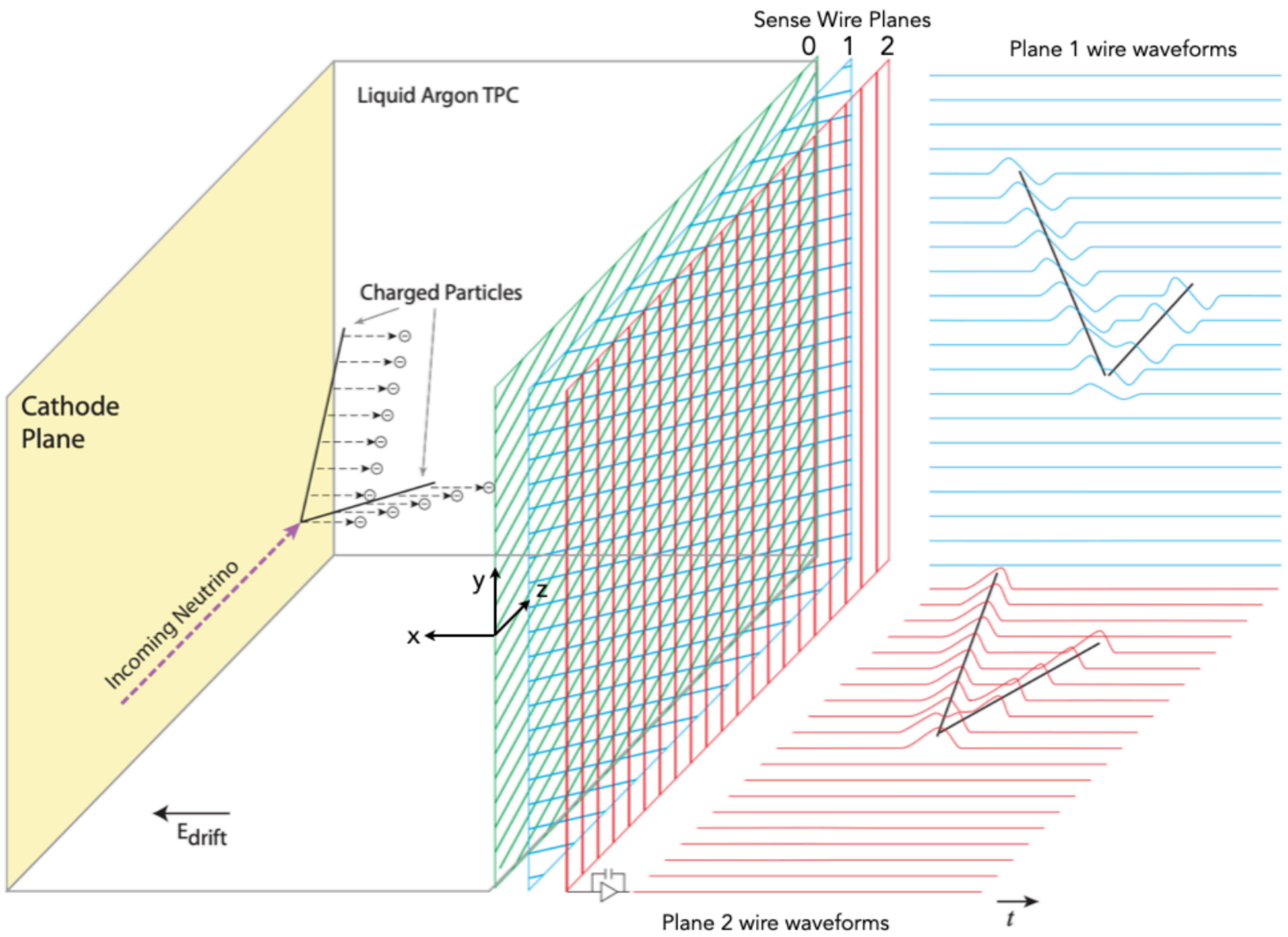

3 planes allow for 3D reco

MicroBooNE detector

- Charged particles produced in neutrino interactions ionize the argon, ionization electrons drift in electric field towards anode planes
- Sense wires detect the incoming charge, producing beautiful detector data images
- Full detail of neutrino interaction with O(mm) spatial resolution and calorimetric information
- Fast scintillation light detected by PMT system for triggering and cosmic rejection

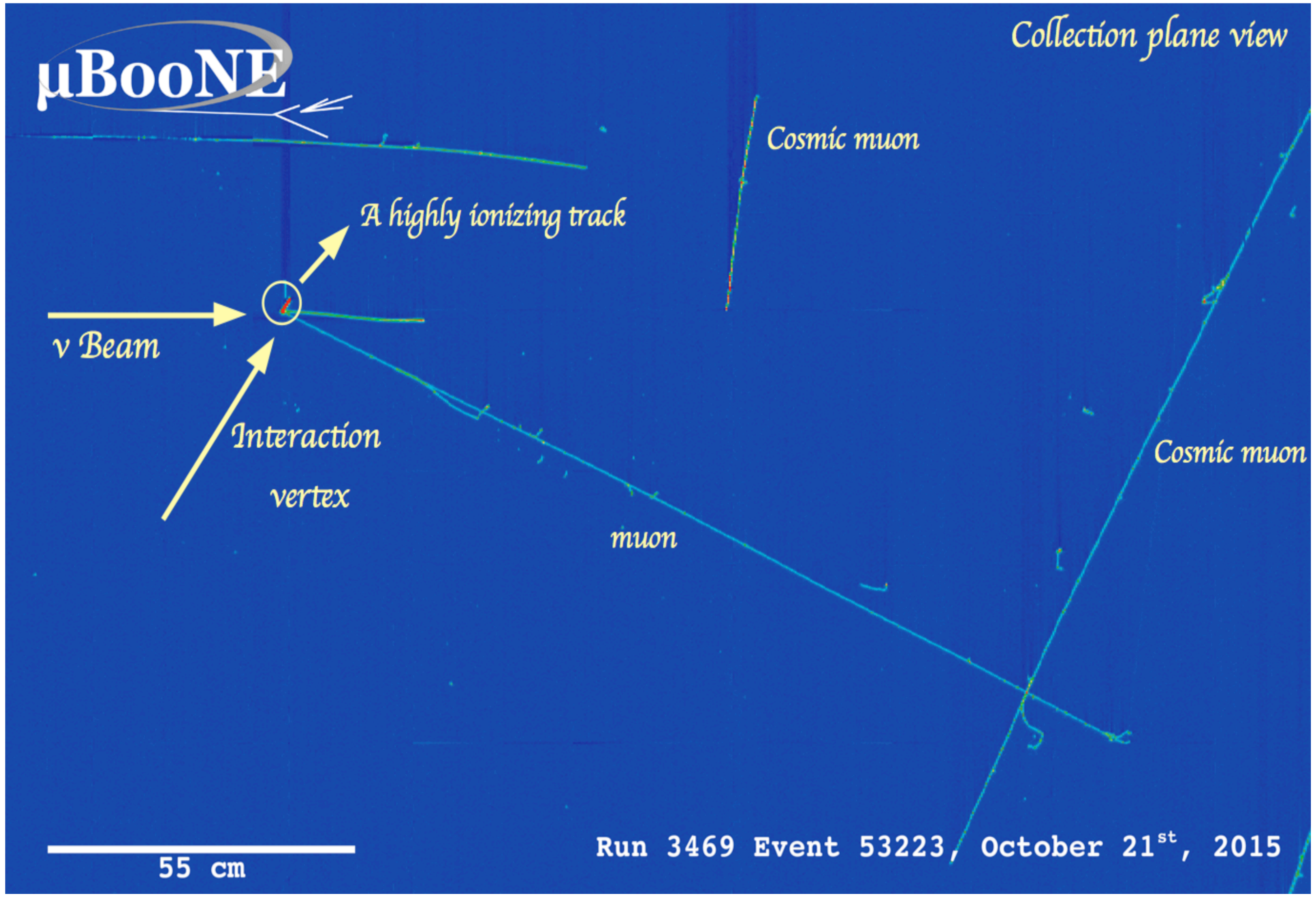

axes: time vs wire - color scale: charge

Fermilab

Superior detector capabilities

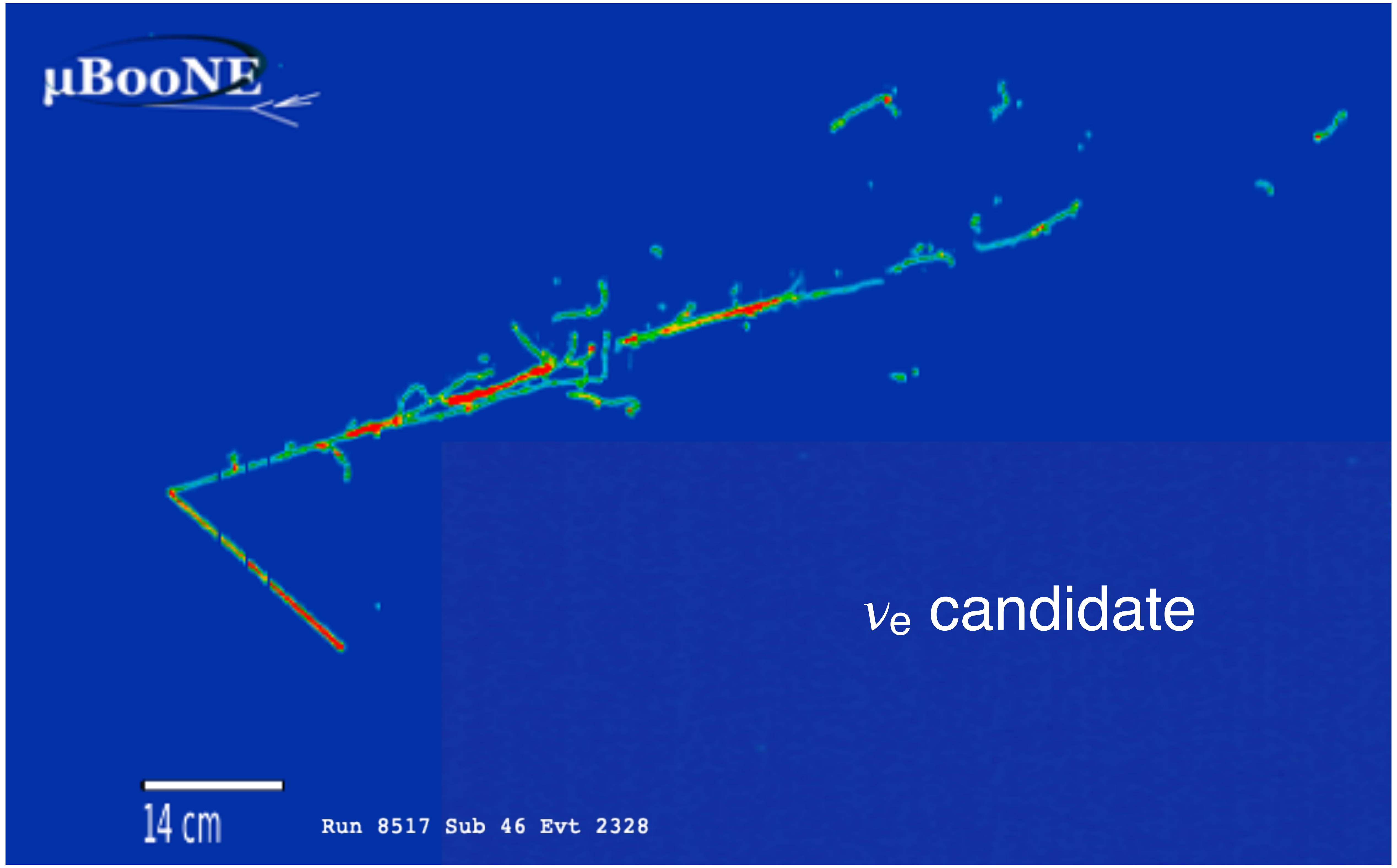

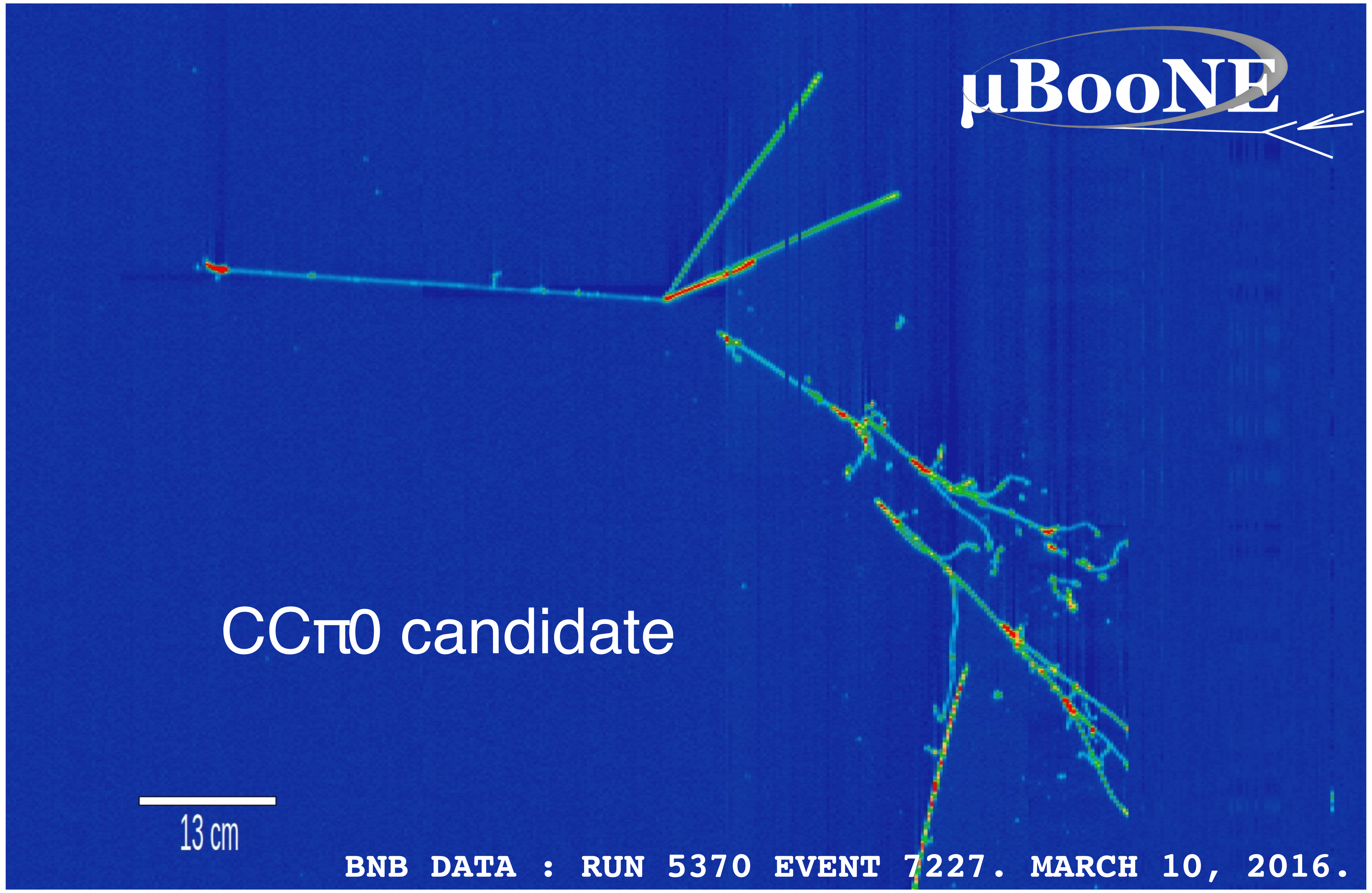

Superior detector capabilities: e/g separation

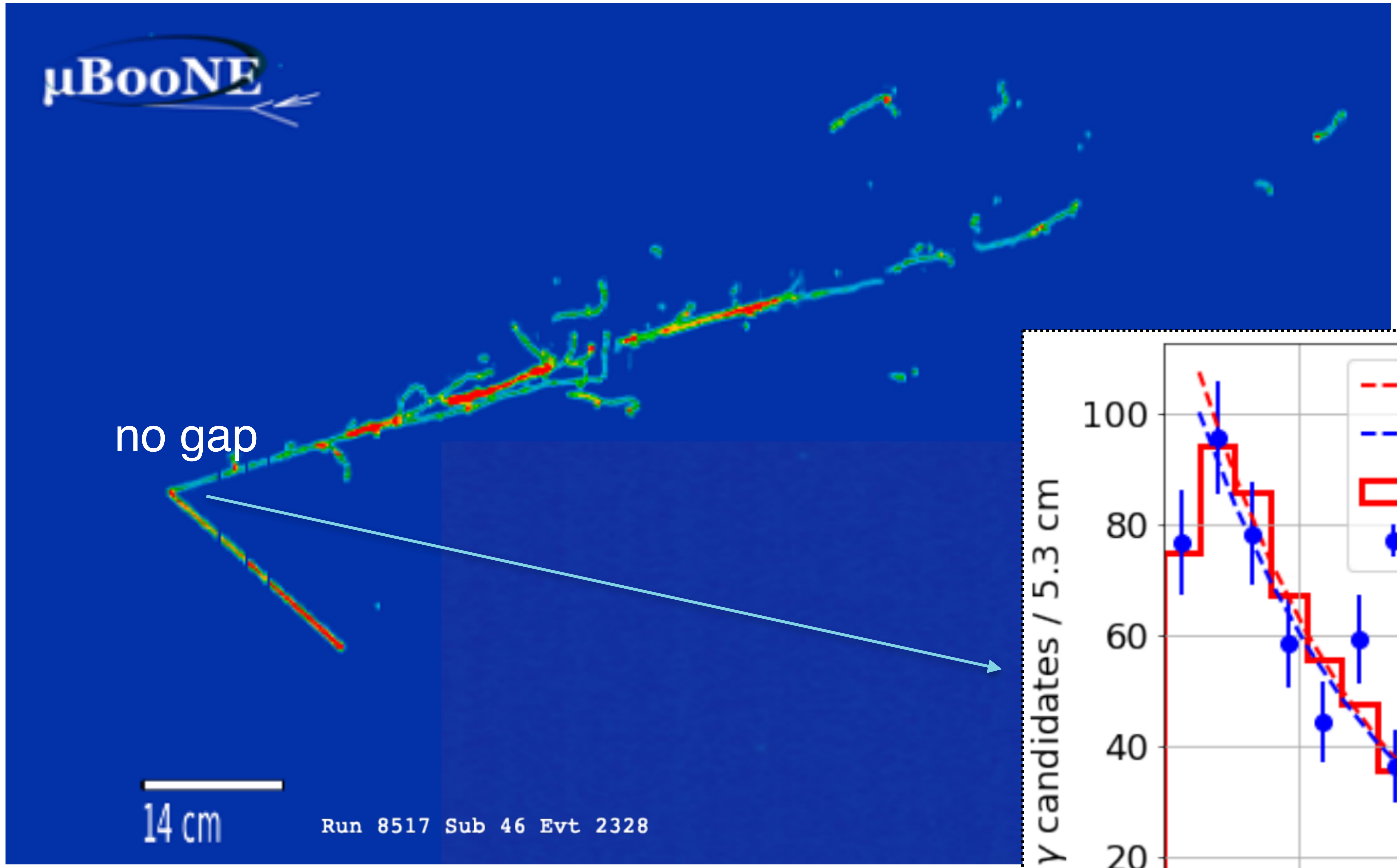

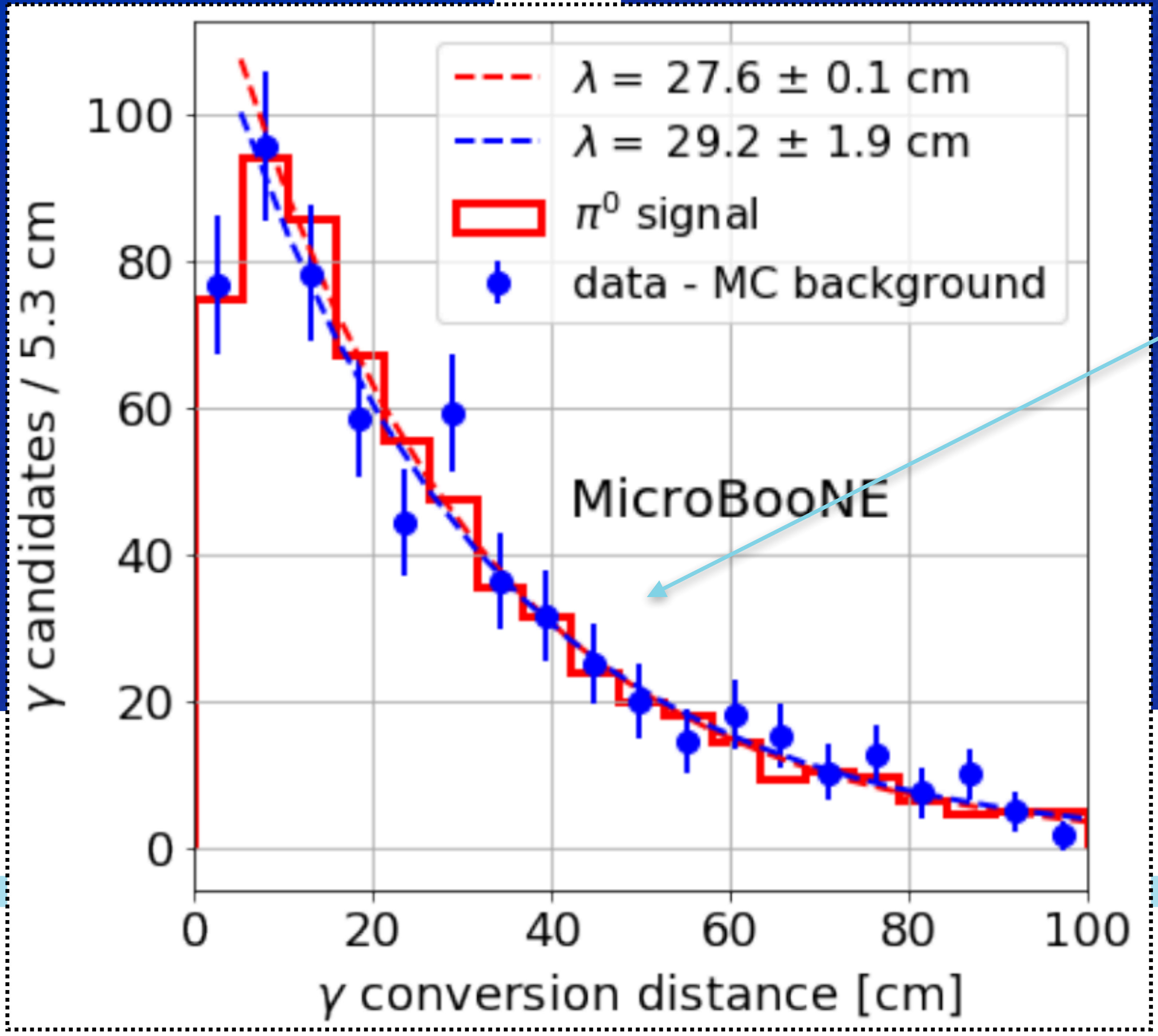

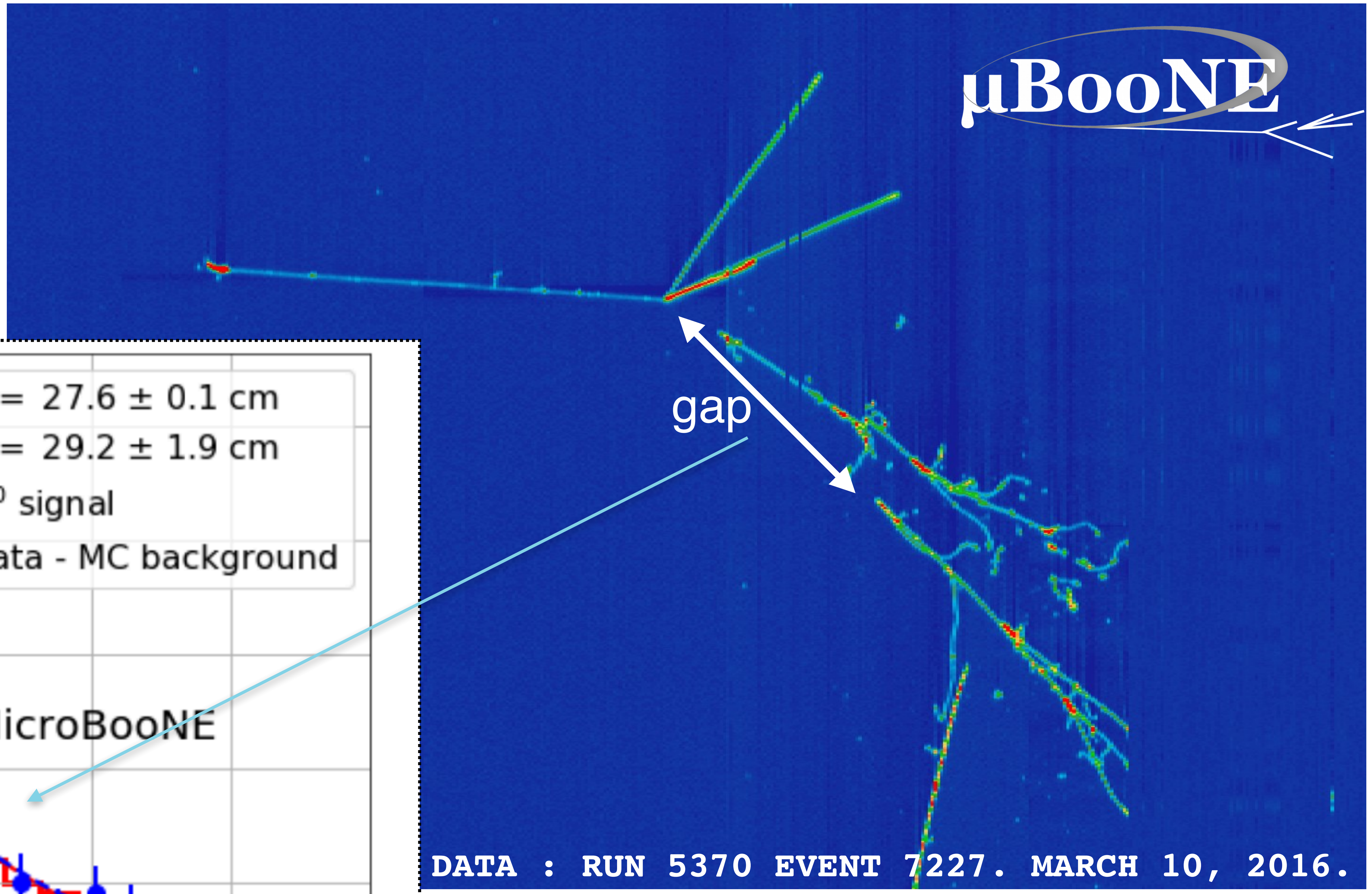

JINST 15, P02007 (2020)

Fermilab

Superior detector capabilities: e/g separation

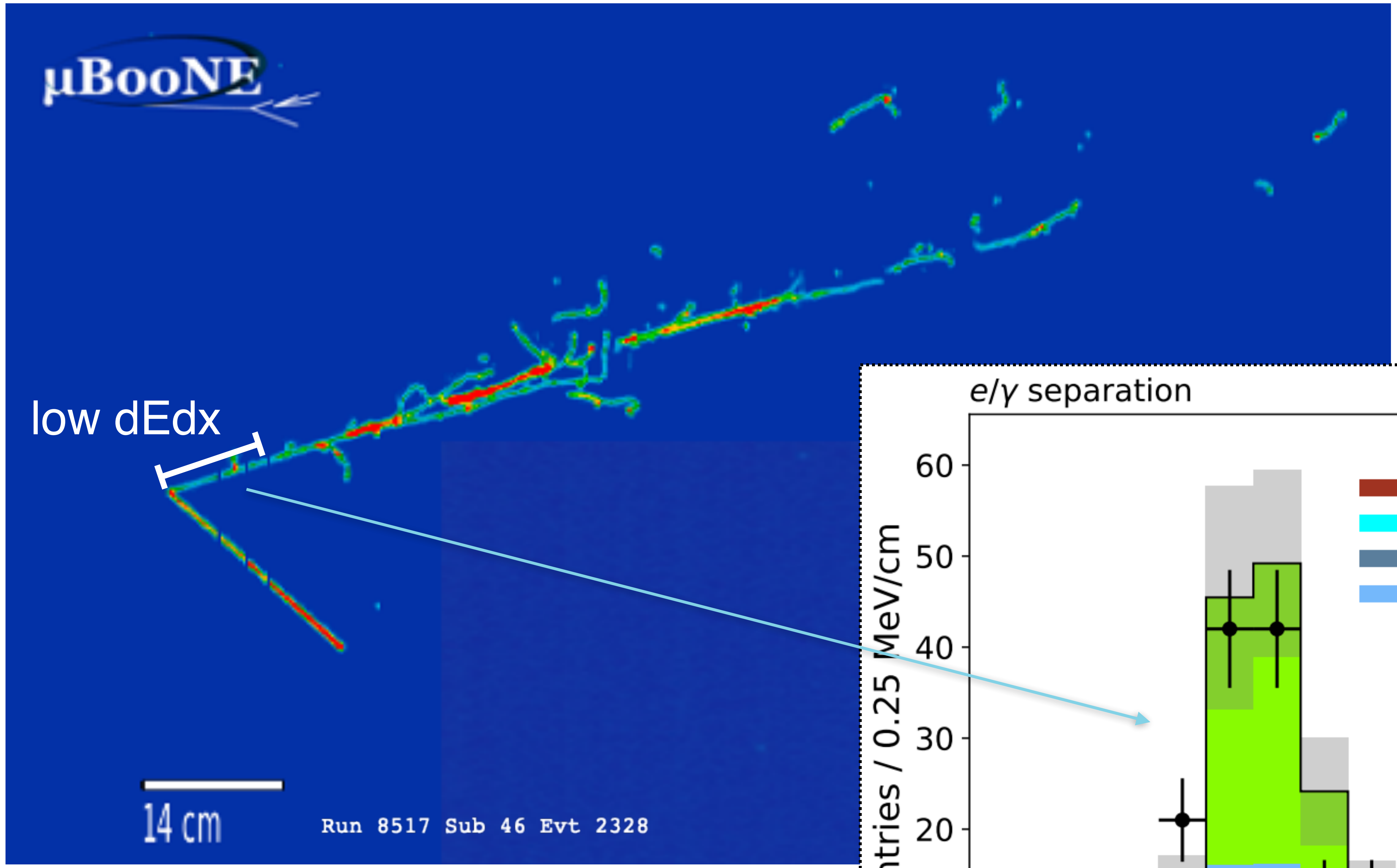

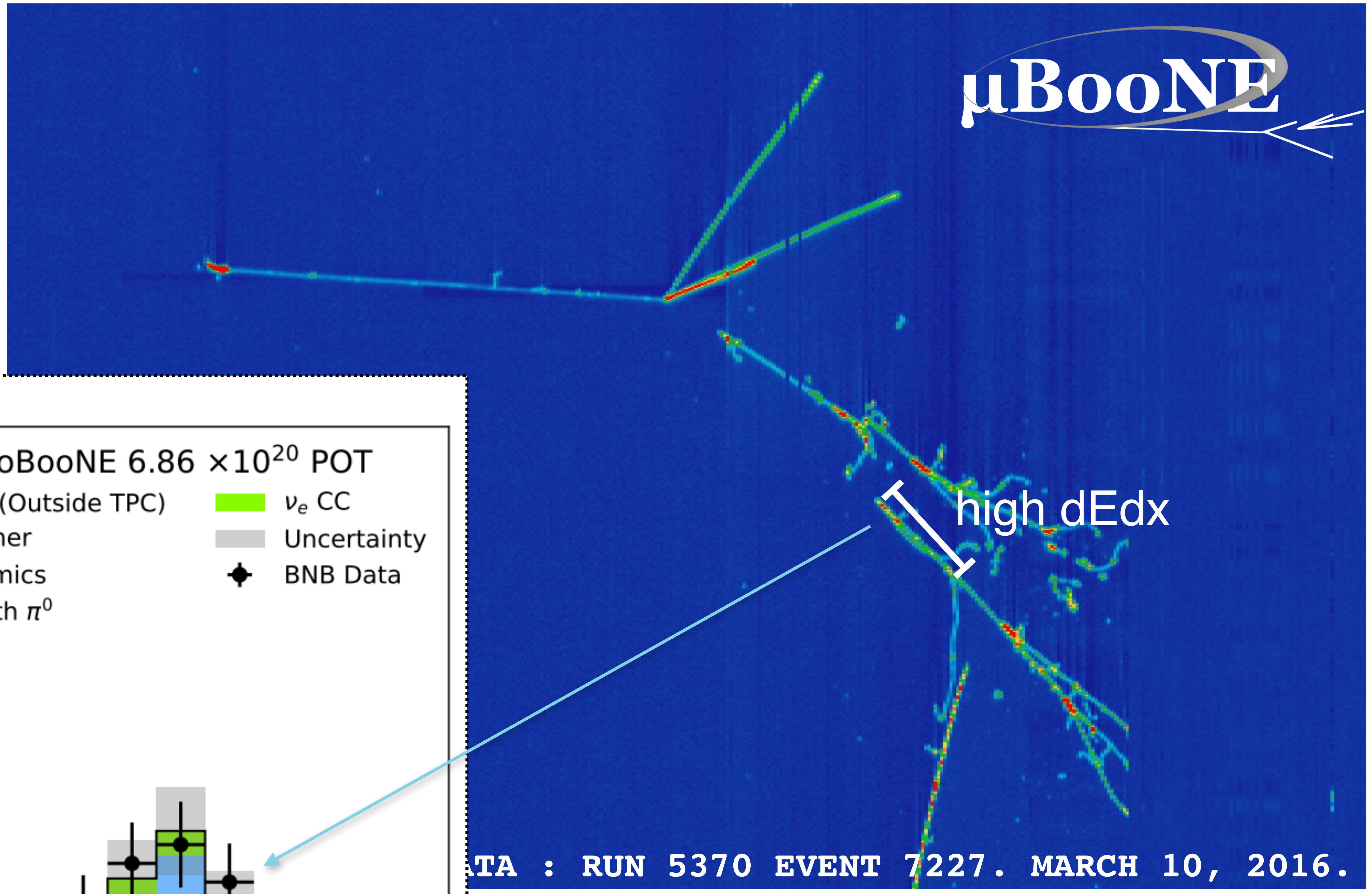

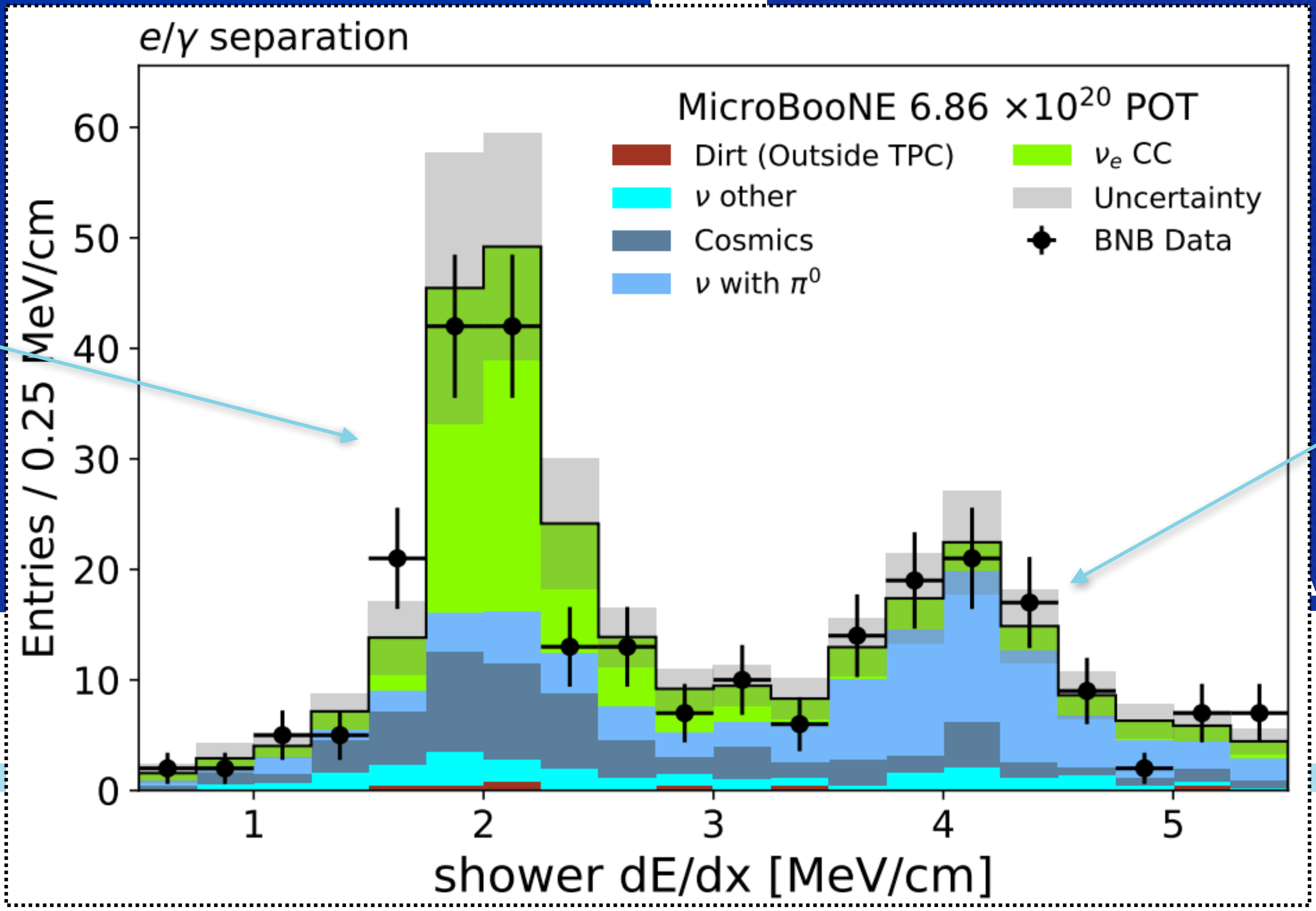

arXiv:2110.14065

Fermilab

Superior detector capabilities: proton detection

JHEP 12 (2021) 153

Fermilab

PRD 103, 052002 (2021)

Searching for the MB excess in uB

- Our first tests of the MB excess look for the signature of leading interpretations of the excess:
  - ν_e events (oscillation)
  - neutral current (NC) $\Delta \to \gamma$

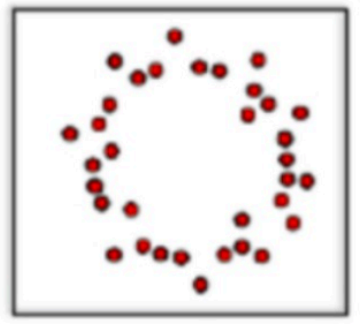

Electron,

photon

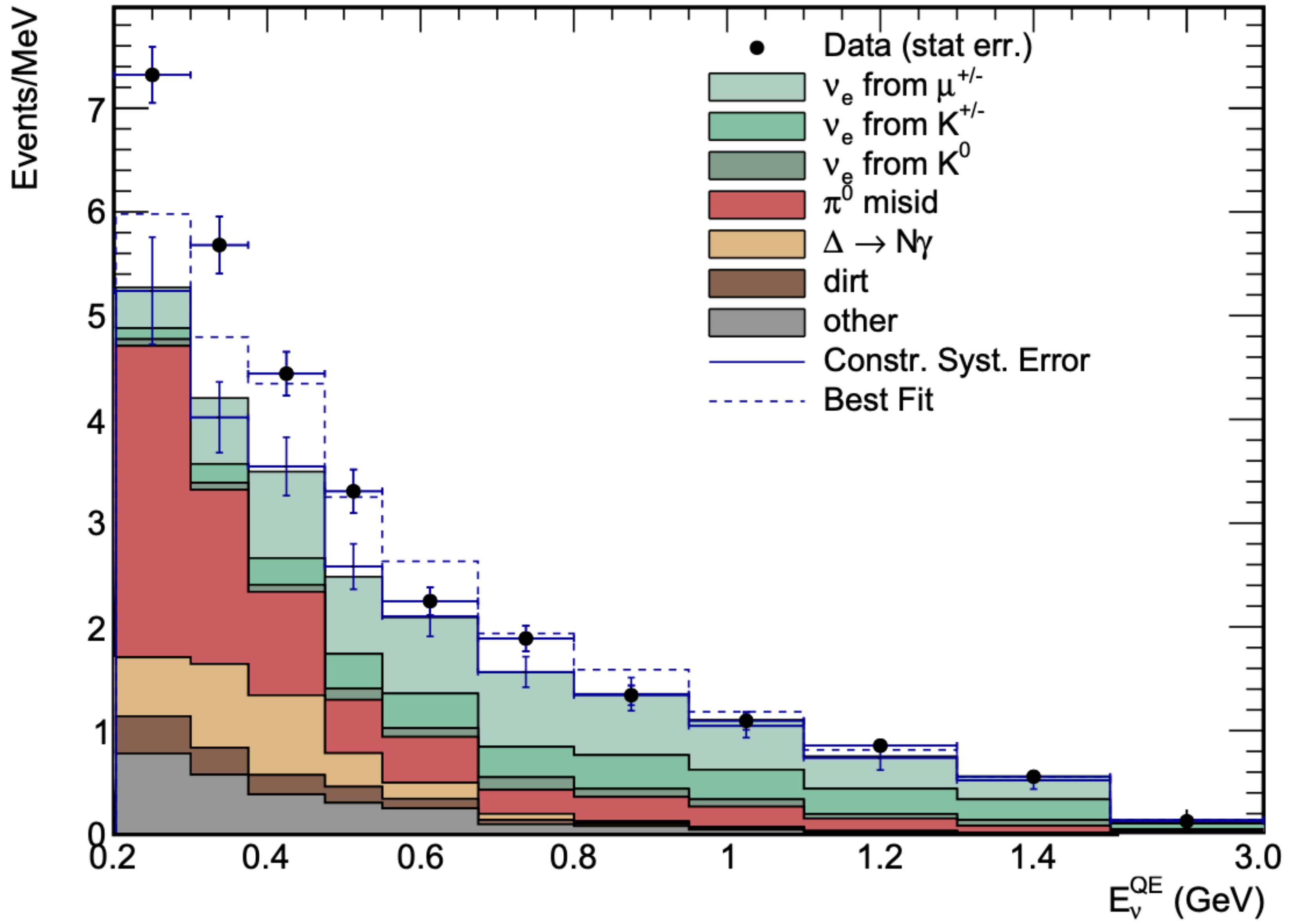

Fermilab

Searching for the MB excess in uB

- Our first tests of the MB excess look for the signature of leading interpretations of the excess:
  - ν_e events (oscillation)
  - neutral current (NC) $\Delta \rightarrow \gamma$
- Define empirical signal model in uB based on unfolded MB E_ν data excess

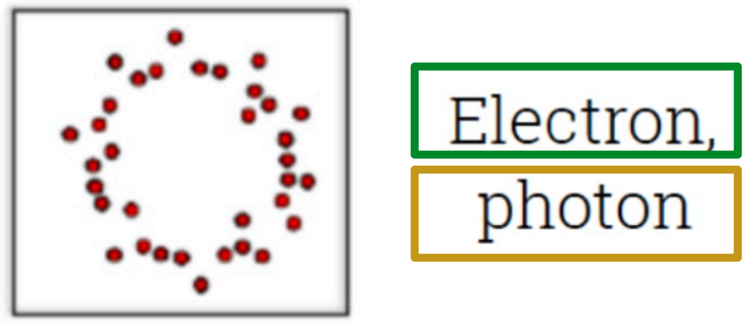

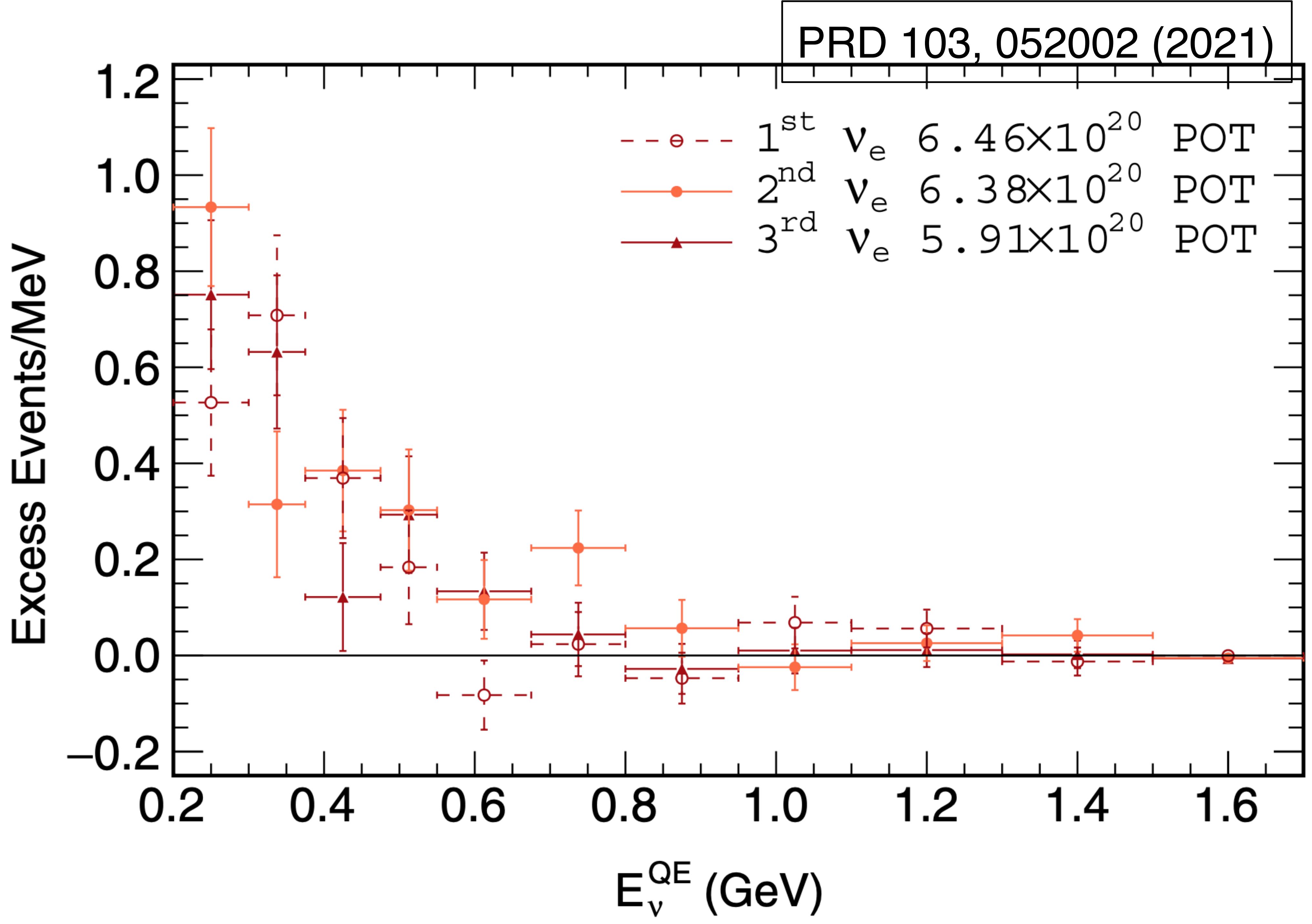

Searching for the MB excess in uB

- Our first tests of the MB excess look for the signature of leading interpretations of the excess:
  - ν_e events (oscillation)
  - neutral current (NC) $\Delta \rightarrow \gamma$

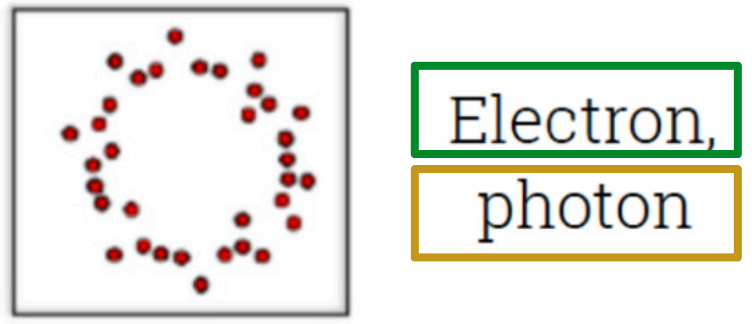

- Define empirical signal model in uB based on unfolded MB E_ν data excess
  - Prediction in uB is then obtained from a scale factor to the nominal prediction for that process
- Signal in uB can be tested as
  - simple hypothesis H0 vs H1
  - signal strength fit (normalization scaling parameter)

PRD 103, 052002 (2021)

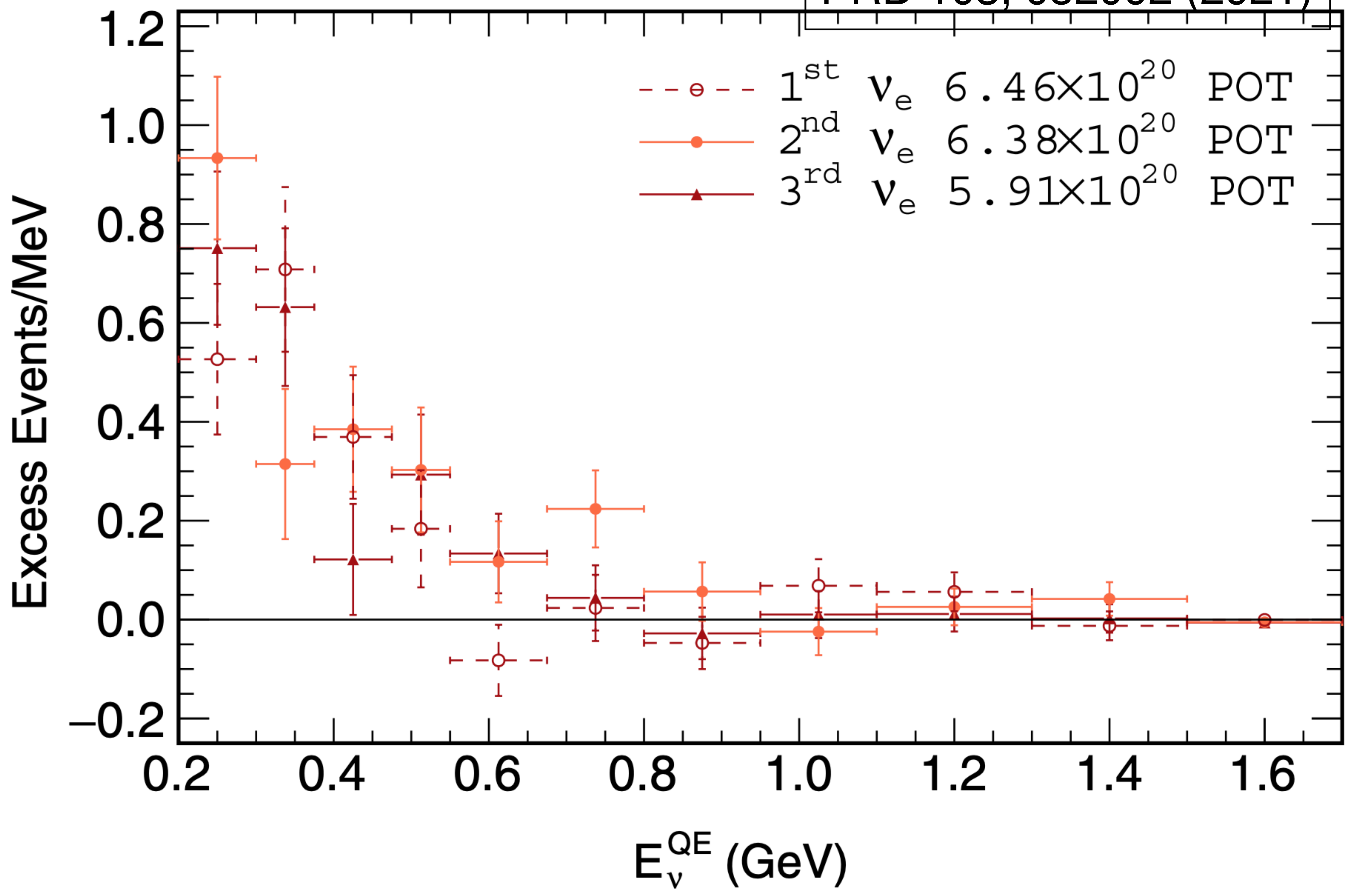

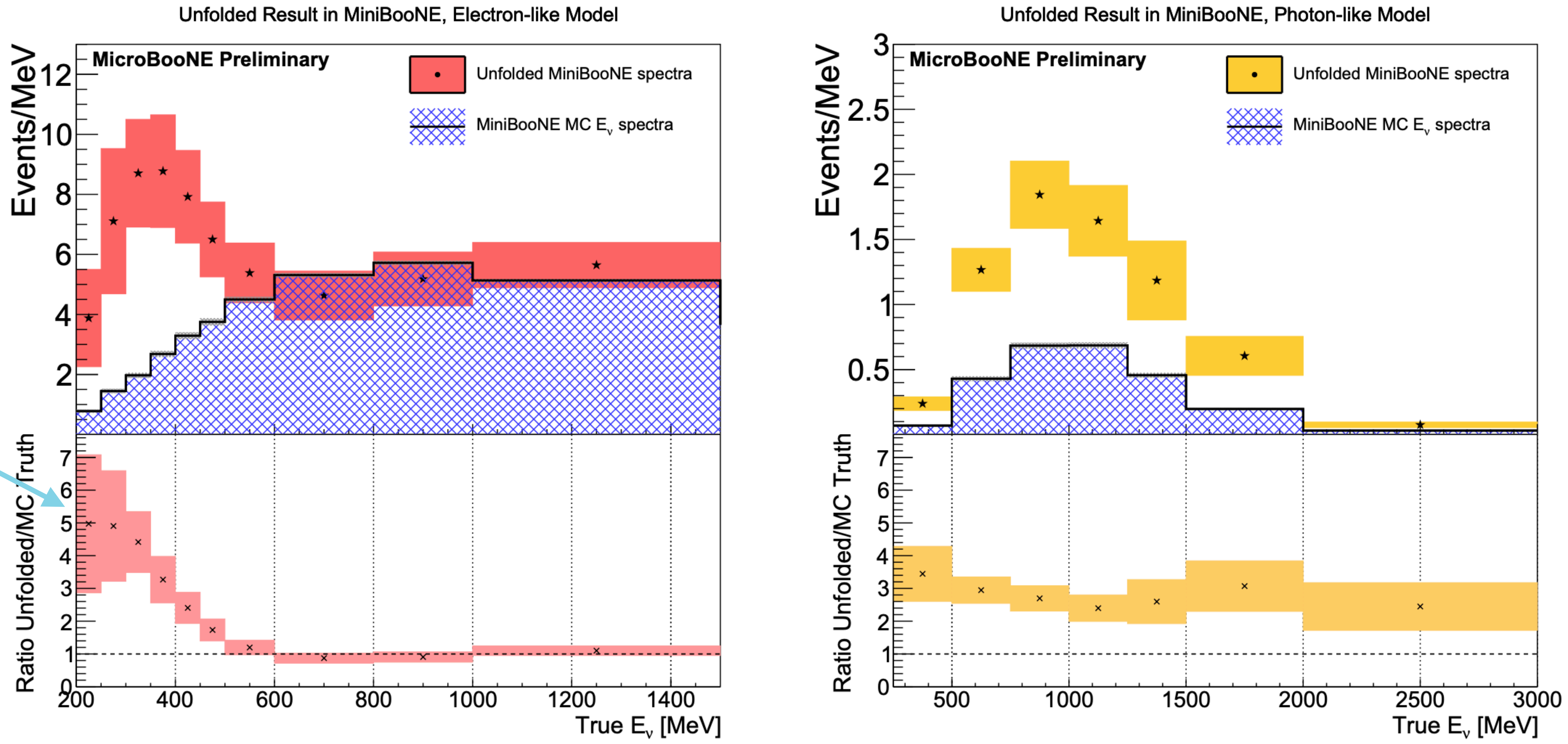

MICROBOONE-NOTE-1043

PRL 128 (2022) 11, 111801

Search for Neutral Current Delta Radiative

- Assume excess is due to ~3x larger NC $\Delta \rightarrow N\gamma$
- Apply to MicroBooNE to benchmark the analysis wrt excess
- $\Delta \rightarrow N\gamma$ search utilizes $1\gamma1p$ and $1\gamma0p$ events which are fit simultaneously to maximize signal statistics
- Major challenge is understanding and rejecting NC π^0 backgrounds
  - In situ measurement used to constrain the background

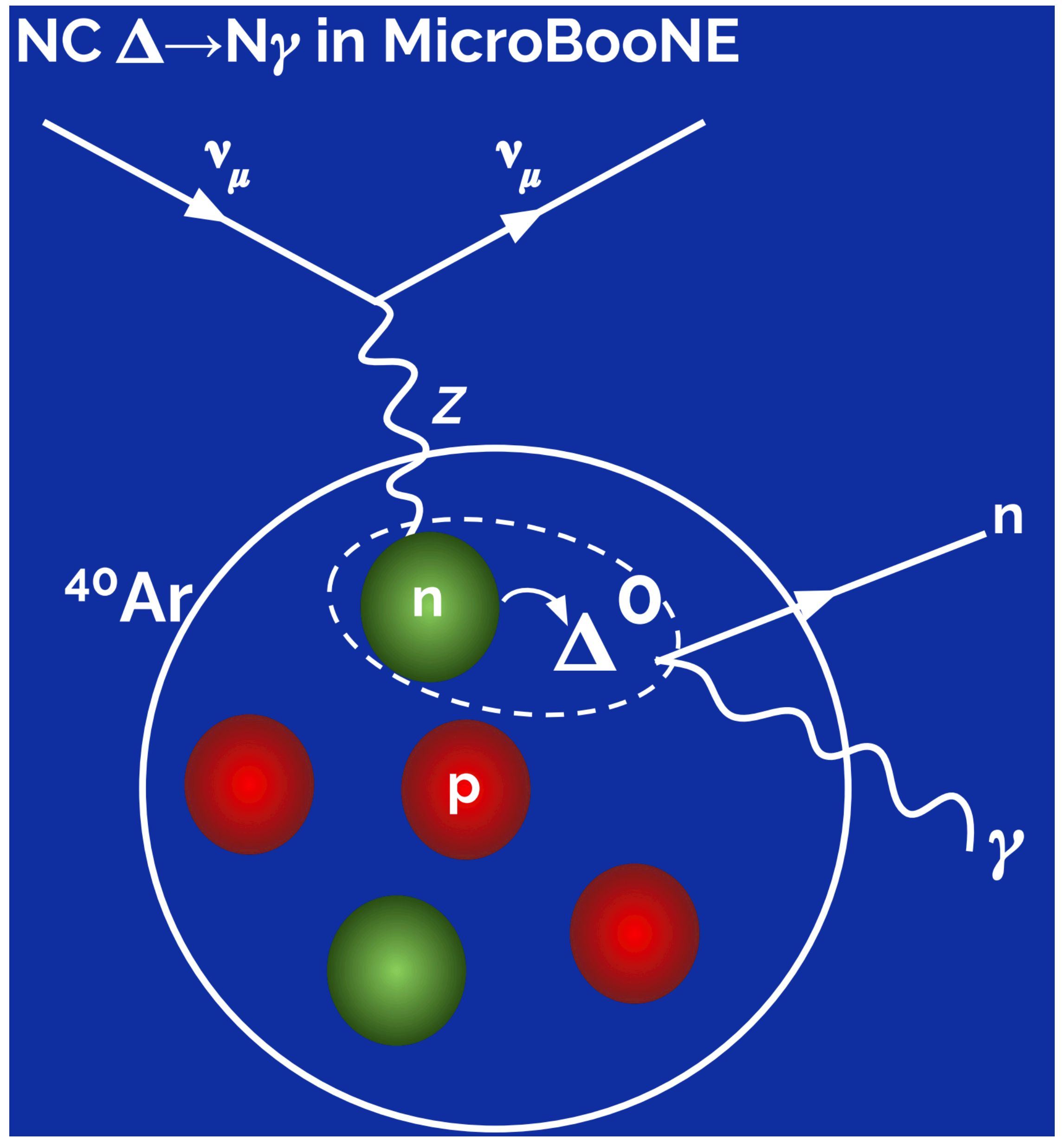

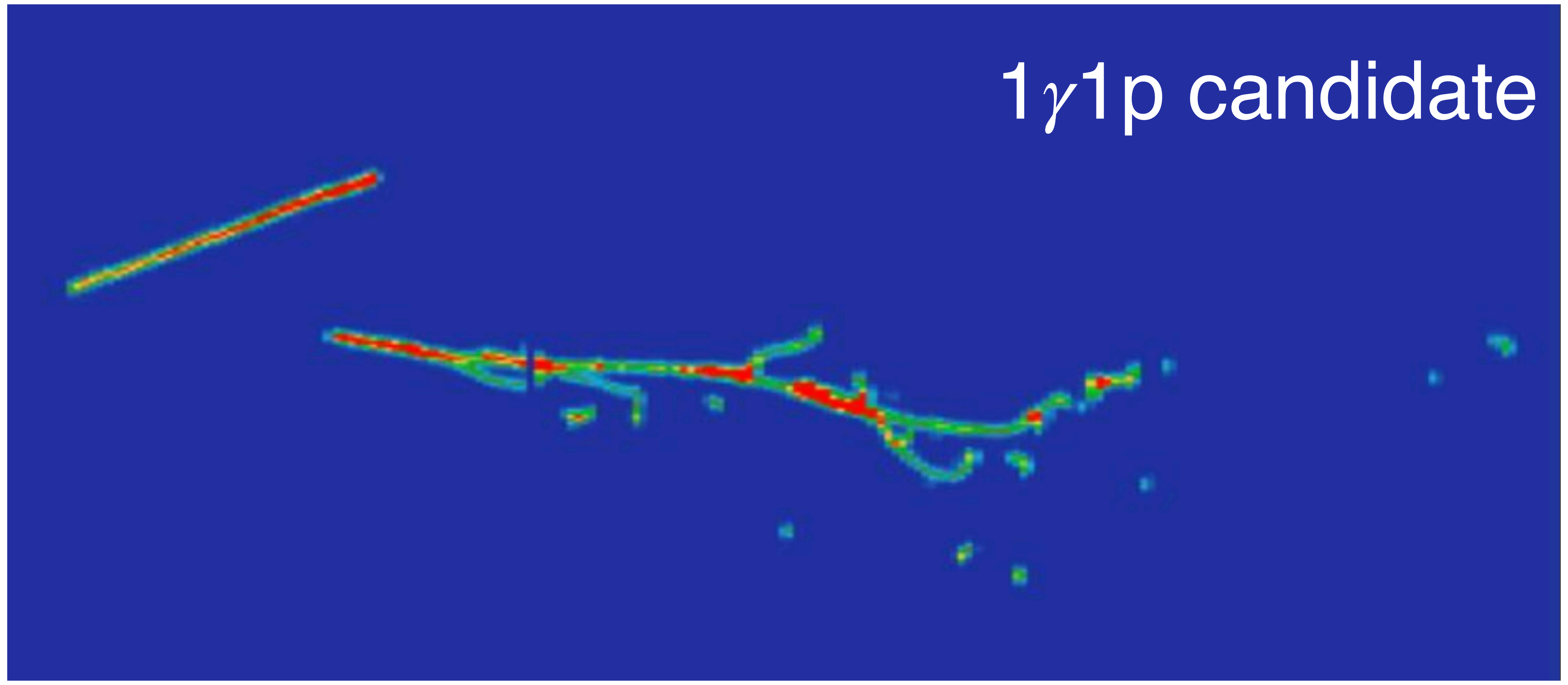

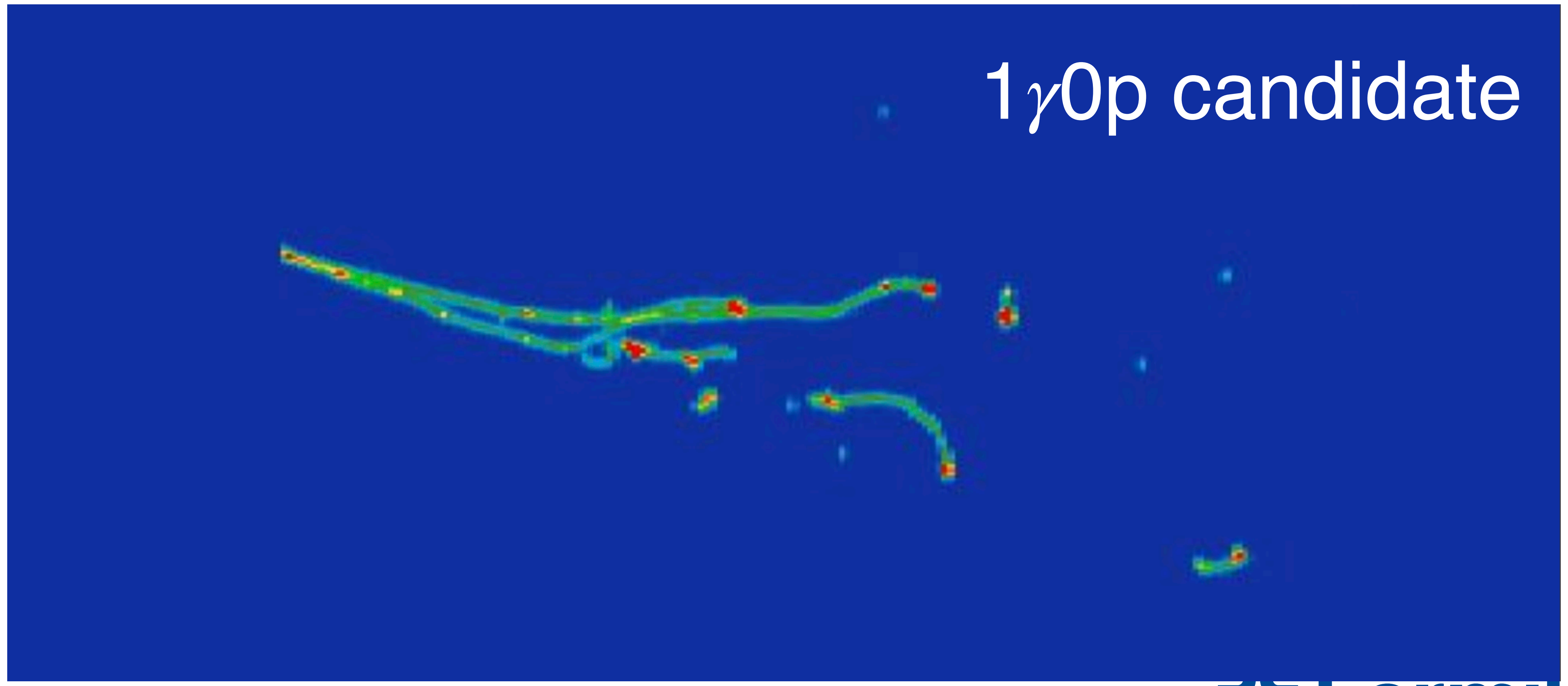

PRL 128 (2022) 11, 111801

NC Delta Radiative - Results

- Observe data-MC agreement within error in both channels
  - overall deficit is similar to observation in NC π^0 control regions

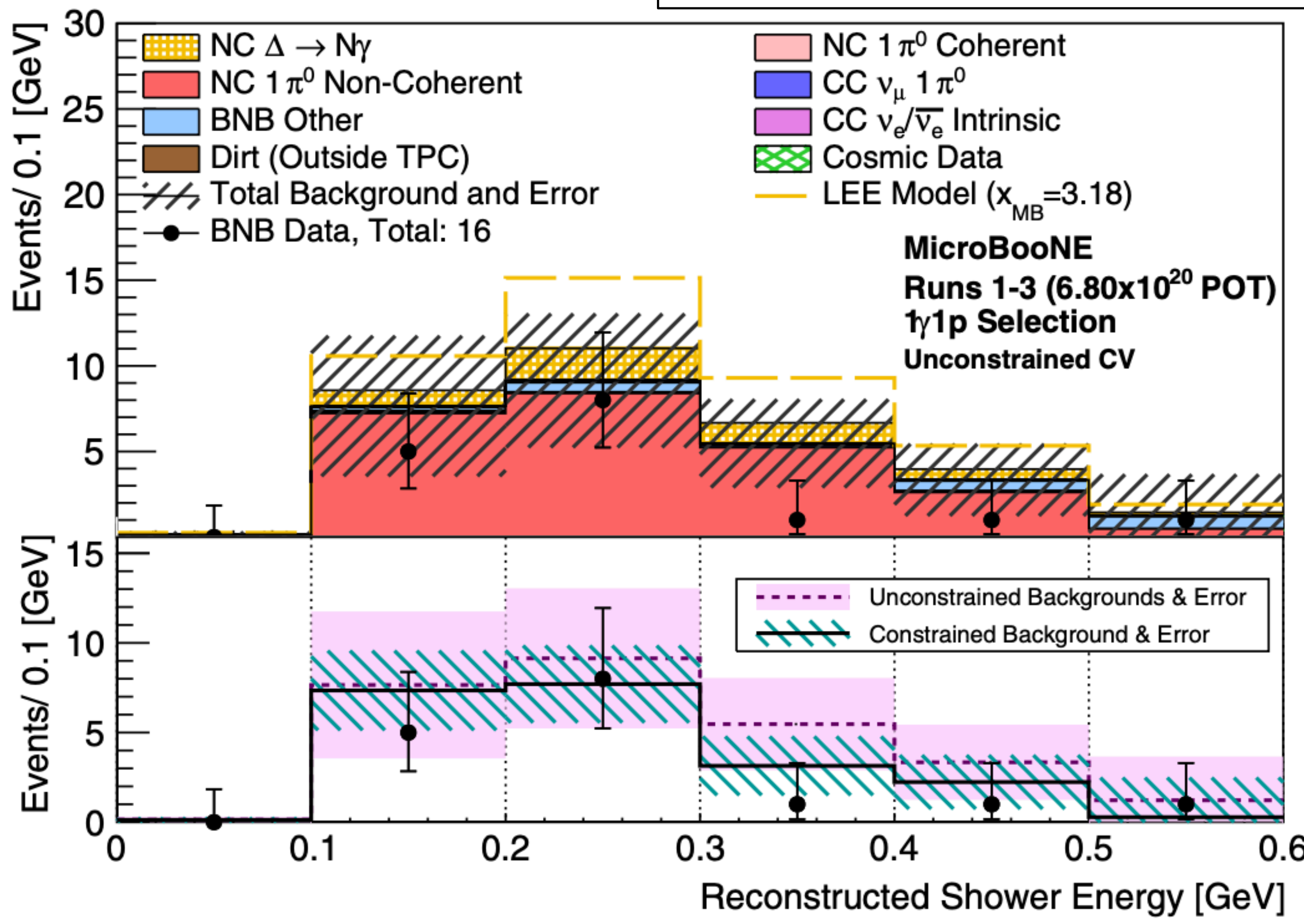

(a)

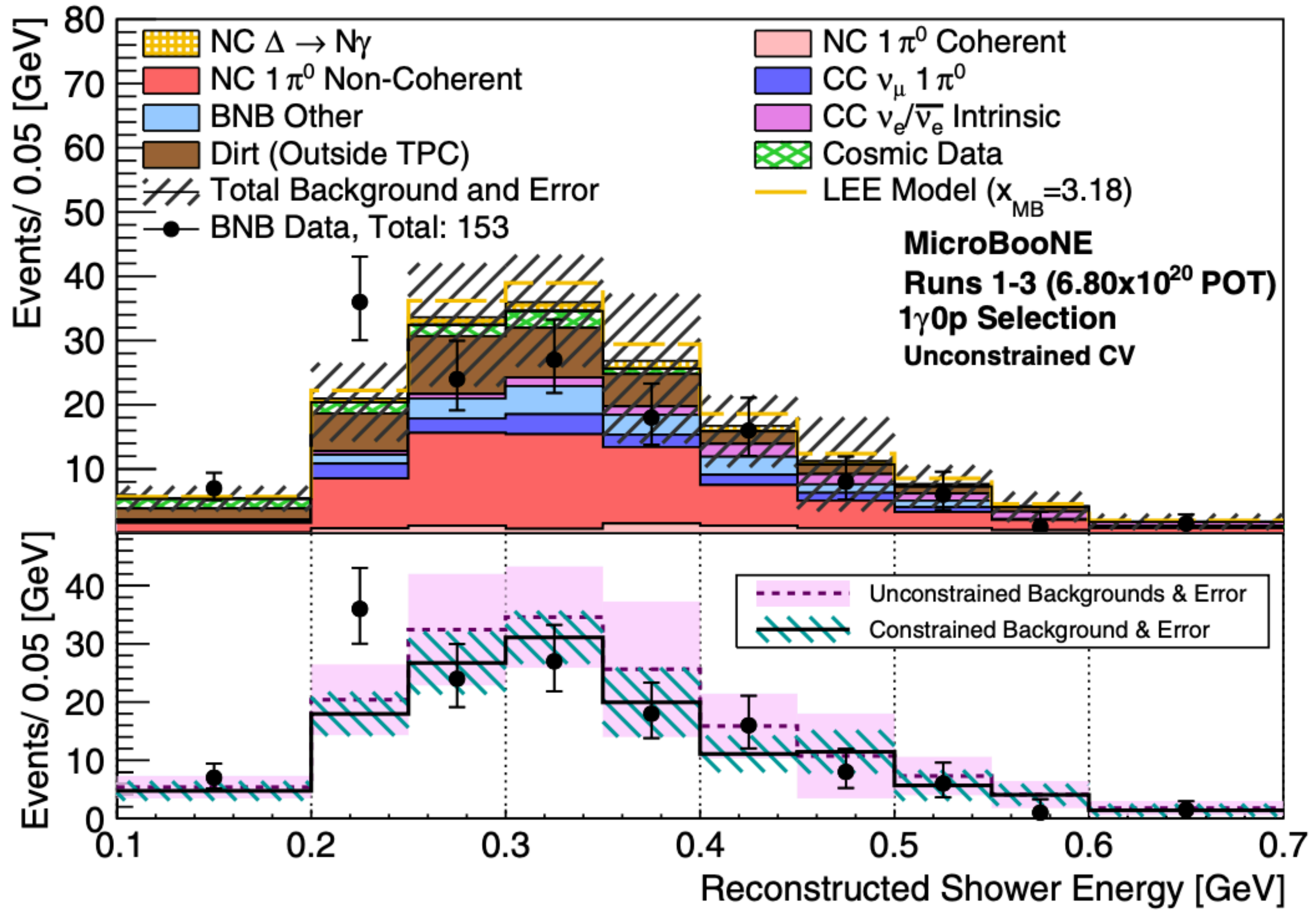

(b)

Fermilab

PRL 128 (2022) 11, 111801

NC Delta Radiative - Results

- Observe data-MC agreement within error in both channels
  - overall deficit is similar to observation in NC π^0 control regions
- Control regions used to update prediction, improving agreement with data
  - no excess consistent with NC $\Delta \rightarrow \gamma$ is observed

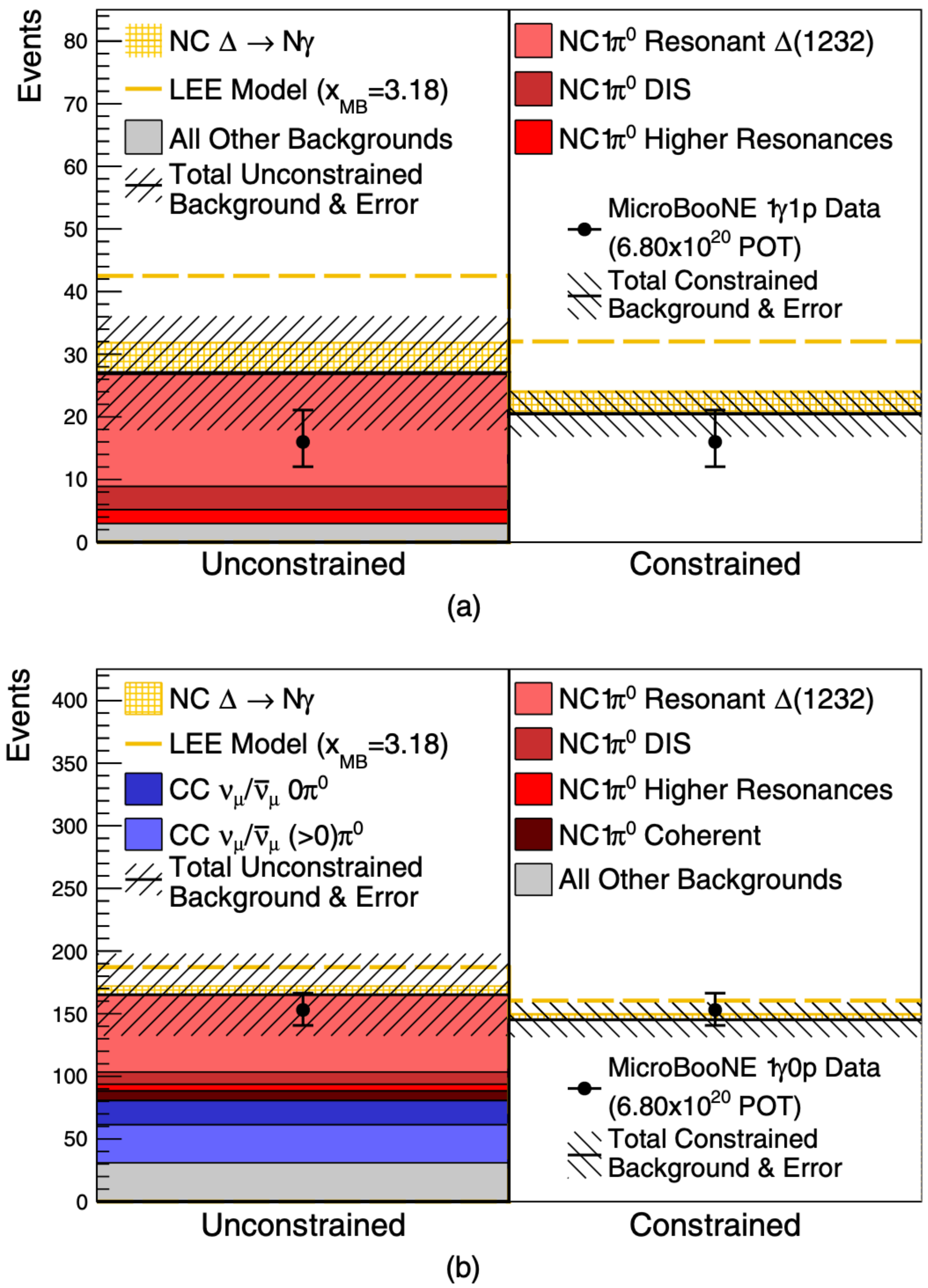

Fermilab

PRL 128 (2022) 11, 111801

NC Delta Radiative - Results

- Observe data-MC agreement within error in both channels
  - overall deficit is similar to observation in NC π^0 control regions
- Control regions used to update prediction, improving agreement with data
  - no excess consistent with NC $\Delta \rightarrow \gamma$ is observed
- Limits can be interpreted in terms of:
  - LEE signal strength < 3 at 90% CL
  - Branching ratio for Delta radiative decay < 1.8%
  - Cross section < $20 \cdot 10^{-42}$ cm^{-2}/nucleon

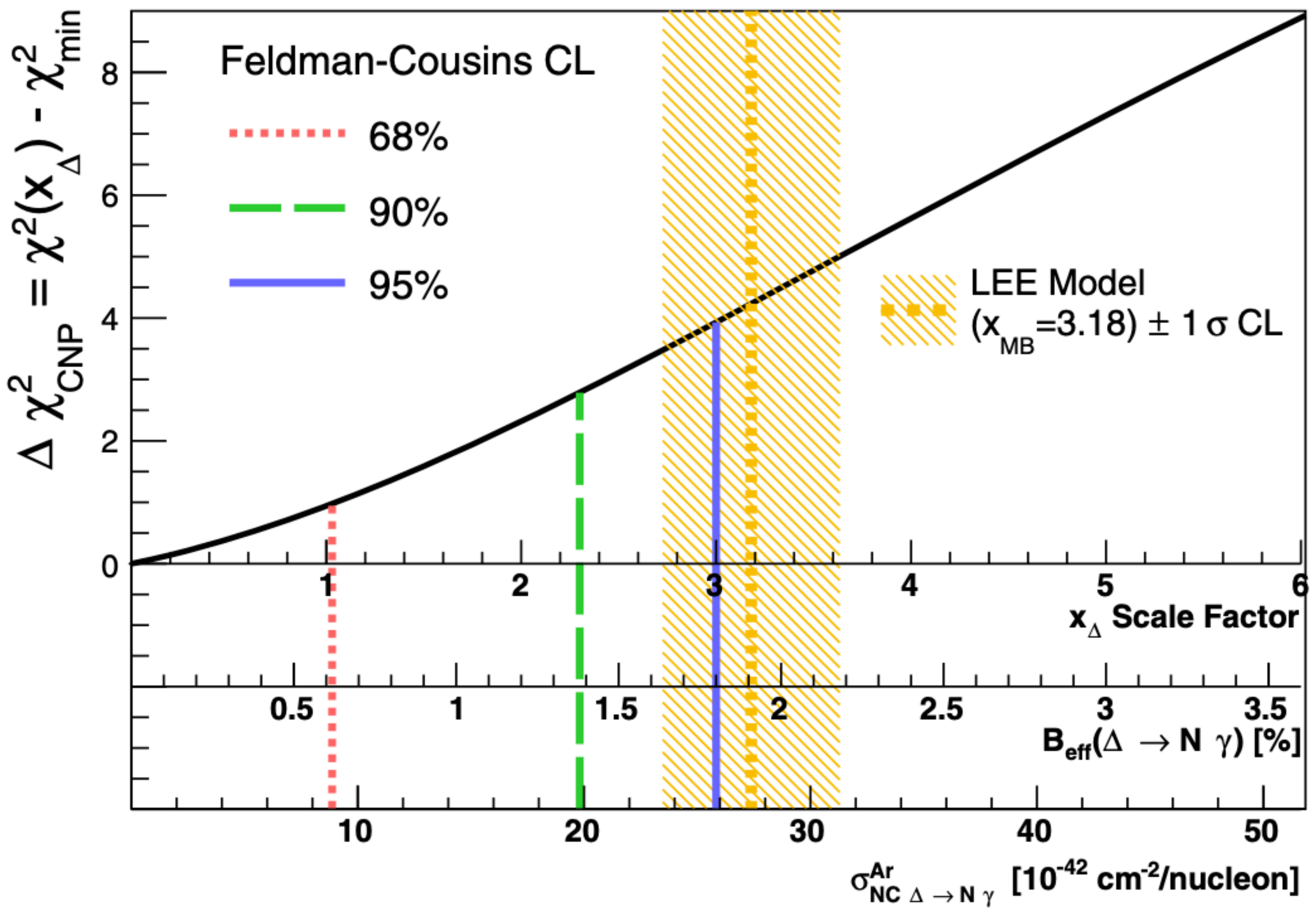

Fermilab

Search for an Excess of Electron Neutrino Interactions

Three complementary analyses testing different final states and using different reconstruction tools

Search for an Excess of Electron Neutrino Interactions

Three complementary analyses testing different final states and using different reconstruction tools

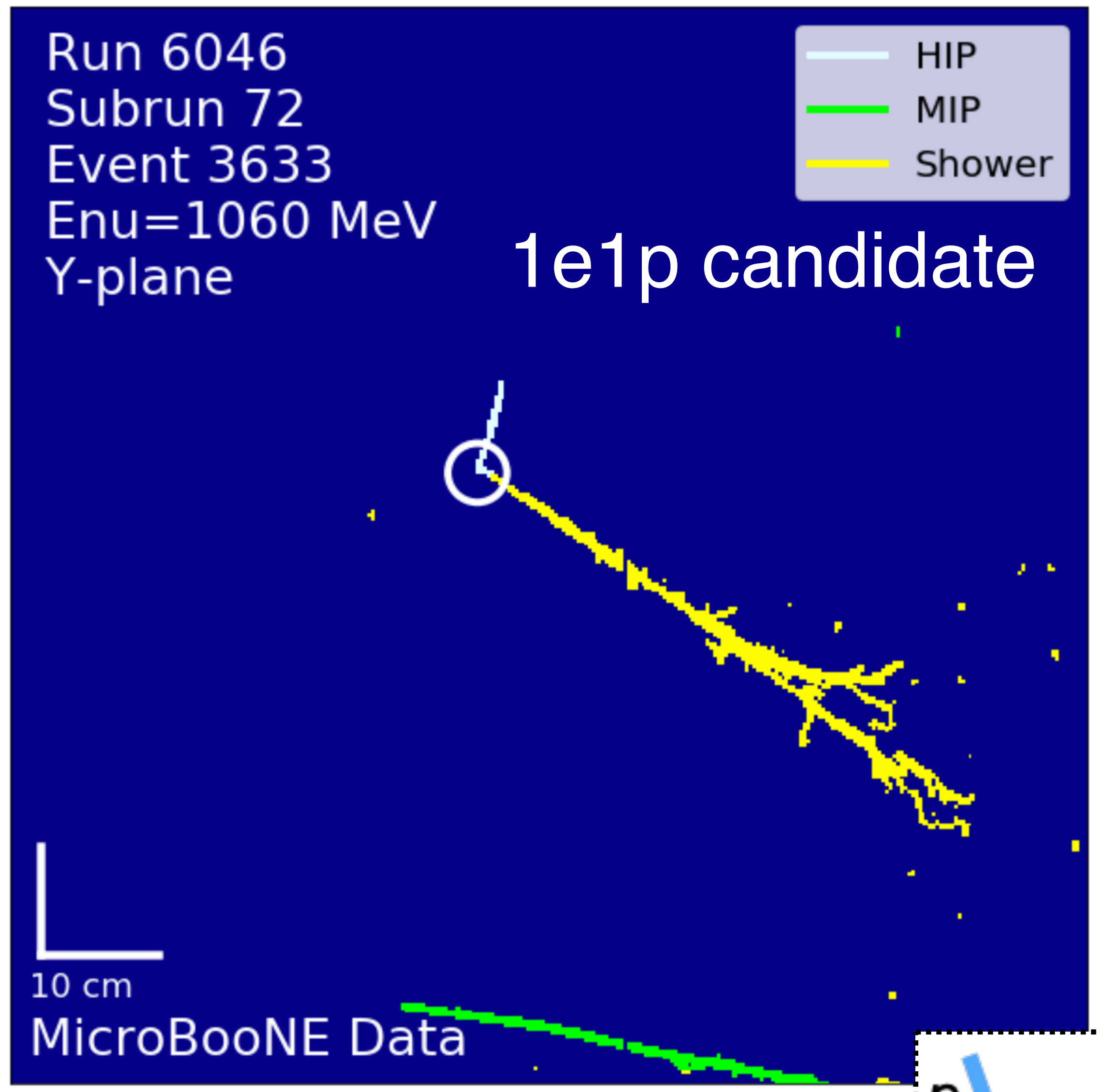

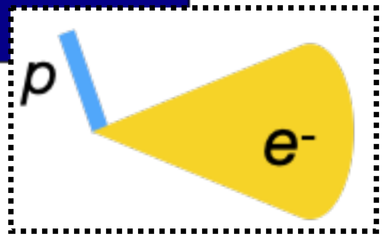

arXiv:2110.14080

CCQE: 1e1p

Dominant interaction at low energies. Leverage image-based reconstruction, including DeepLearning tools

PRD 103, 052012 (2021)

Search for an Excess of Electron Neutrino Interactions

Three complementary analyses testing different final states and using different reconstruction tools

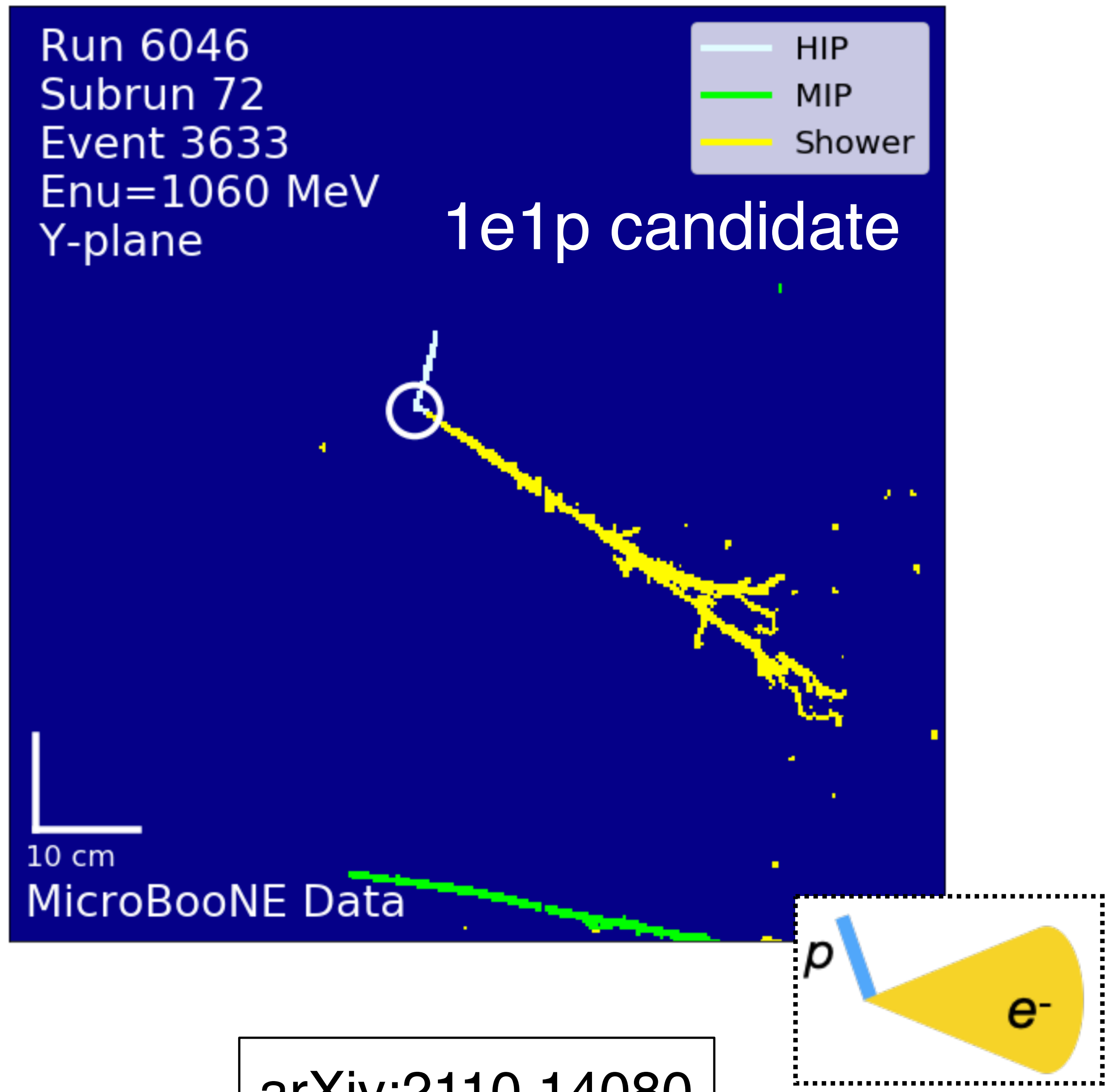

arXiv:2110.14080

CCQE: 1e1p

Dominant interaction at low energies.
Leverage image-based reconstruction, including DeepLearning tools

PRD 103, 052012 (2021)

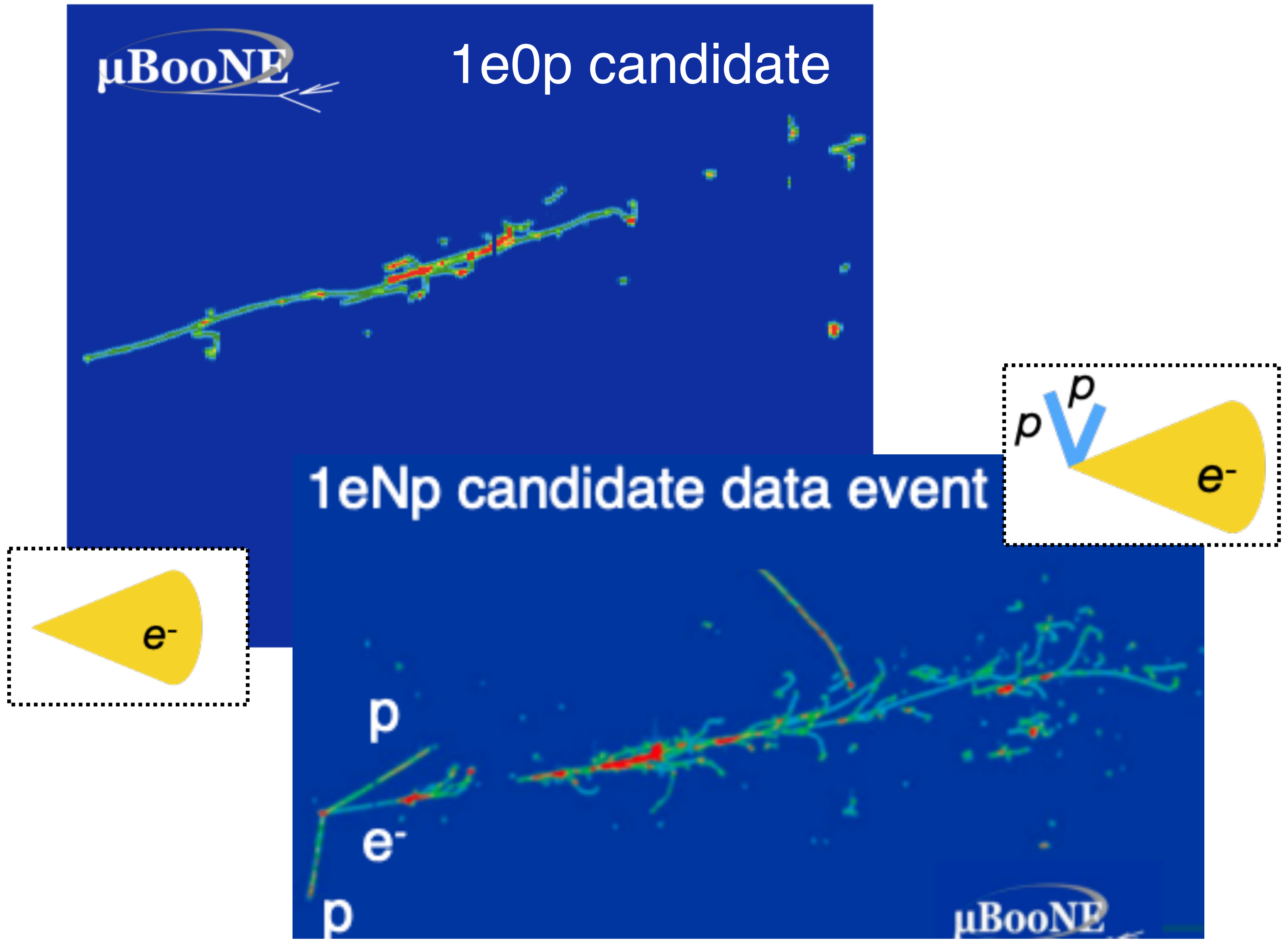

arXiv:2110.14065

Pionless: 1e0p + 1eNp

Match MiniBooNE signal definition.
Use hit-based reconstruction (2D→3D) based on Pandora toolkit

EPJC 78, 1, 82 (2018)

Search for an Excess of Electron Neutrino Interactions

Three complementary analyses testing different final states and using different reconstruction tools

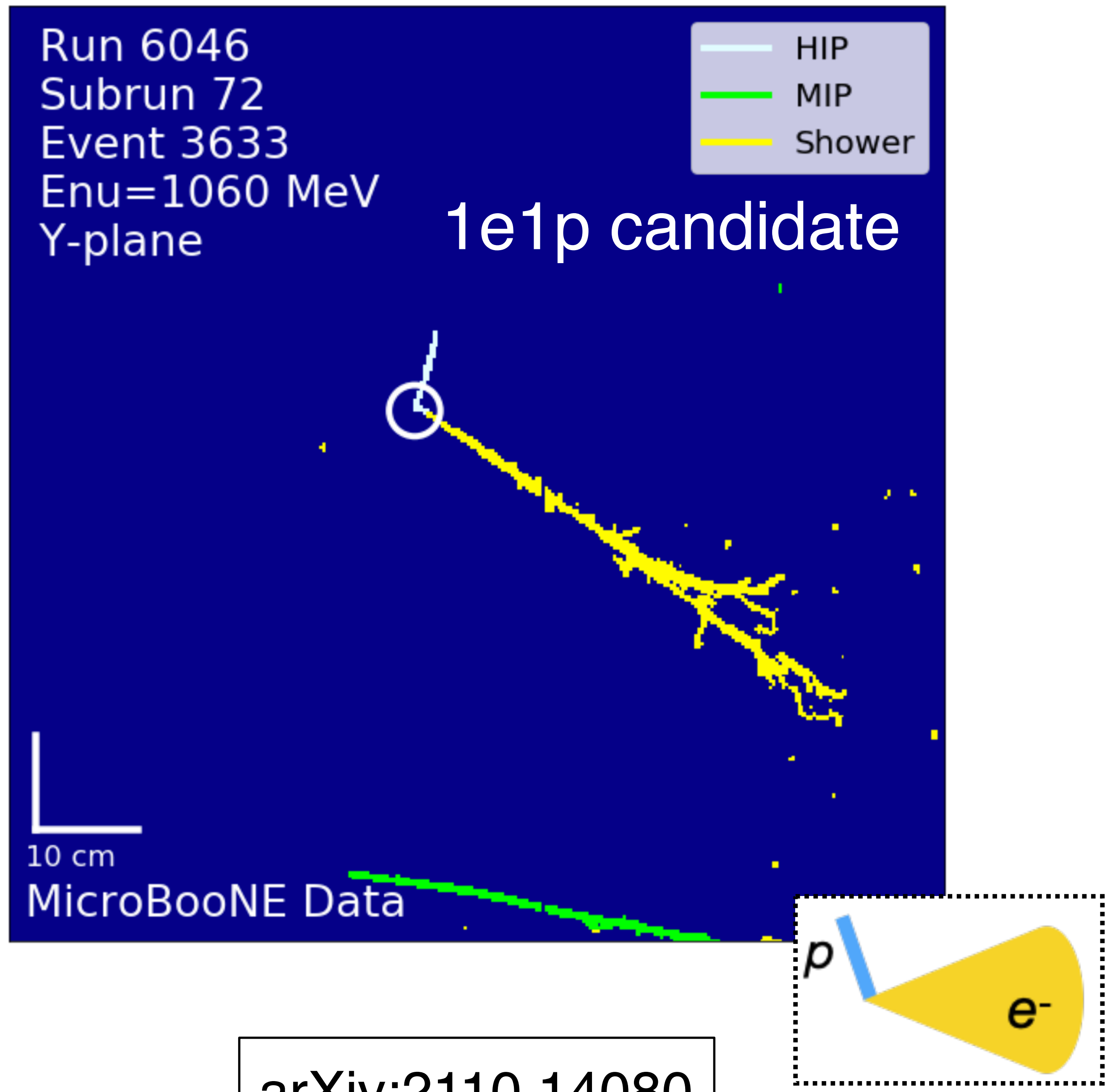

arXiv:2110.14080

CCQE: 1e1p

Dominant interaction at low energies.
Leverage image-based reconstruction, including DeepLearning tools

PRD 103, 052012 (2021)

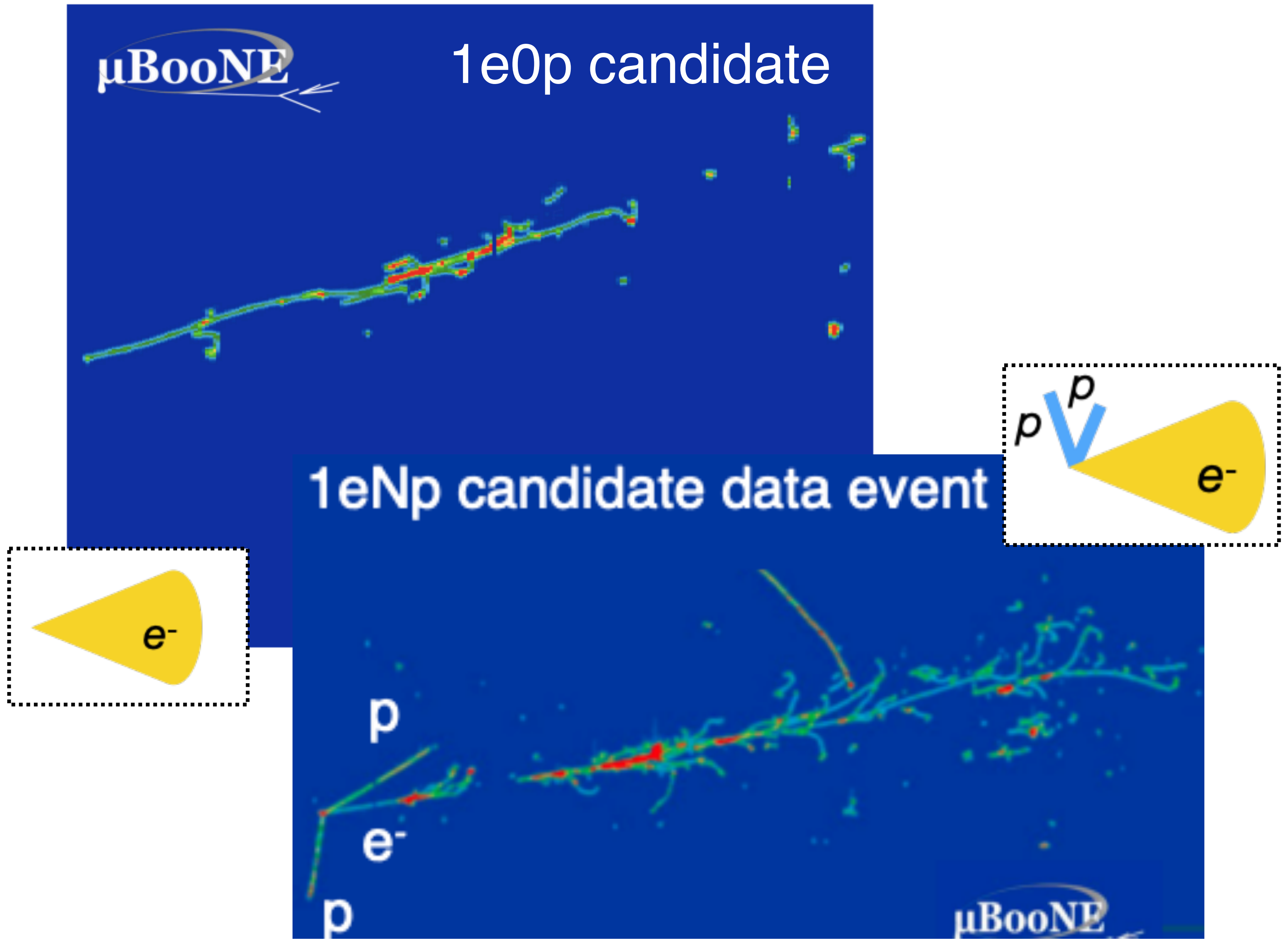

arXiv:2110.14065

Pionless: 1e0p + 1eNp

Match MiniBooNE signal definition.
Use hit-based reconstruction (2D→3D) based on Pandora toolkit

EPJC 78, 1, 82 (2018)

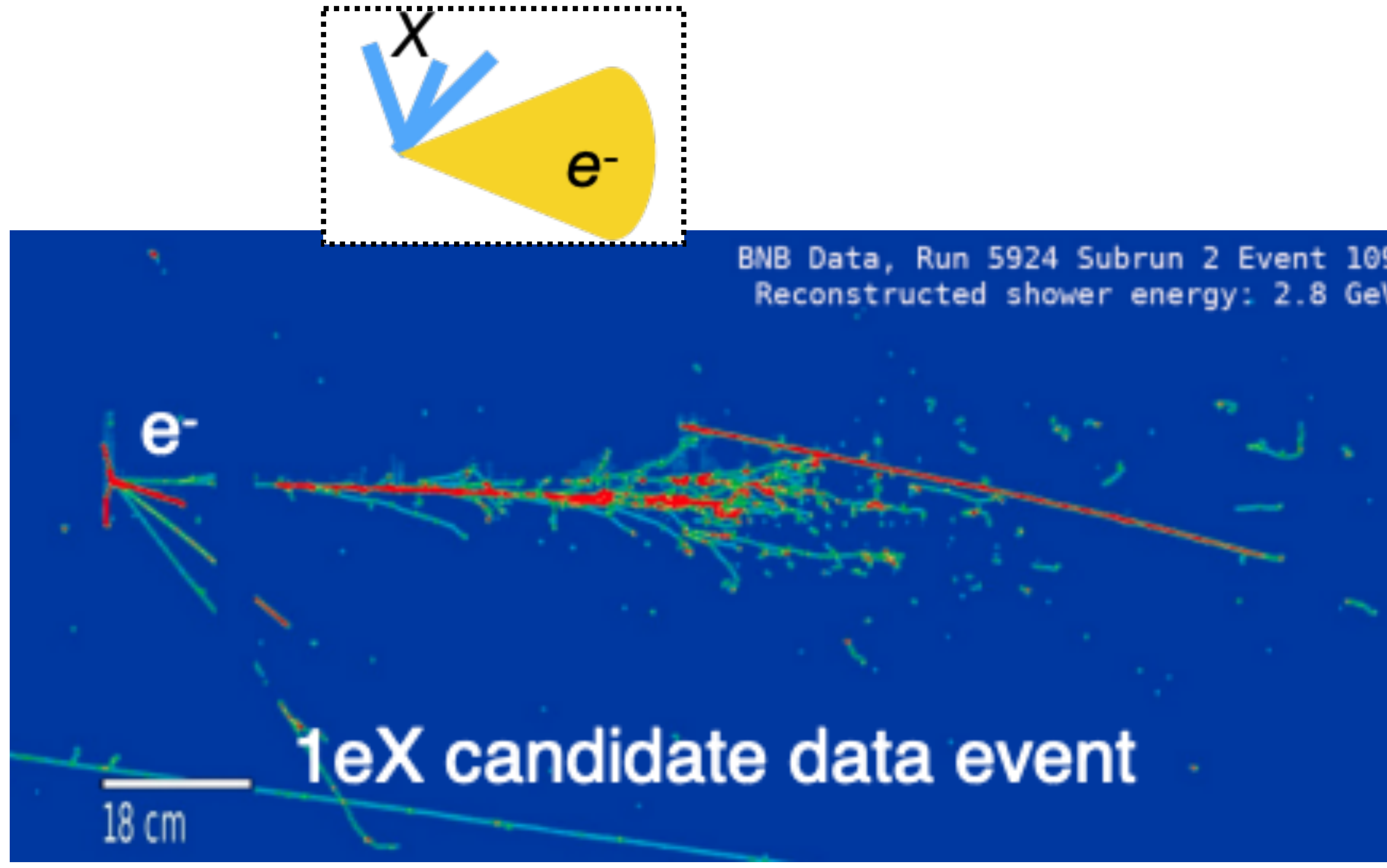

arXiv:2110.13978

Inclusive: 1eX

Largest statistics and sensitivity.
Use tomographic reconstruction, native 3D, based on Wire-Cell

JINST 17 (2022) P01037

Common Analysis Flow

(1) PRD 105 (2022) 7, 072001
(2) JINST 14, P04004 (2019)
(3) EPJC 79, 673 (2019)
(4) PRApp. 15, 064071 (2021)
(5) JINST 16 (2021) 12, T12017
(6) JINST 15, P02007 (2020)
(7) PRD 103, 092003 (2021)
(8) JHEP 12 (2021) 153
(9) EPJC 82 (2022) 5, 454
(10) JINST 16, P09025 (2021)
(11) JINST 15, P12037 (2020)

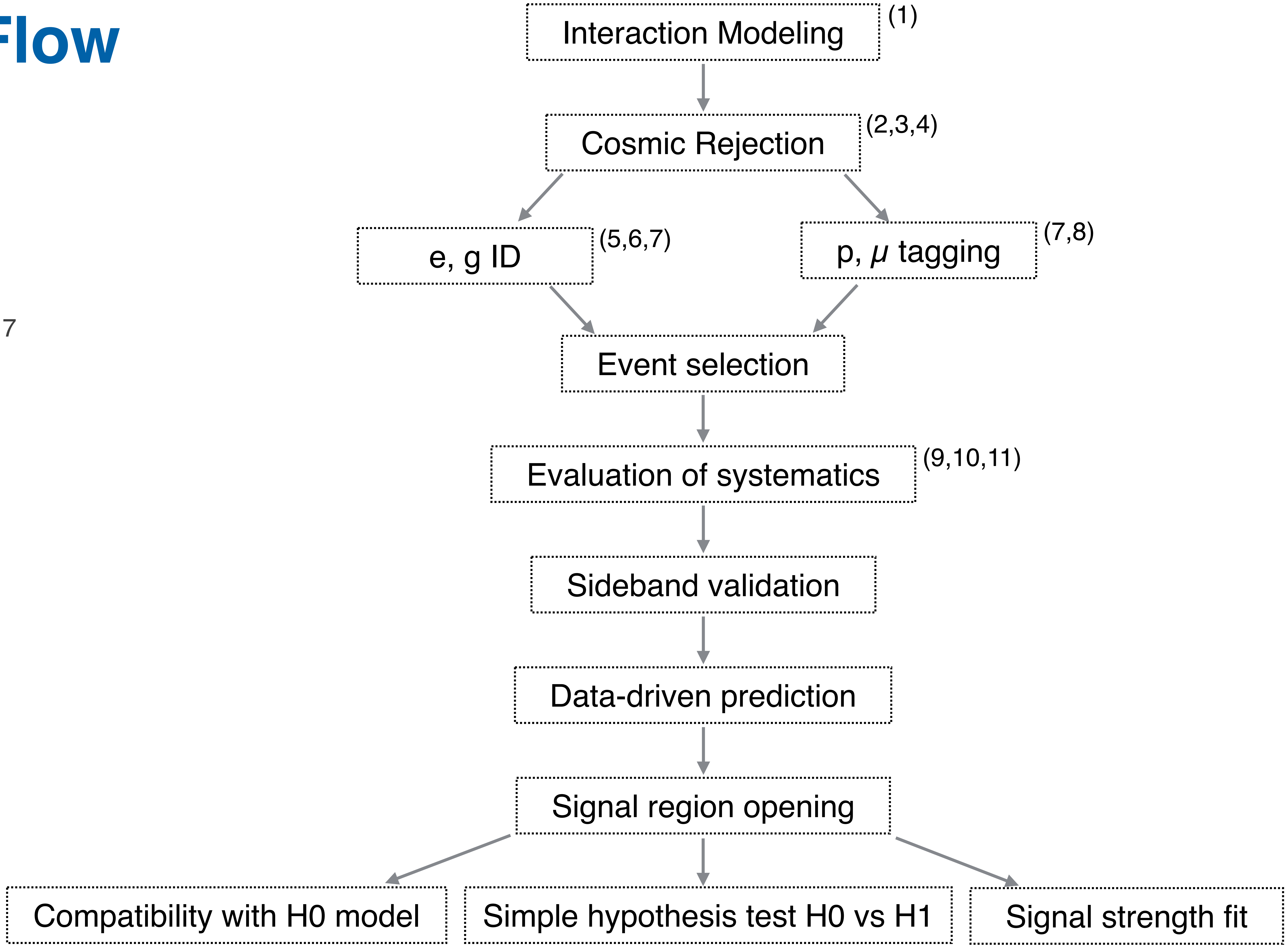

Common Analysis Flow

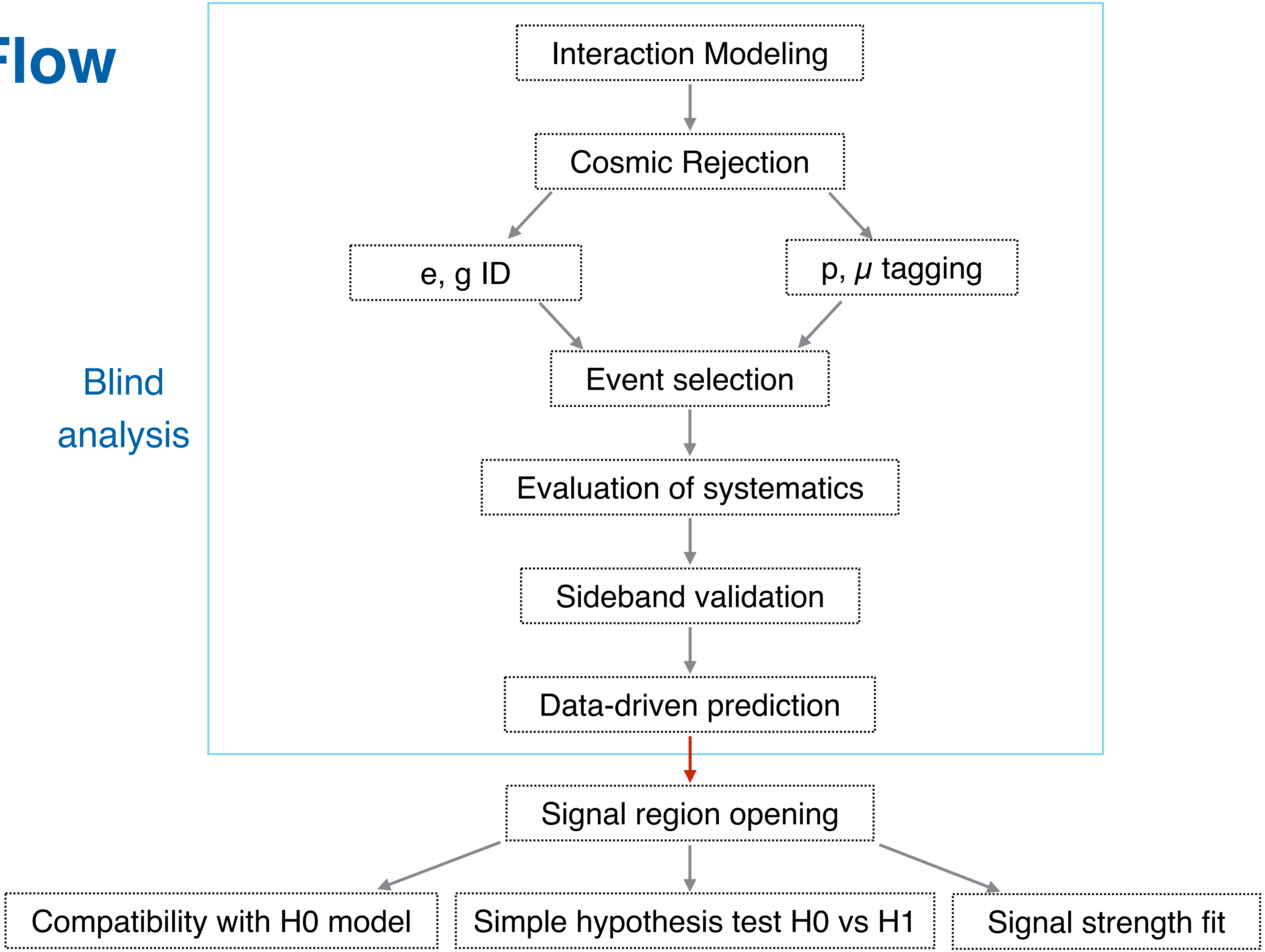

Common Strategy: data-driven prediction

- Correlations between ν_μ and ν_e events due to flux parentage and interaction
- Prediction from nominal modeling is "corrected" using ν_μ data, based on covariance matrix formalism

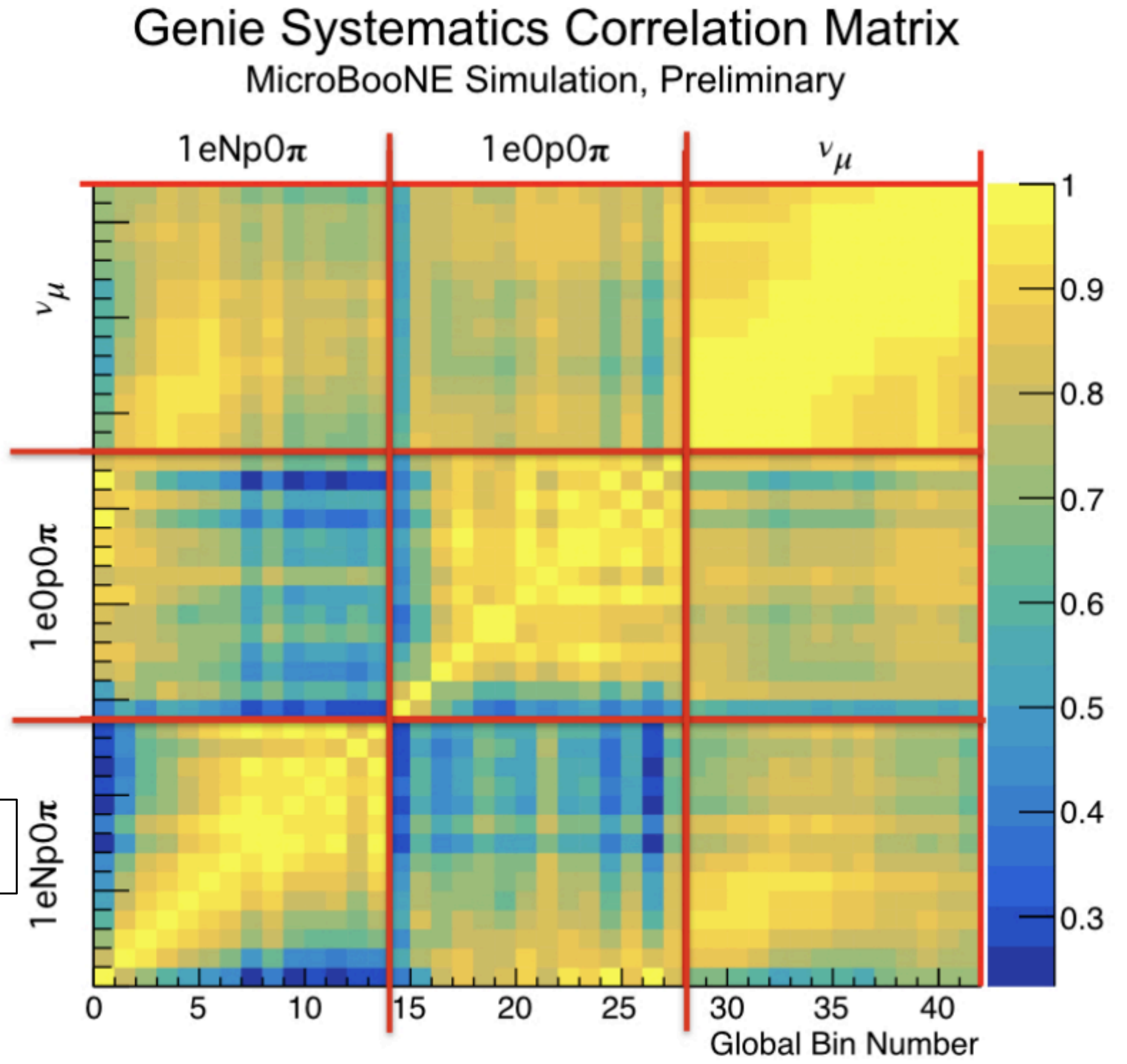

MICROBOONE-NOTE-1085

arXiv:2110.14065

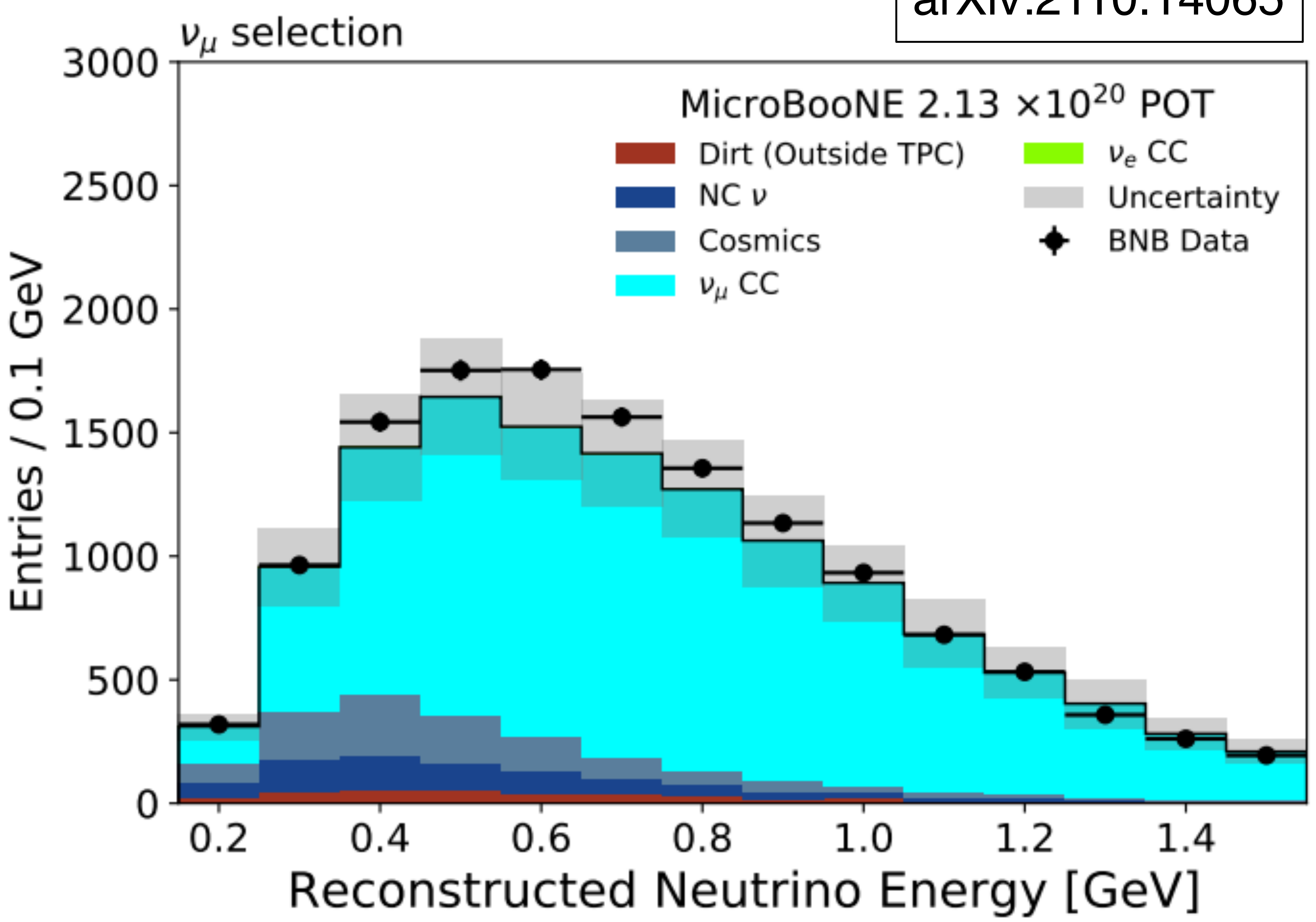

Fermilab

Common Strategy: data-driven prediction

- Correlations between ν_μ and ν_e events due to flux parentage and interaction
- Prediction from nominal modeling is "corrected" using ν_μ data, based on covariance matrix formalism
- The prediction is updated in two aspects: the central value and the systematics
  - systematics are significantly reduced thanks to the in-situ measurement

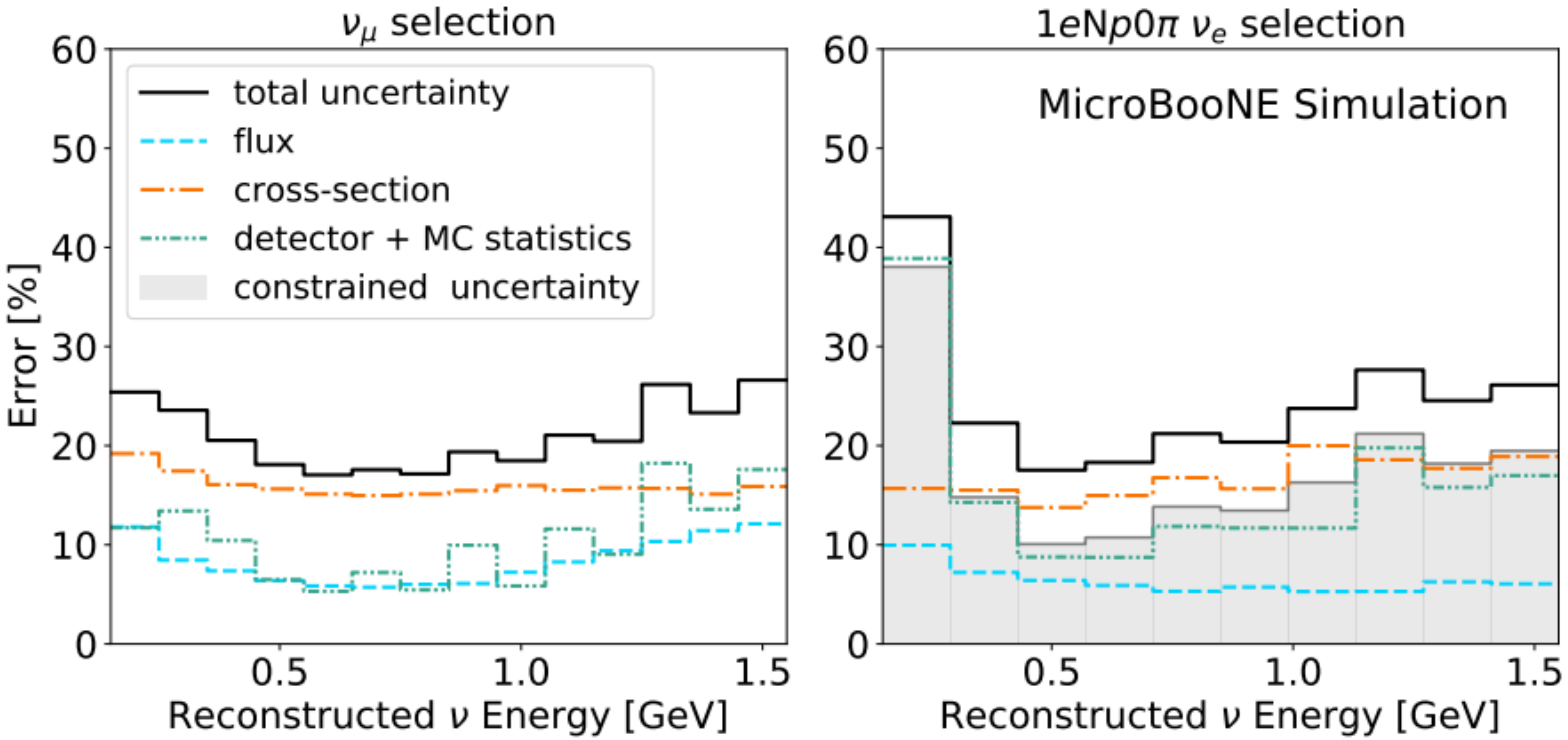

arXiv:2110.14065

Common Strategy: Blind Analysis and Sideband Validations

arXiv:2110.14065

- Signal region was kept blind until the last stage of the analysis to avoid bias
- Reconstruction and analysis developed on small-size (<1/10) open dataset
- Validated in high statistics control regions
  - e.g. π^0 mass peak for shower energy scale
- Unique validation dataset given by ν_e events from NuMI beam (off-axis)

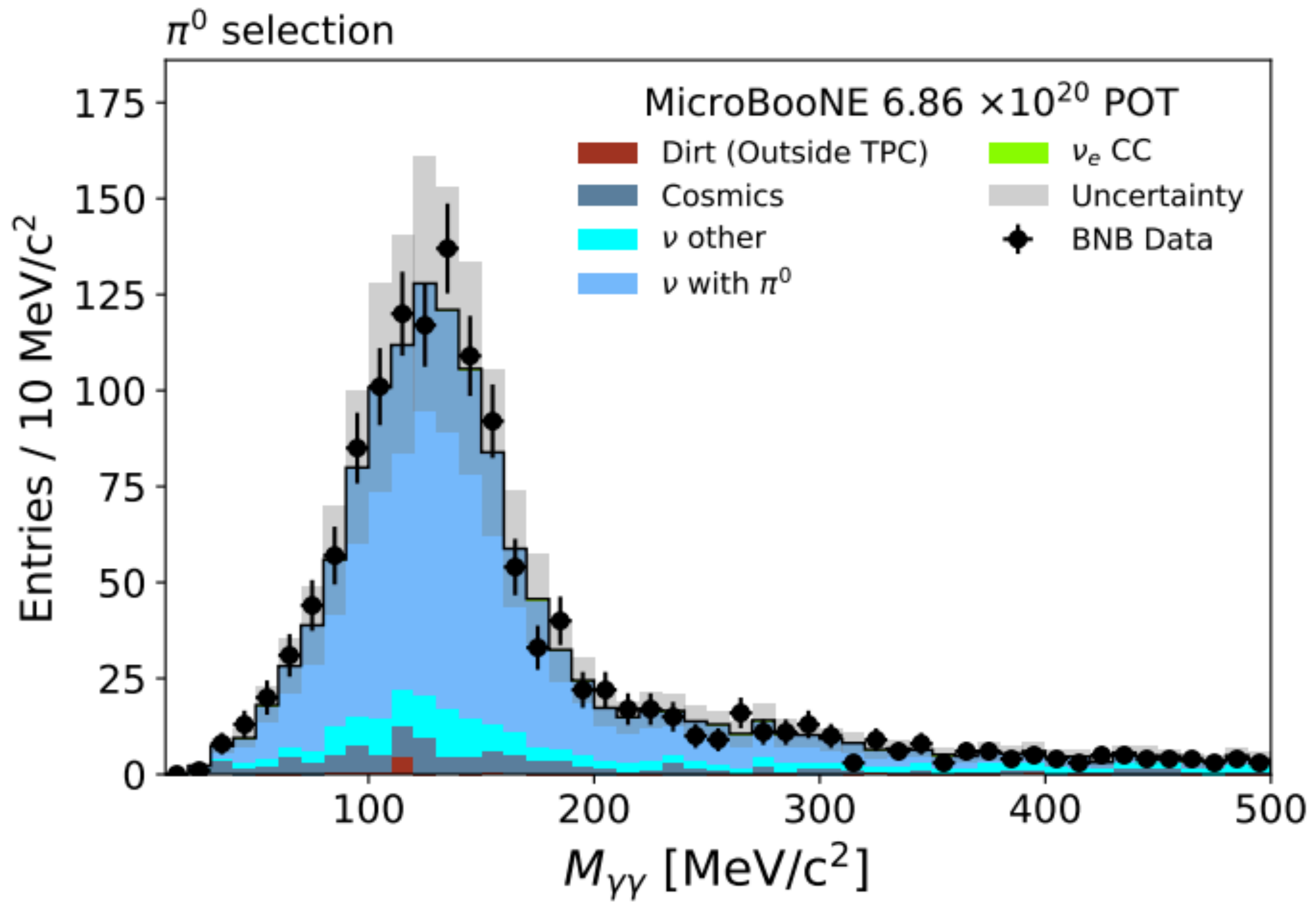

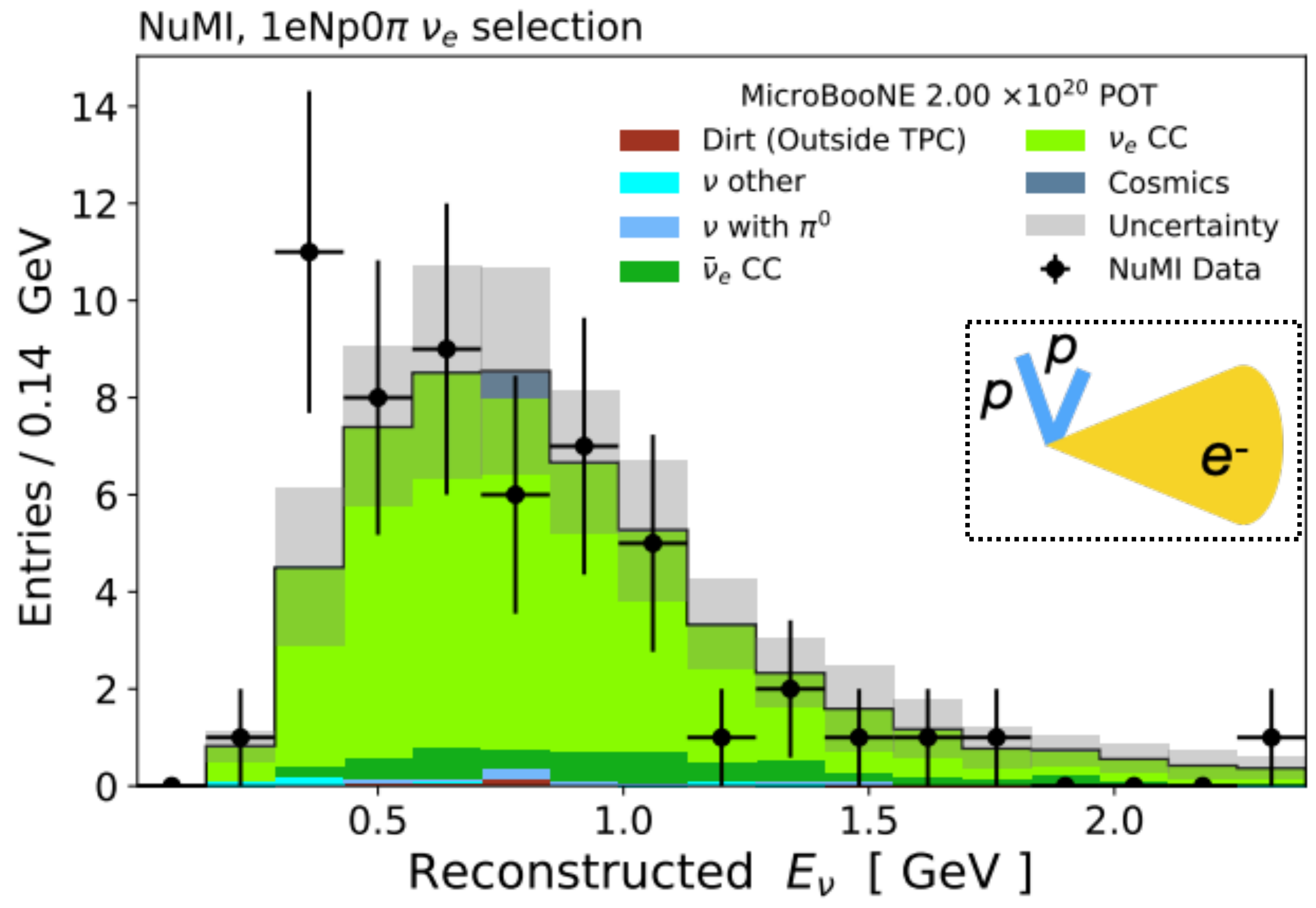

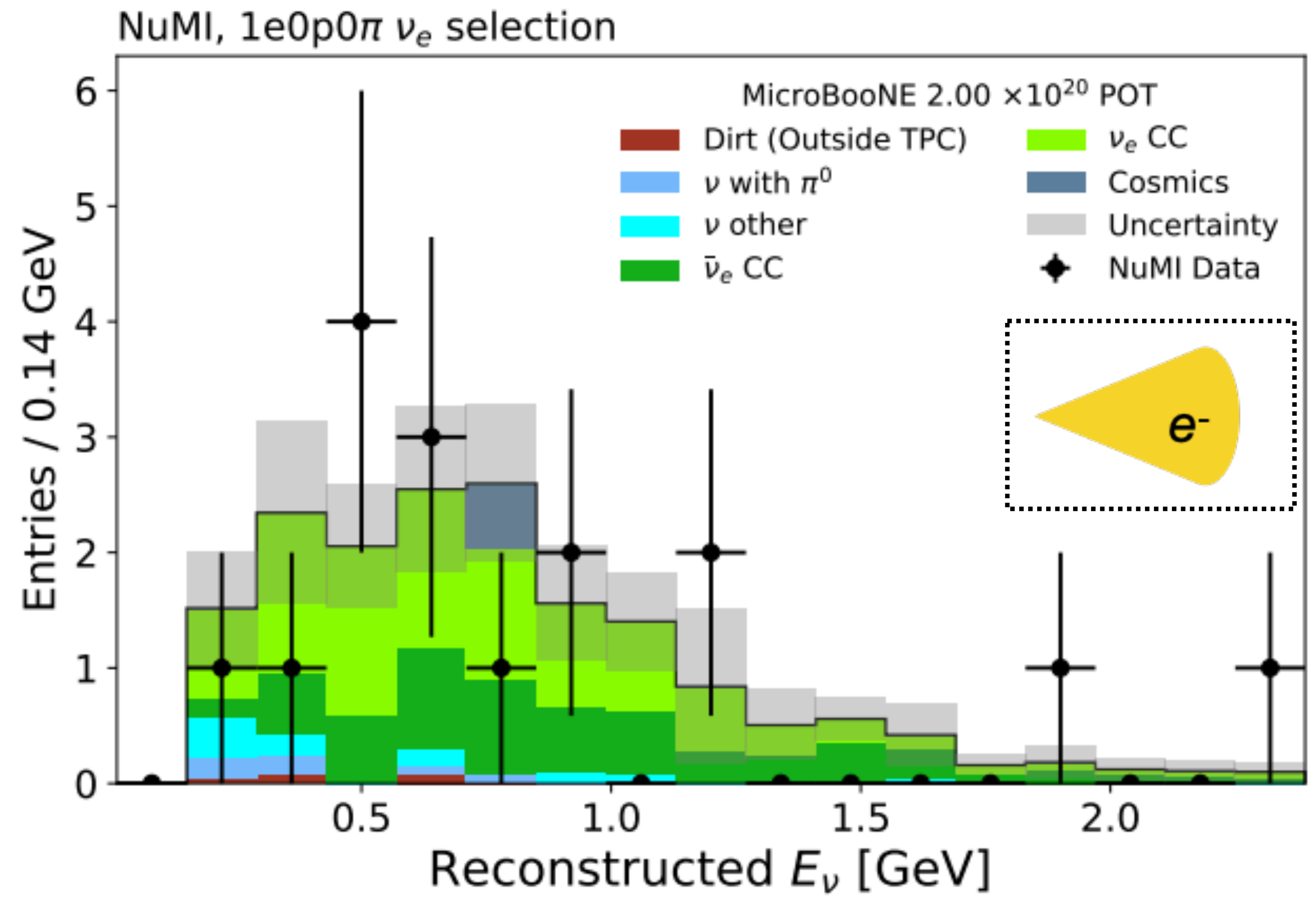

Results: nominal (no excess) ν_e model prediction

- Unblinded data is fitted in pre-defined intervals, is found to be in agreement with ν_e model prediction
  - frequentist p-values are extracted for the energy spectrum:
    - CCQE 1e1p: 0.014
    - 1eNp0π, 1e0p0π: 0.18, 0.13
    - 1eX: 0.85
  - also looked at kinematic variables, confirming good agreement

arXiv:2110.14080

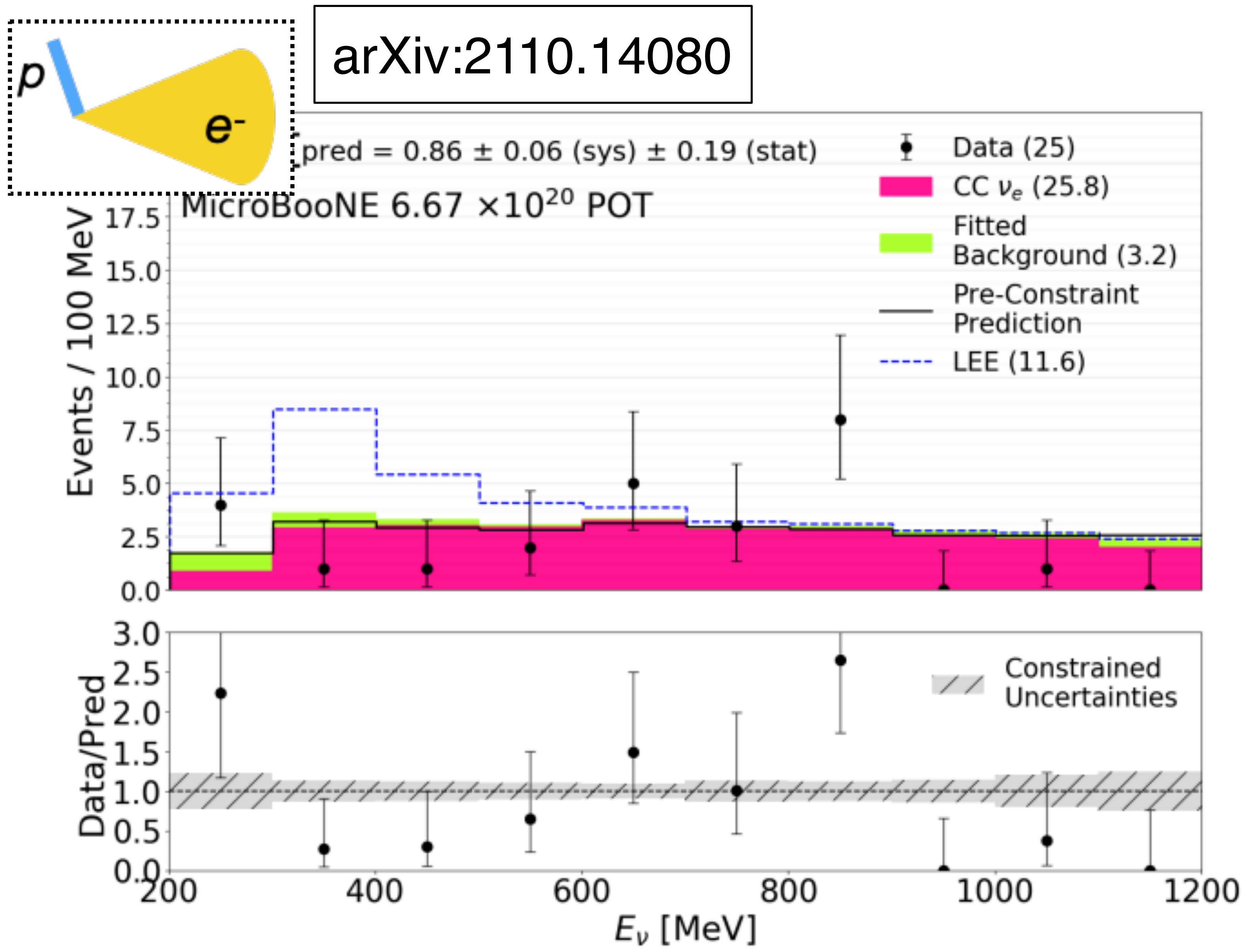

arXiv:2110.14065

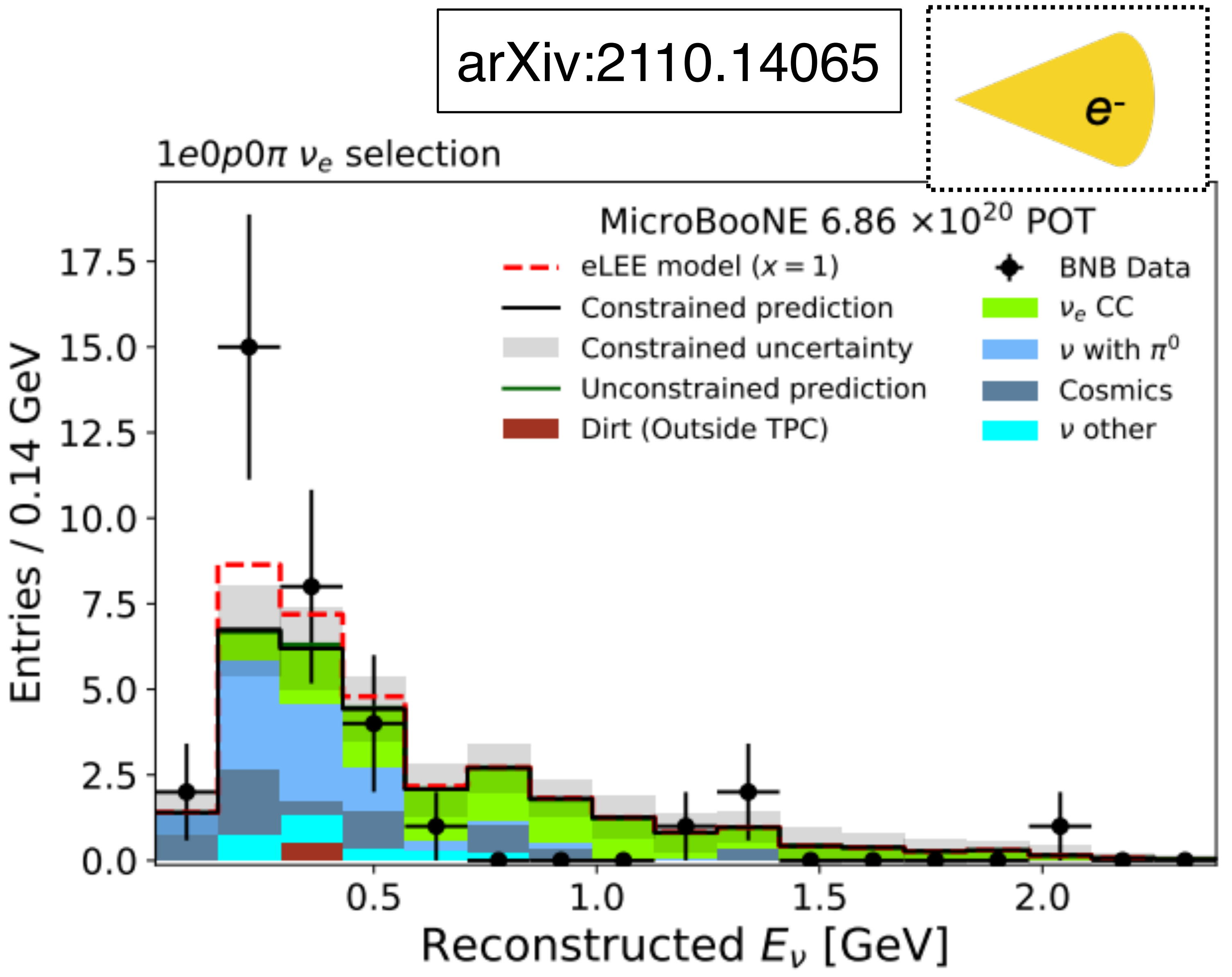

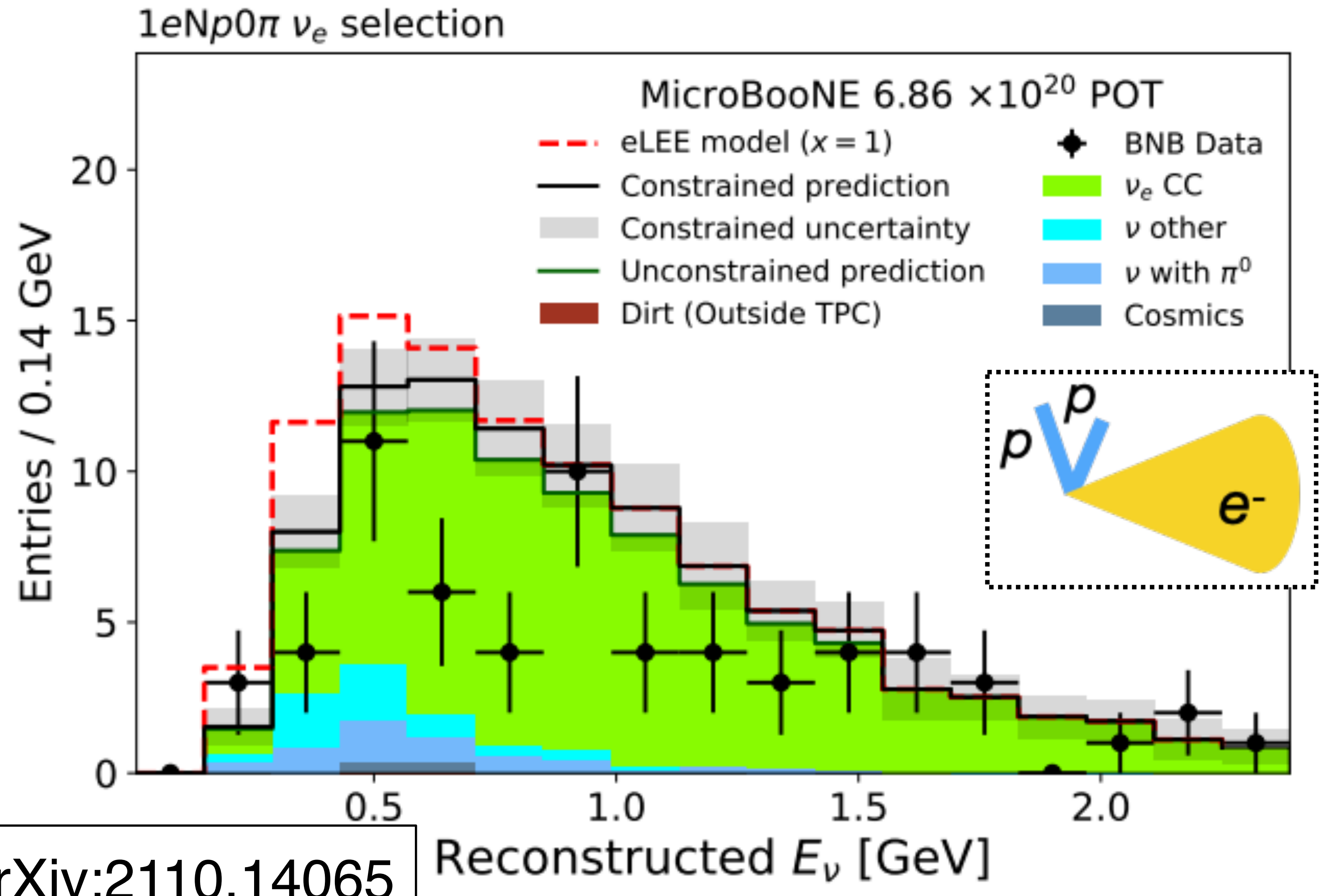

arXiv:2110.14065

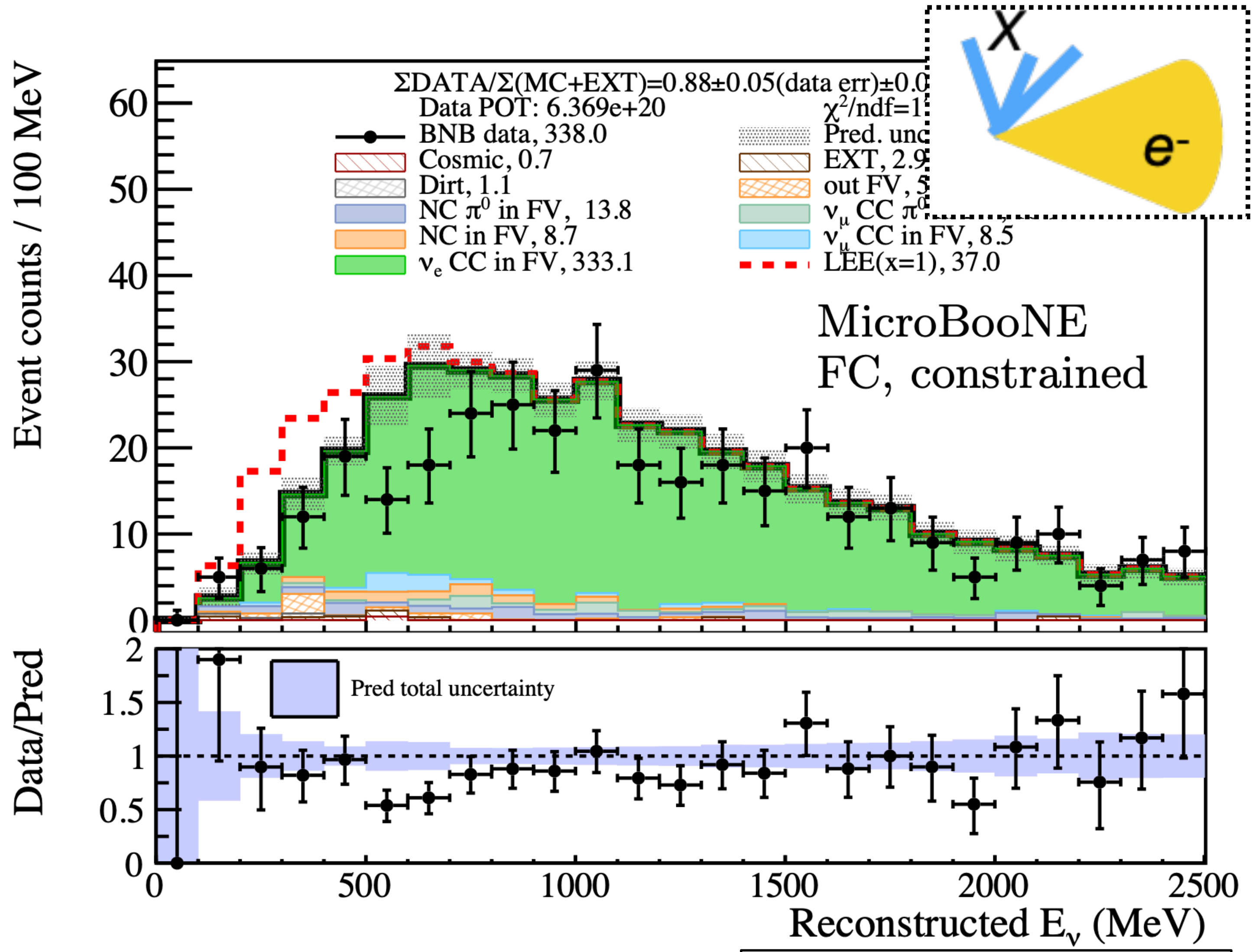

arXiv:2110.13978

arXiv:2110.14054

Results: limits on the eLEE model

- We reject our eLEE model (H1) at >97% CL for all high purity selections
  - including both exclusive (1e1p CCQE, 1eNp0π) and inclusive (1eX) event classes
  - signal strength fit with Feldman Cousins procedure consistent with μ=0

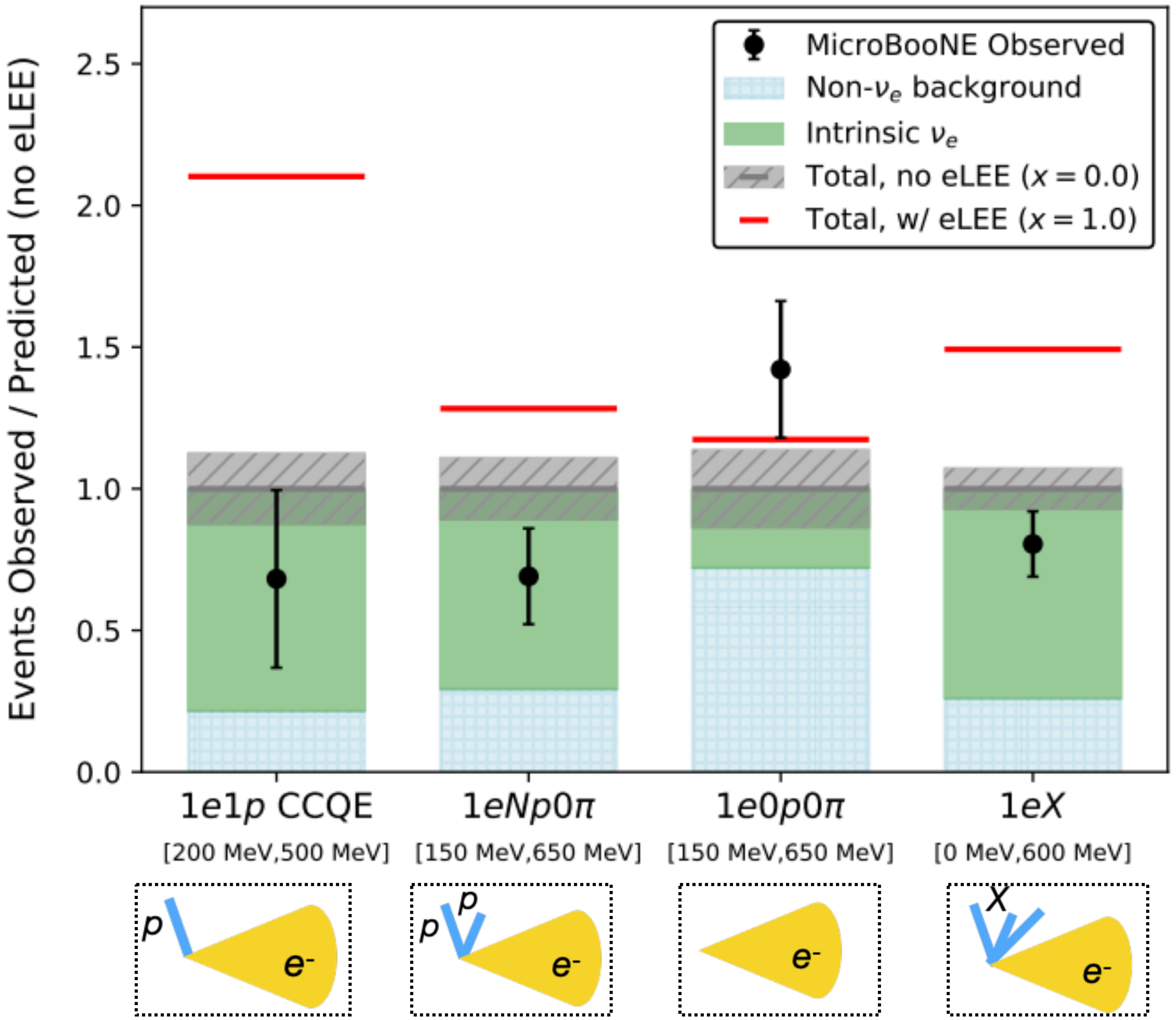

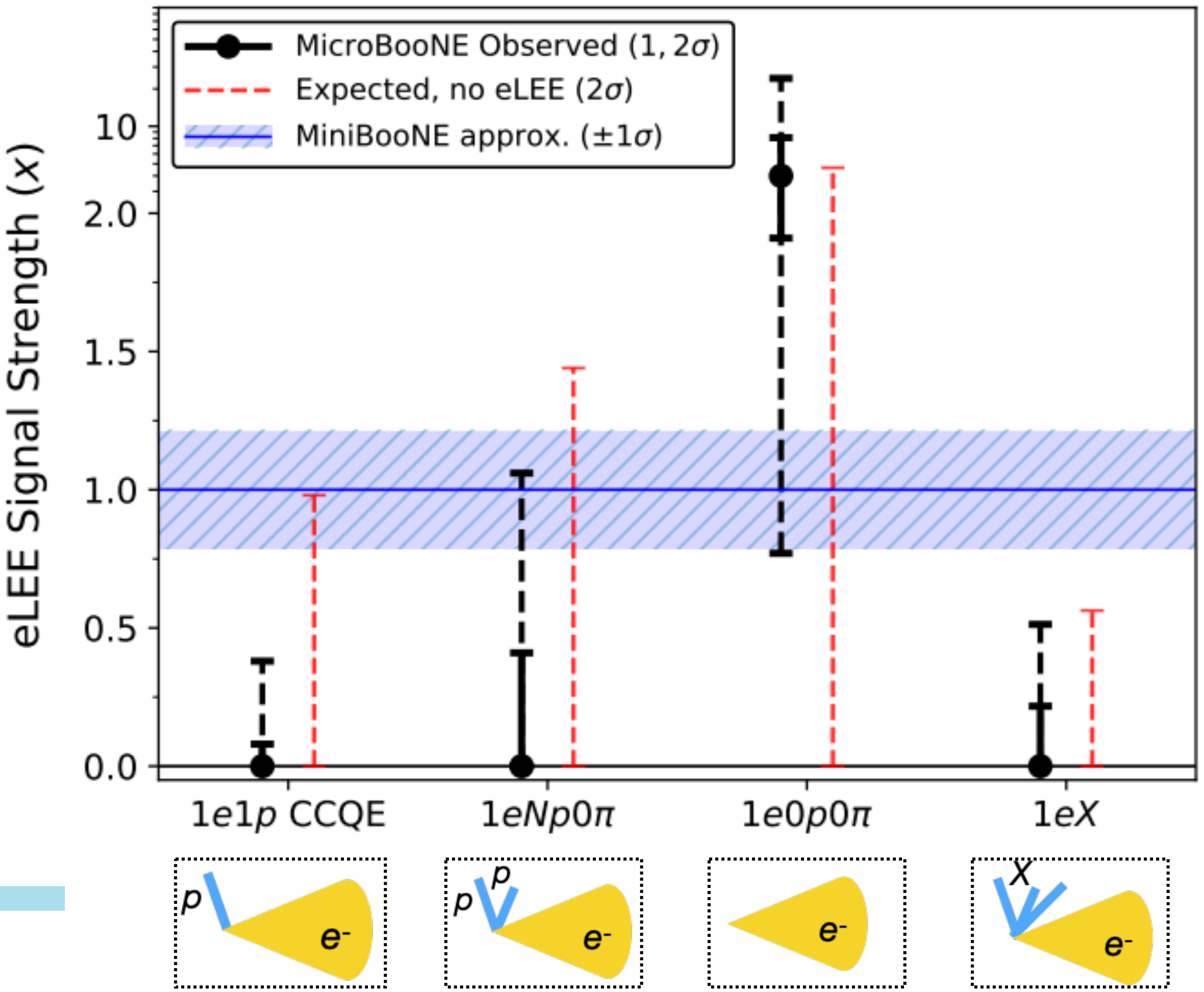

Evolution of LEE analyses

MicroBooNE's first series of LEE search results

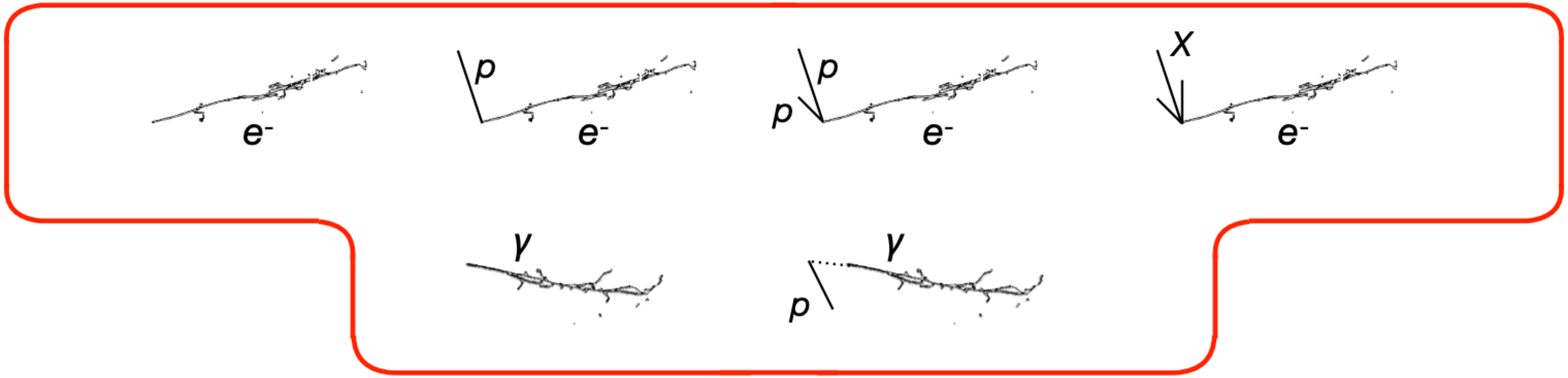

- Investigated if the MiniBooNE excess originates from ν_e or NC $\Delta \rightarrow \gamma$ events
- No evidence for excesses relative to prediction for both processes

Fermilab

Evolution of LEE analyses

MicroBooNE's first series of LEE search results

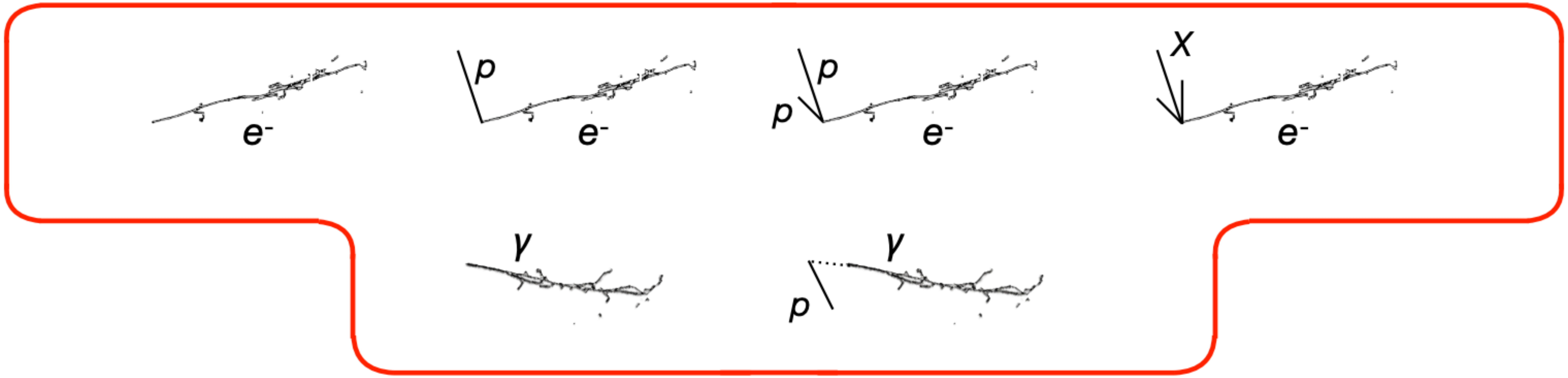

- Investigated if the MiniBooNE excess originates from ν_e or NC $\Delta \rightarrow \gamma$ events
- No evidence for excesses relative to prediction for both processes
- Further steps include:
  - New interpretations of results in terms of oscillations or cross section
  - Search for different BSM explanations for the MB LEE

First results at Nu22 next week!

Topologies compatible with the MiniBooNE excess

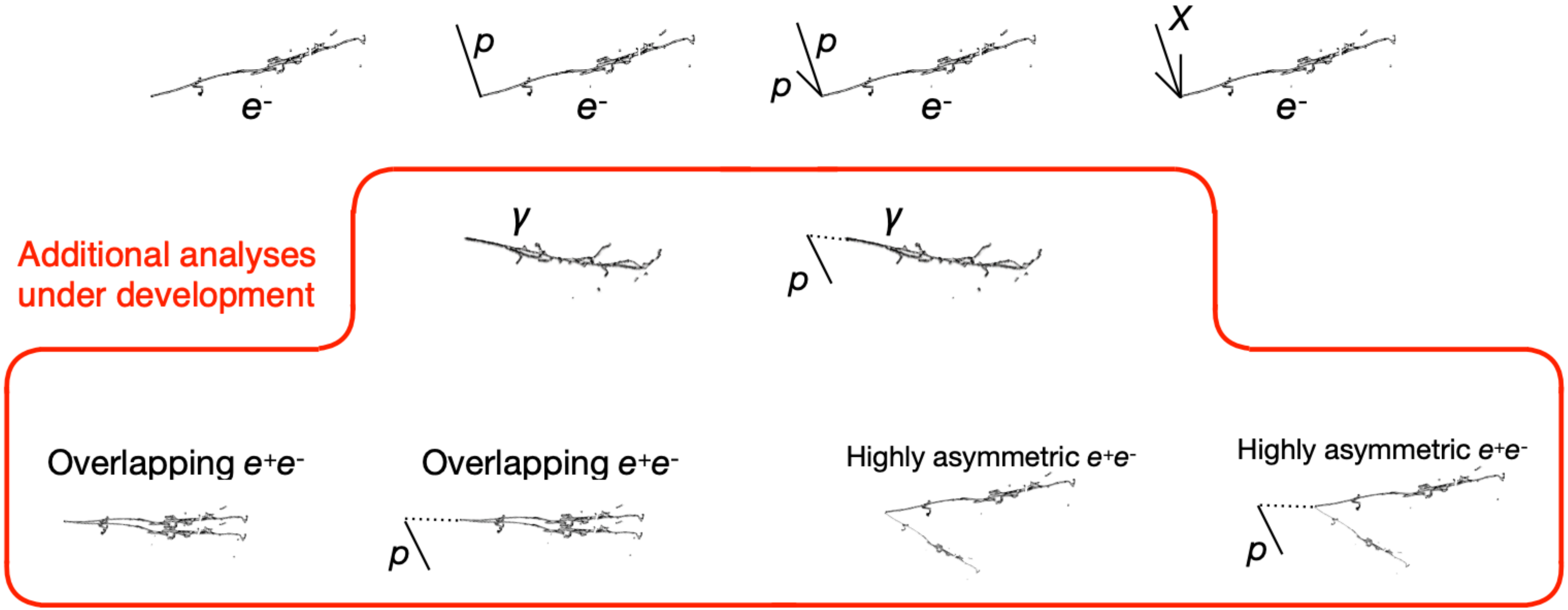

Rich set of BSM models can explain the MiniBooNE excess

- Decay of O(keV) Sterile Neutrinos to active neutrinos
  - *[13] Dentler, Esteban, Kopp, Machado Phys. Rev. D 101, 115013 (2020)*
  - *[14] de Gouvêa, Peres, Prakash, Stenico JHEP 07 (2020) 141*
- New resonance matter effects
  - *[5] Asaadi, Church, Guenette, Jones, Szelc, PRD 97, 075021 (2018)*
  - *[16] Alves, Louis, deNiverville, [hep-ph]2201.00876 (2022)*
- Mixed O(1eV) sterile oscillations and O(100 MeV) sterile decay
  - *[7]Vergani, Kamp, Diaz, Arguelles, Conrad, Shaevitz, Uchida, arXiv:2105.06470*
- Decay of heavy sterile neutrinos produced in beam
  - *[4] Gninenko, Phys.Rev.D83:015015,2011*
  - *[12] Alvarez-Ruso, Saul-Sala, Phys. Rev. D 101, 075045 (2020)*
  - *[15] Magill, Plestid, Pospelov, Tsai Phys. Rev. D 98, 115015 (2018)*
  - *[11] Fischer, Hernandez-Cabezudo, Schwetz, PRD 101, 075045 (2020)*
  - *[17] Dutta, Kim, Thompson, Thornton, Van de Water [hep-ph]2110.11944*
- Decay of upscattered heavy sterile neutrinos or new scalars mediated by Z' or more complex higgs sectors
  - *[1] Bertuzzo, Jana, Machado, Zukanovich Funchal, PRL 121, 241801 (2018)*
  - *[2] Abdullahi, Hostert, Pascoli, Phys.Lett.B 820 (2021) 136531*
  - *[3] Ballett, Pascoli, Ross-Lonergan, PRD 99, 071701 (2019)*
  - *[10] Dutta, Ghosh, Li, PRD 102, 055017 (2020)*
  - *[6] Abdallah, Gandhi, Roy,Phys. Rev. D 104, 055028 (2021)*
- Decay of axion-like particles
  - *[8] Chang, Chen, Ho, Tseng, Phys. Rev. D 104, 015030 (2021)*
- A model-independent approach to any new particle
  - *[9] Brdar, Fischer, Smirnov, PRD 103, 075008 (2021)*

Produces True Electrons

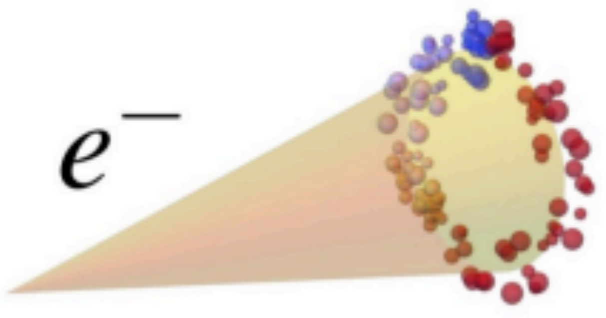

Produces True Photons

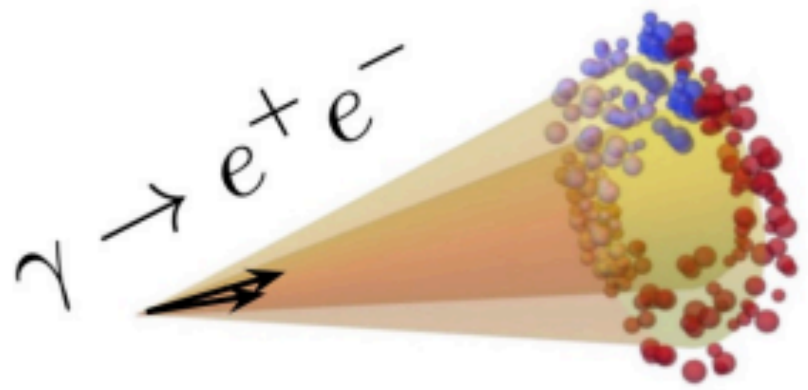

Produces e^+e^- pairs

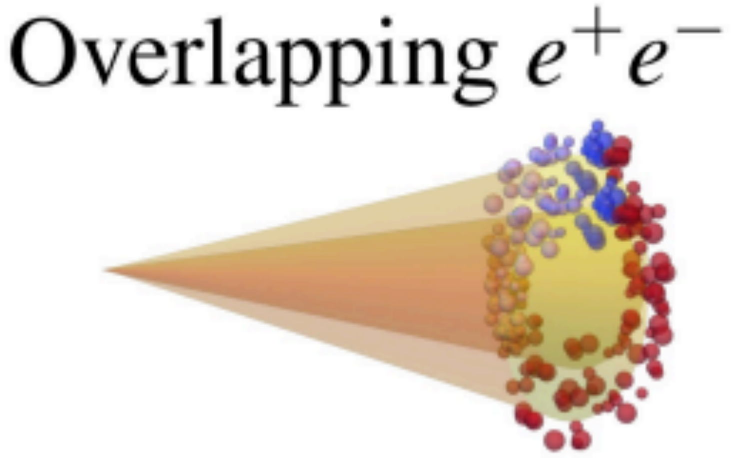

Leverage the power of LArTPC technology to distinguish between models based on exclusive final state topologies!

Fermilab

A couple of examples

PRL121, 241801

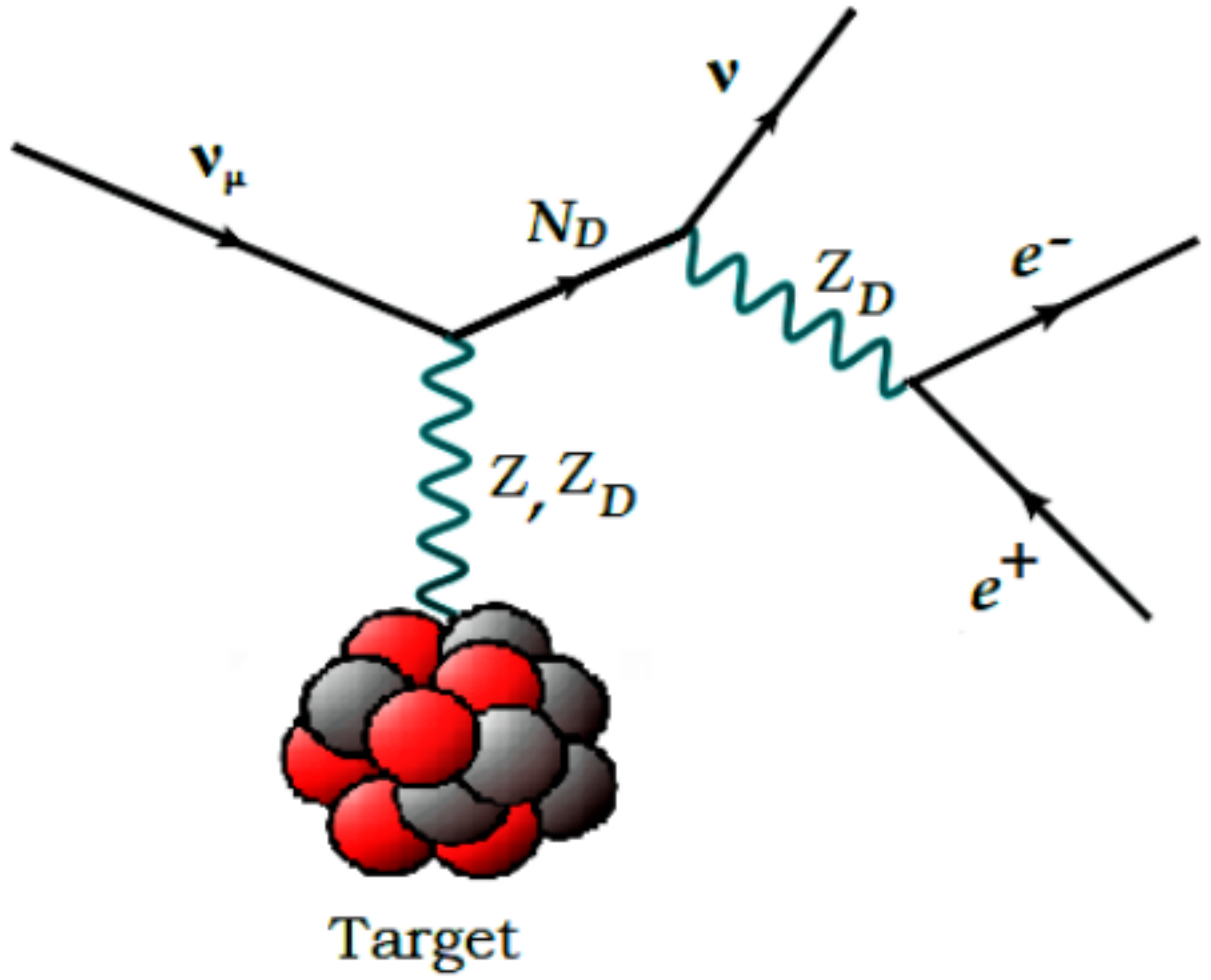

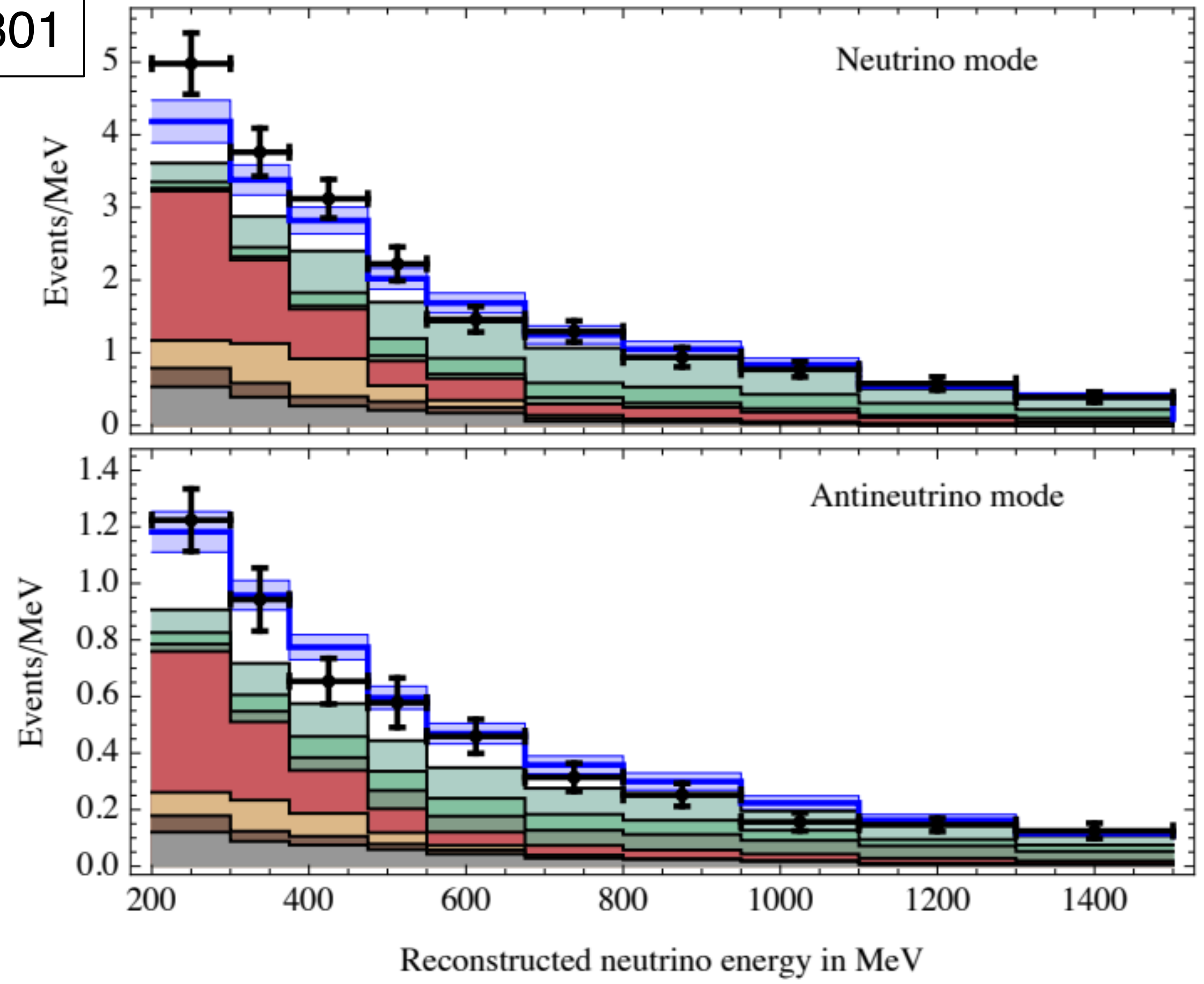

- Dark neutrino portal
  - with dark Z' decay
  - could explain MiniBooNE: if e^+e^- resolved as single shower

- Dark matter produced in beamline
  - scattering off argon

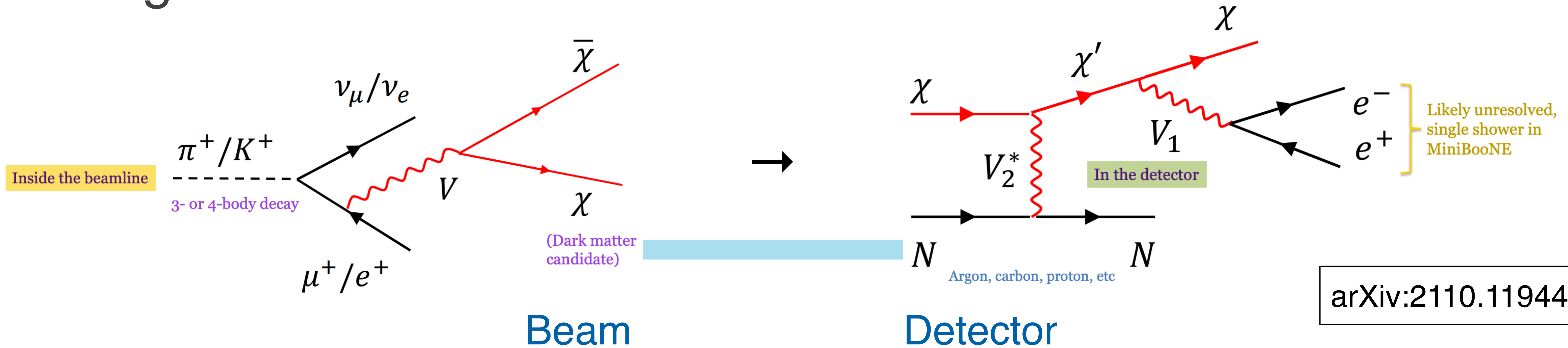

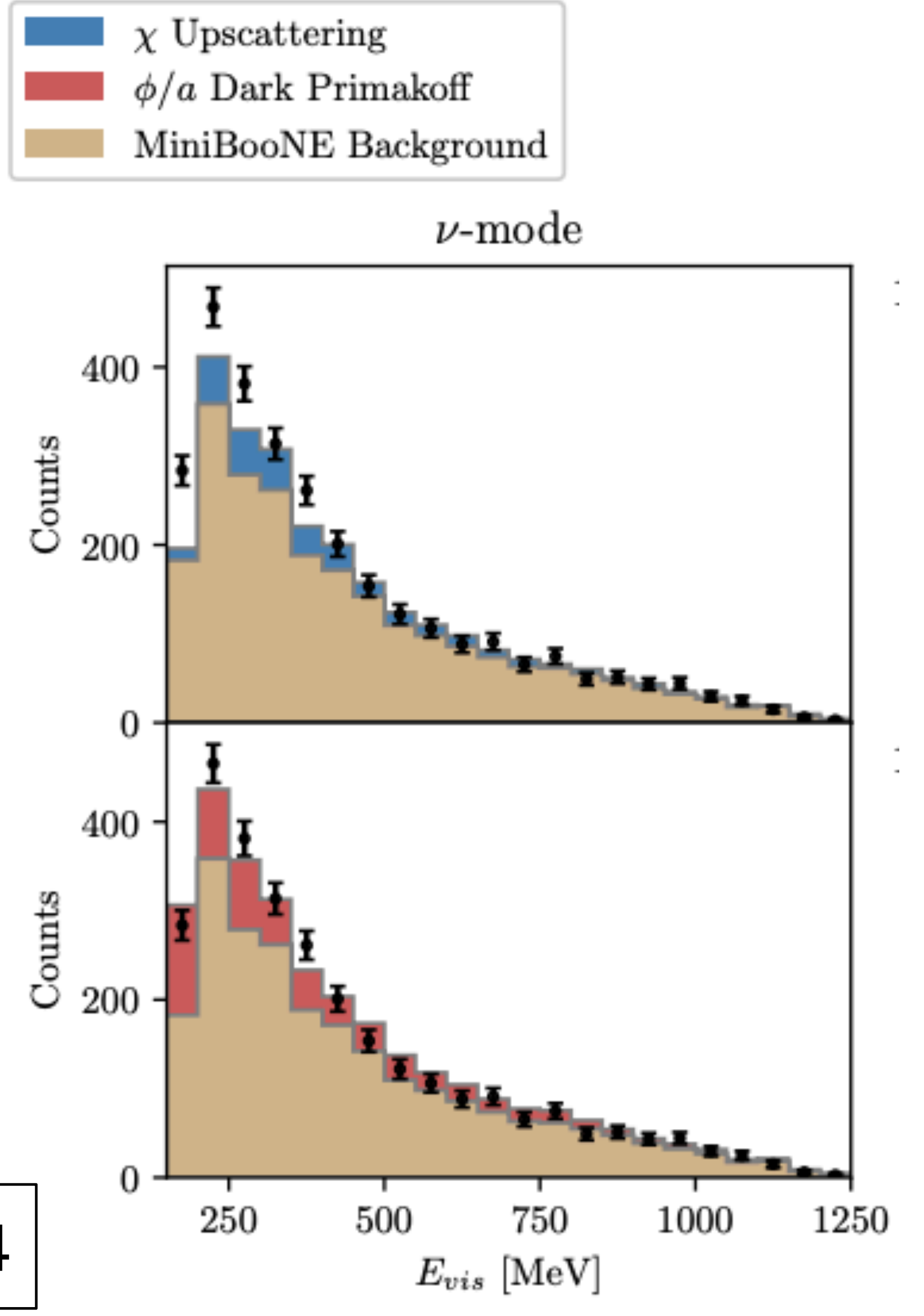

arXiv:2110.11944

BSM Searches in uB: e^+e^-

- MicroBooNE has been producing a rich set of BSM searches, including
  - heavy neutral leptons, n-nbar oscillations, supernovae ν reconstruction, Higgs portal scalars

PRD 101, 052001 (2020) | MICROBOONE-NOTE-1113-PUB | JINST 16, P02008 (2021)

- The Higgs portal scalar search in particular pioneered e^+e^- searches in uB
  - "Portal" to the dark sector, via a dark scalar mixing with the Higgs
  - Kaons decaying to scalar particle in beam, then scalar decays to fermion pair in detector
  - Our first search uses kaons decaying at rest in the NuMI beam dump
  - Limits are competitive, extend exclusion in mixing vs mass parameter space
- Analyses in BNB data including unresolved e^+e^- pairs will be key to test further BSM interpretations of the MB excess

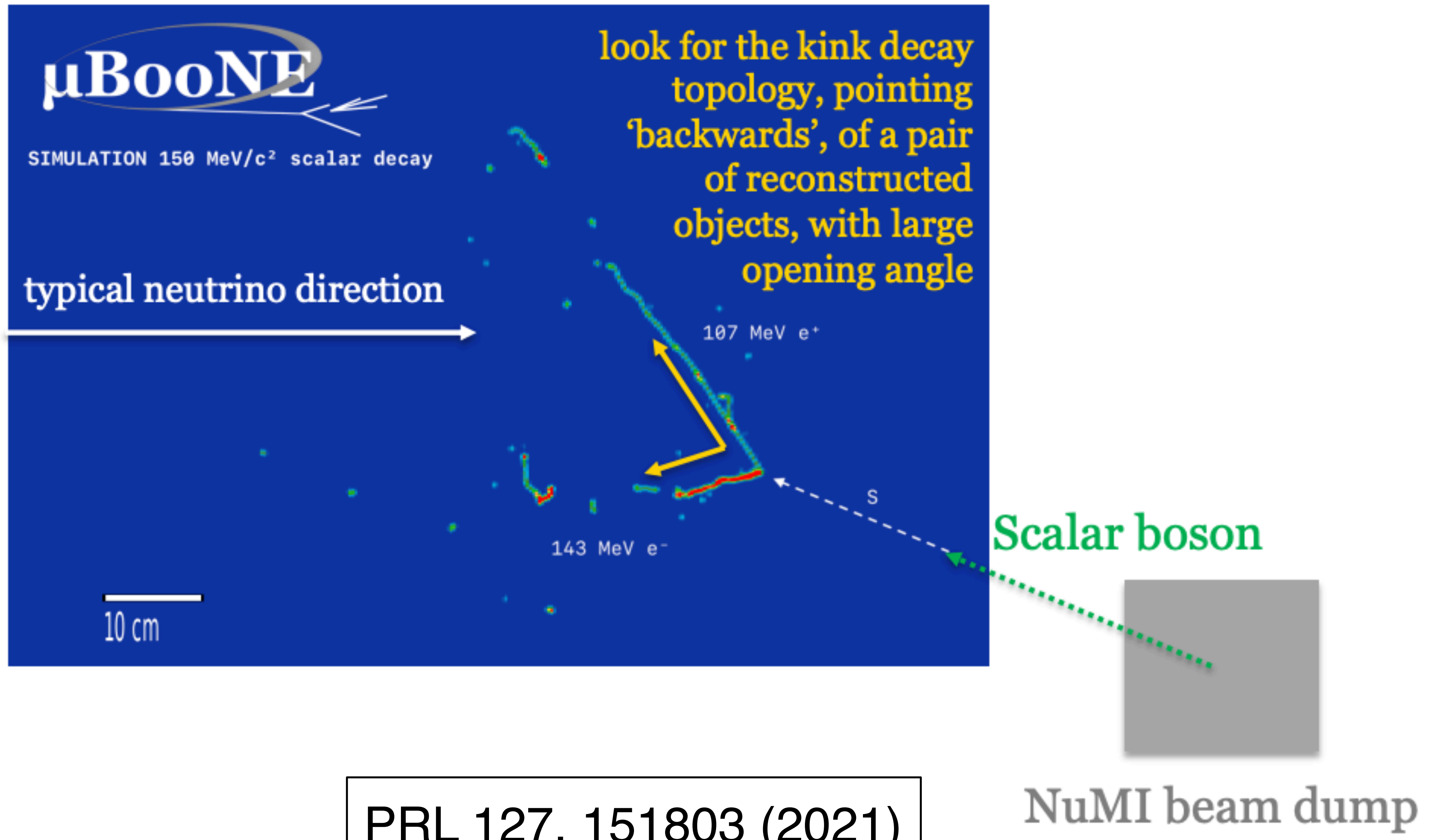

PRL 127, 151803 (2021)

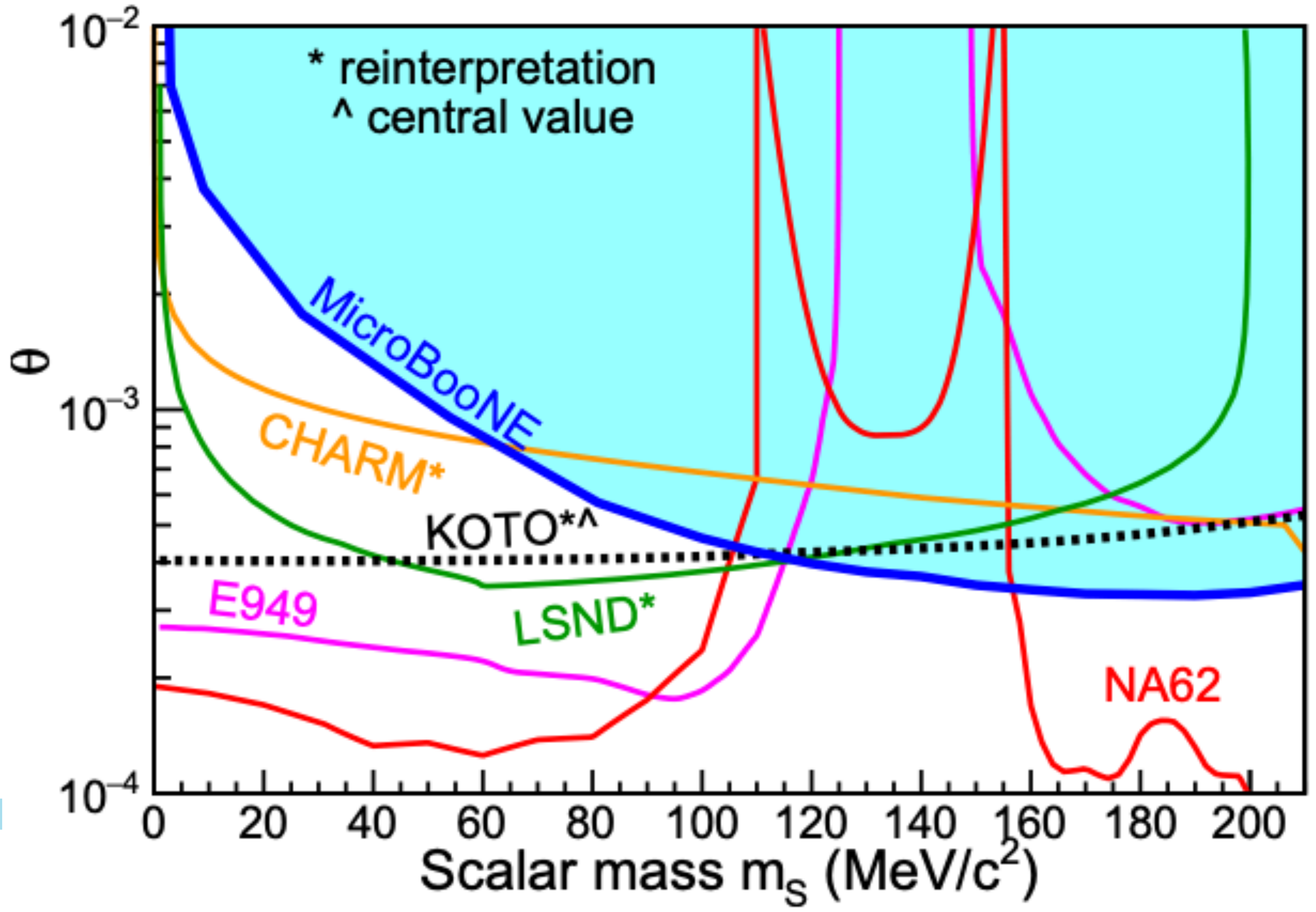

See also Yeon-jae Jwa's talk earlier in paralle session

Conclusions

- Era of precision neutrino physics with LArTPC experiments has started
- Puzzle of short baseline neutrino anomalies is not yet complete
  - MicroBooNE has addressed the leading explanations of the MiniBooNE anomaly
- MicroBooNE is still looking for cuts in the canvas of the SM picture

Thank you!

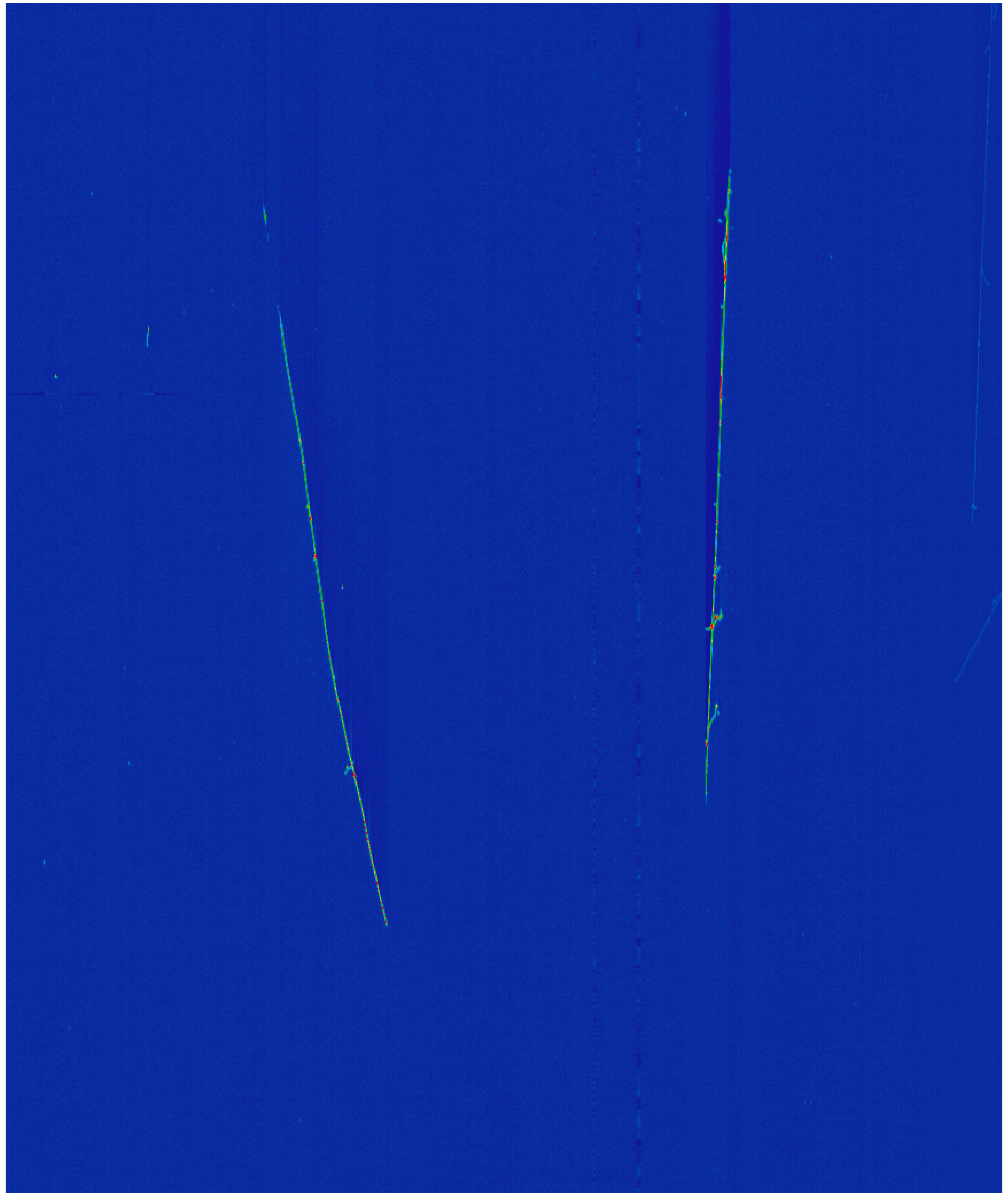

MicroBooNE, EXT data, 2019

Backup slides

HNL Search in MicroBooNE

PRD 101, 052001 (2020)

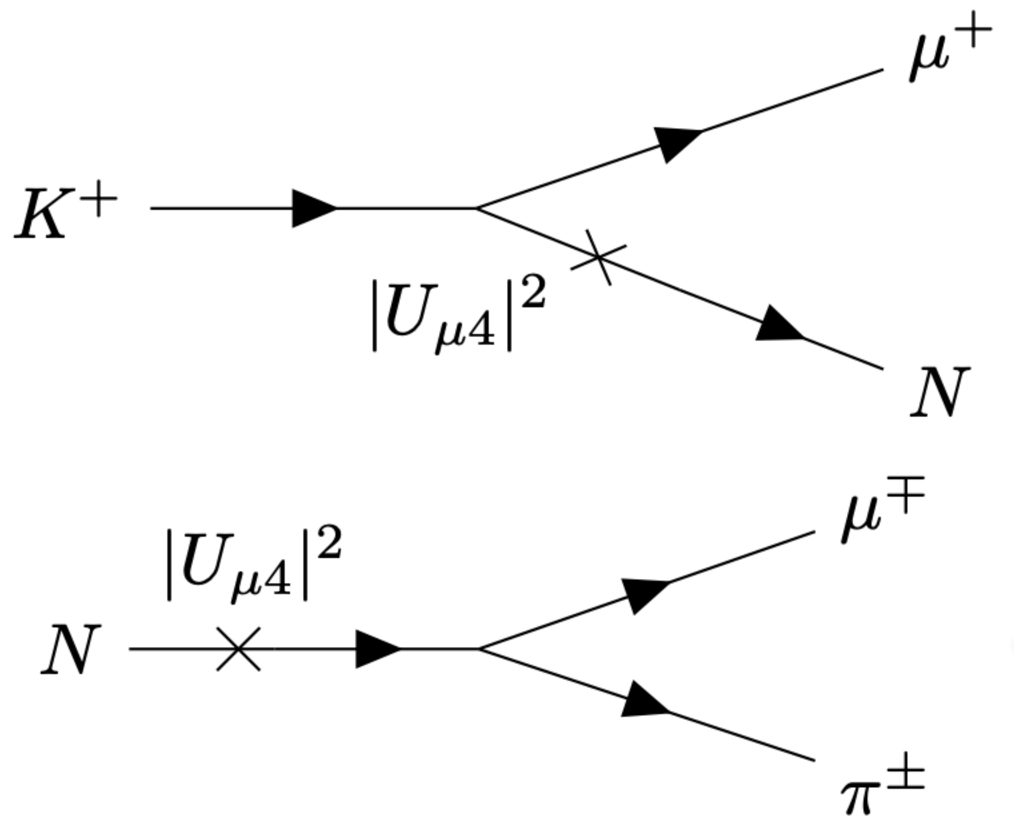

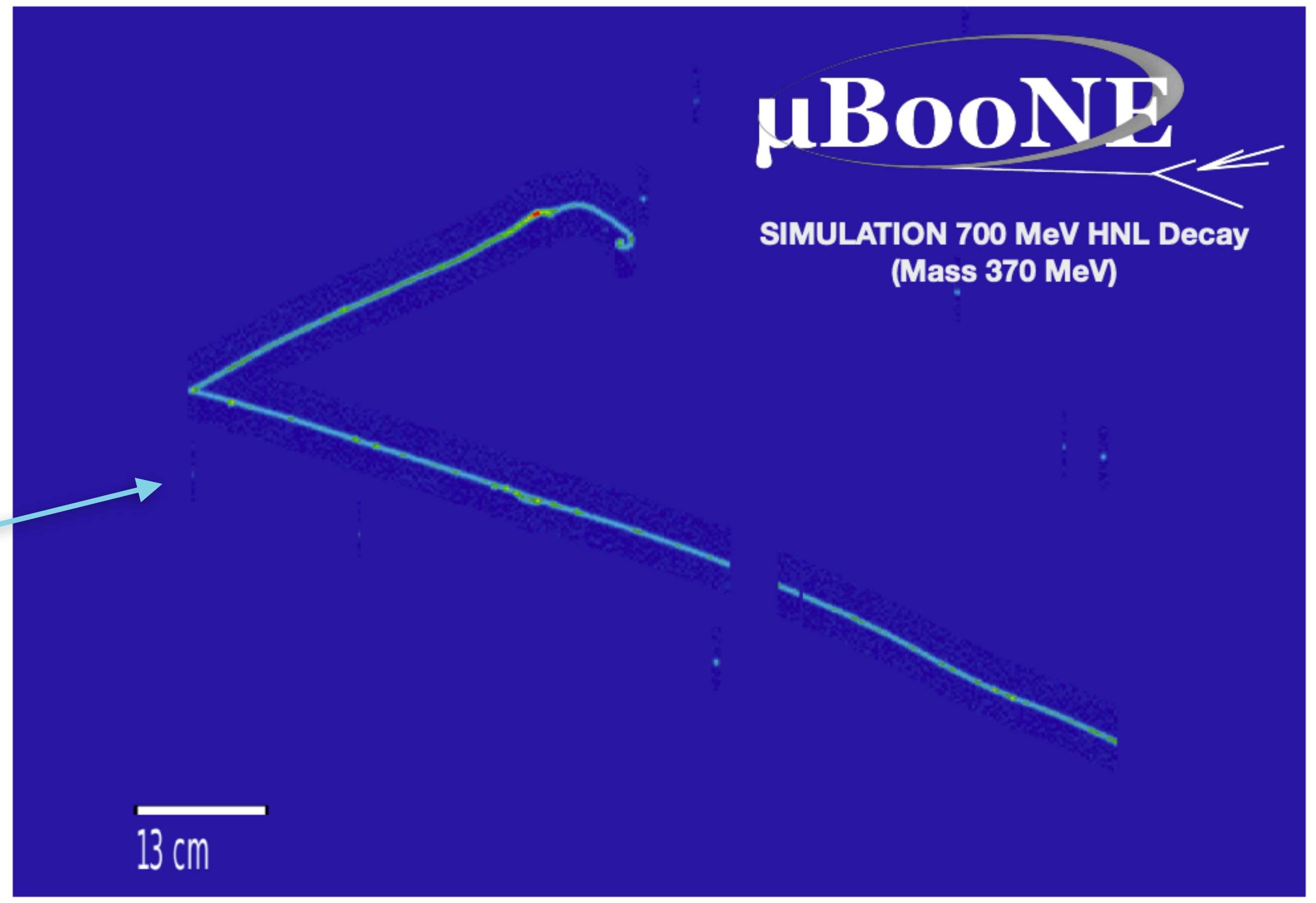

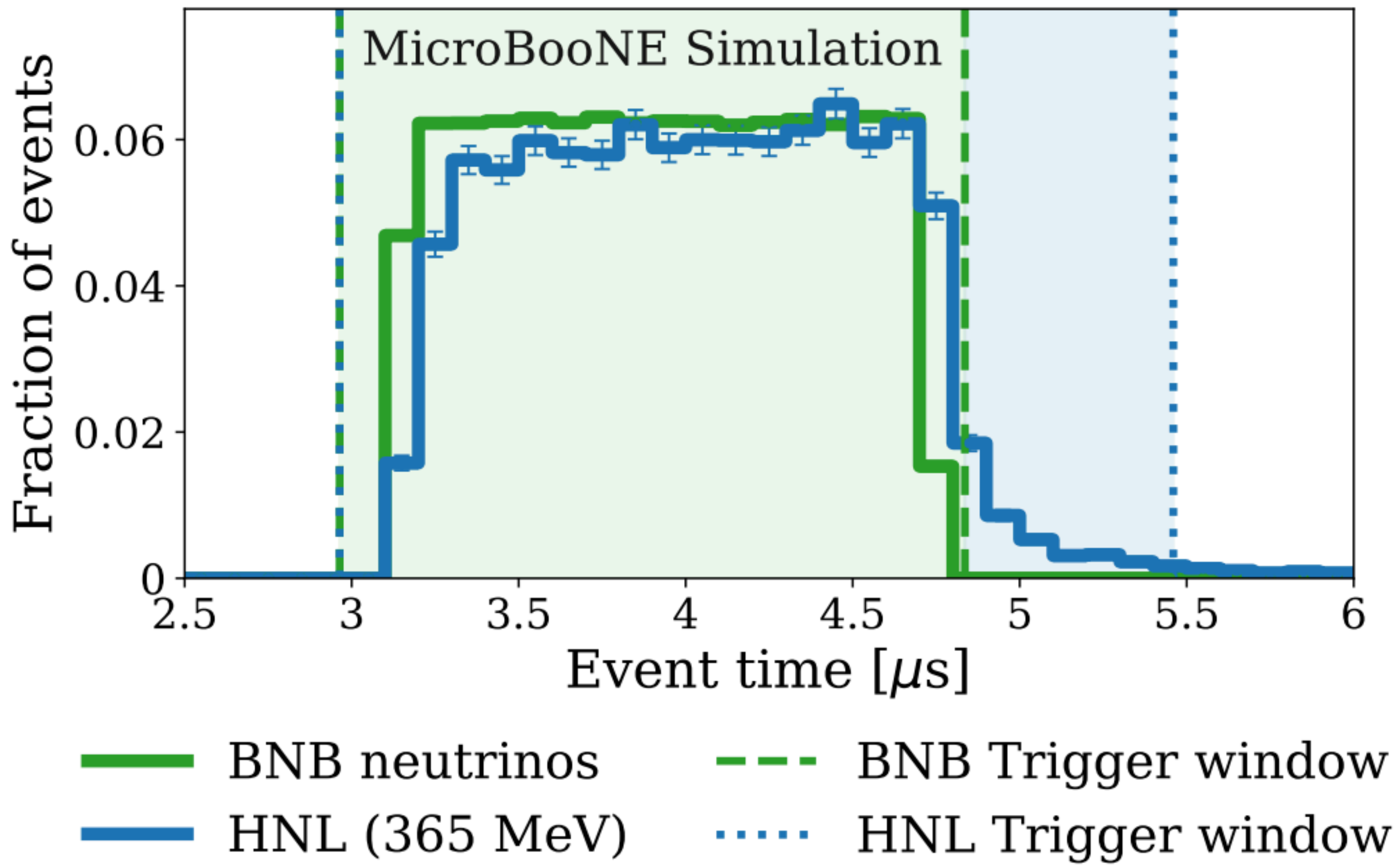

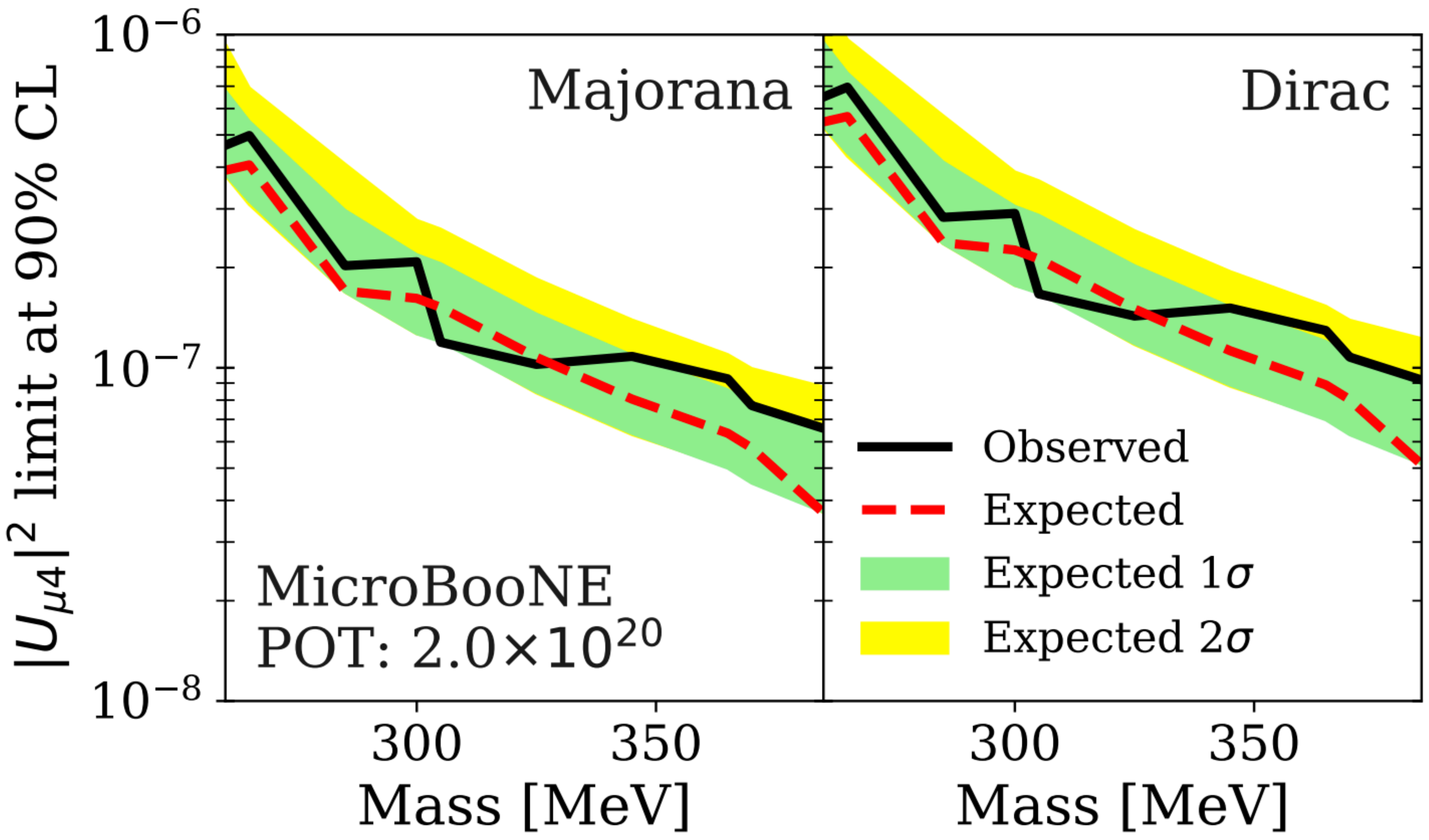

Test of Null Hypothesis

Channel	χ^2	χ^2/dof	p-value
$1eNp0\pi$	15.2	1.52	0.182
$1e0p0\pi$	16.3	1.63	0.126
$1eNp0\pi + 1e0p0\pi$	31.50	1.58	0.098

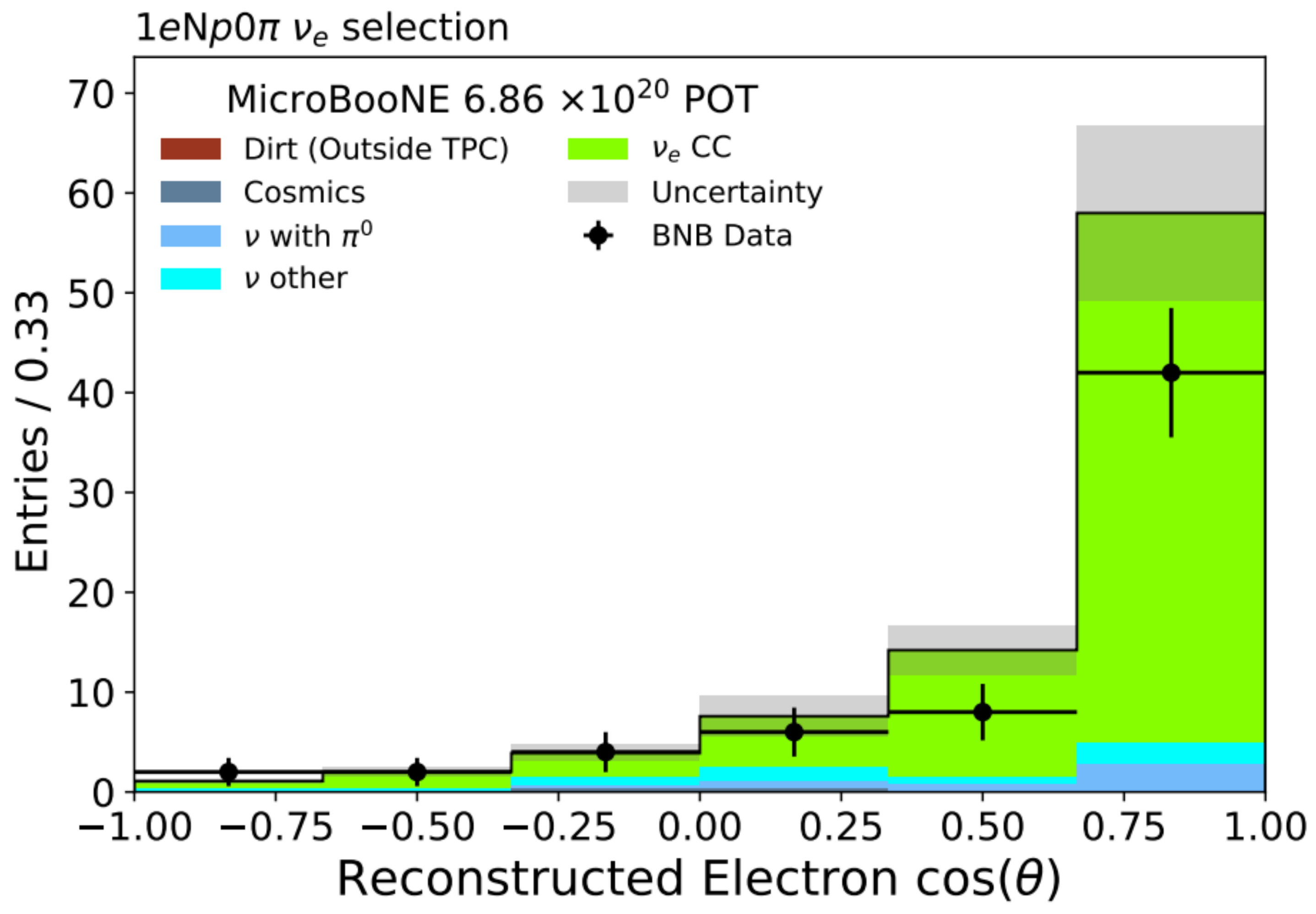

(a) Electron angle relative to beam direction.

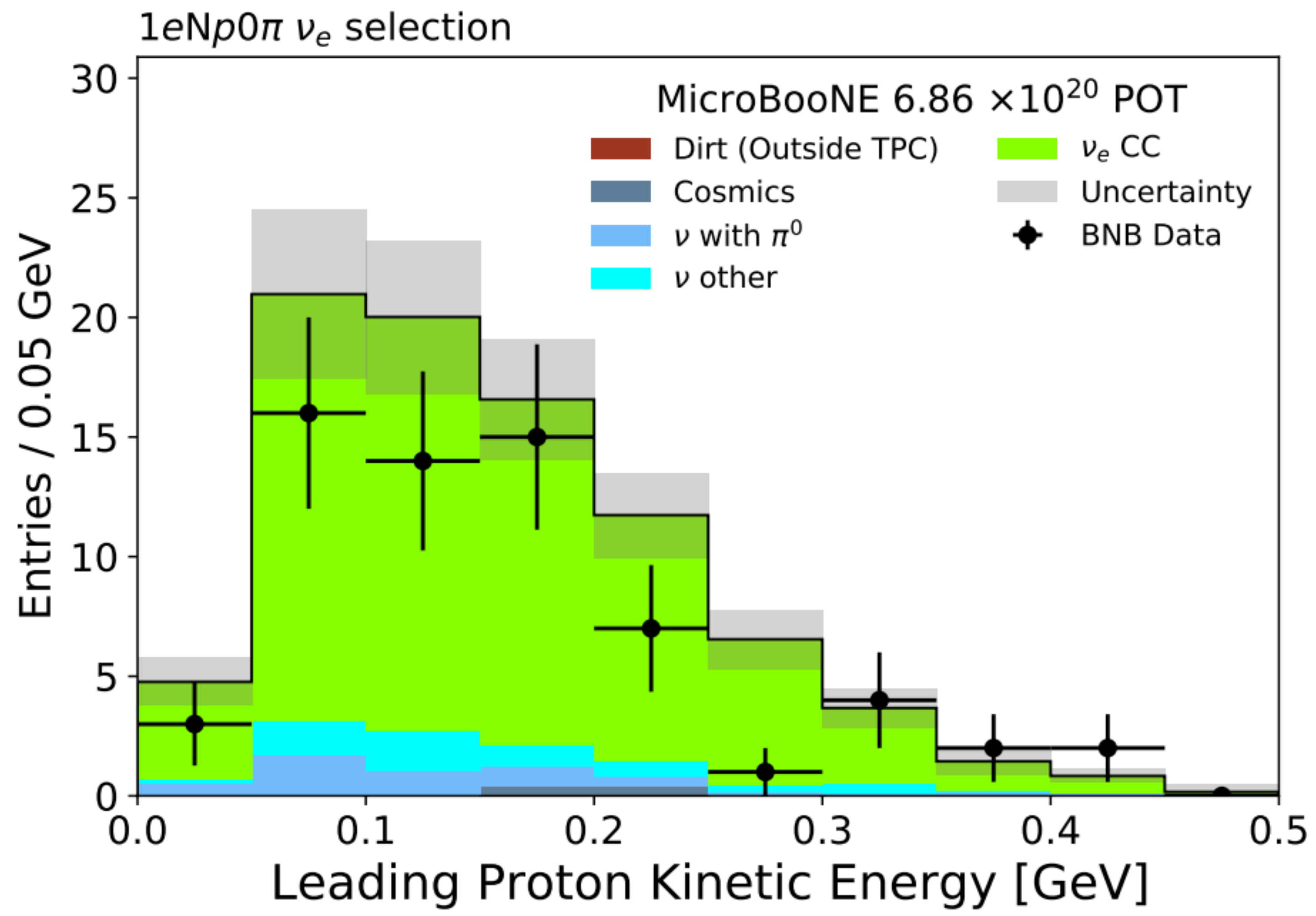

(b) Proton kinetic energy.

arXiv:2110.14065

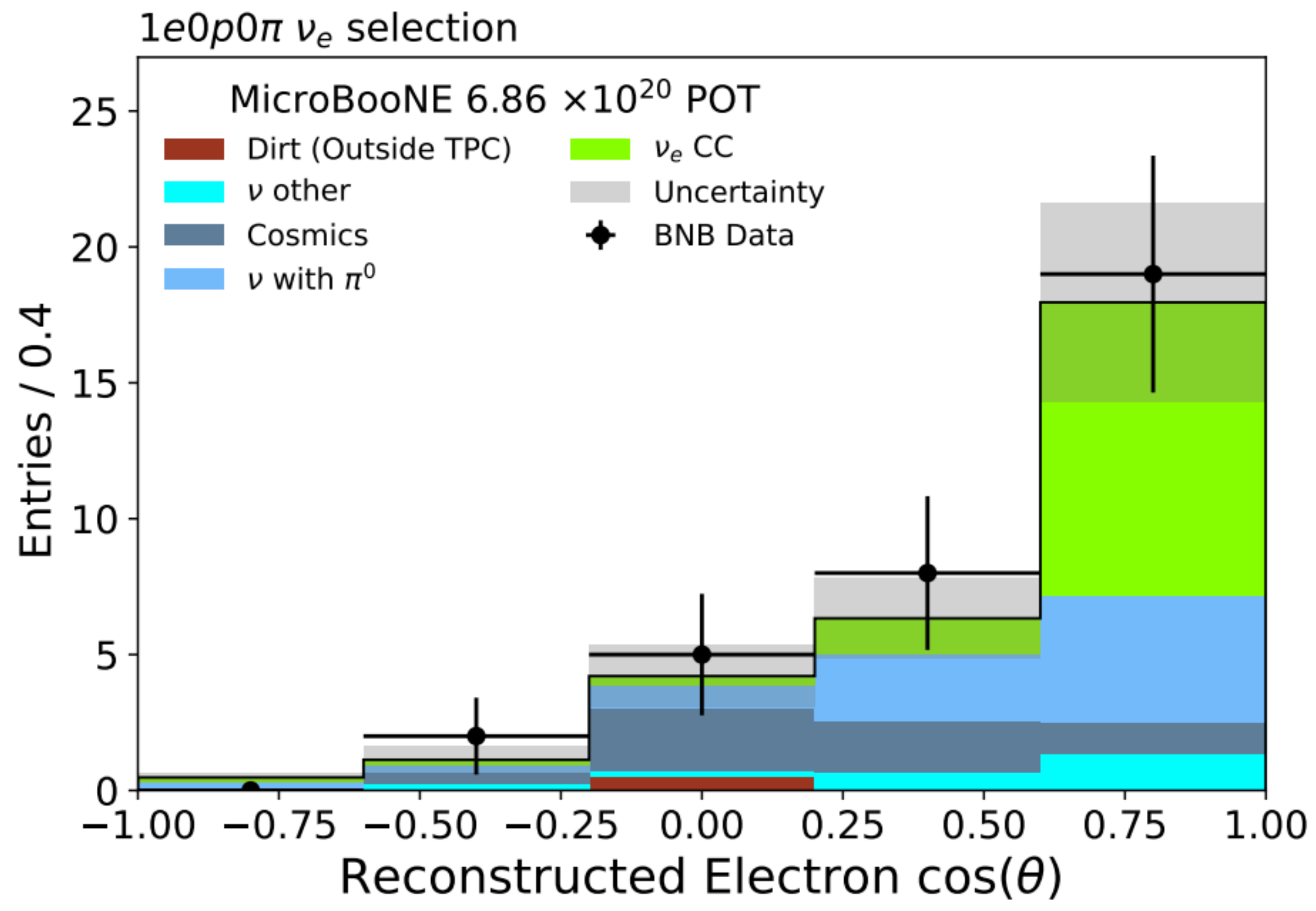

(a) All selected events.

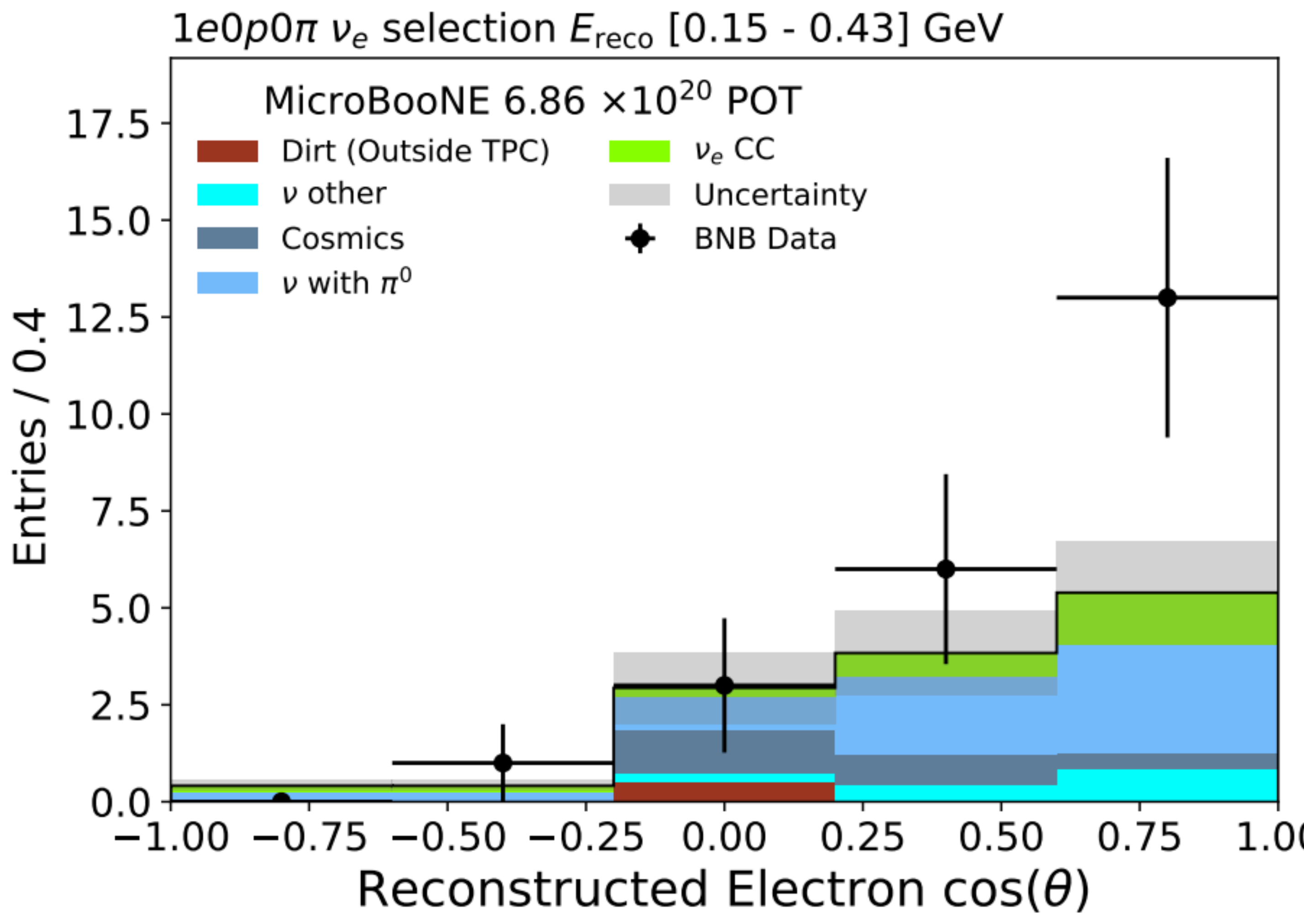

(b) Low energy selected events from 0.15–0.43 GeV.

Fermilab

Simple Hypothesis Test

arXiv:2110.14065

Channel	obs. $\Delta\chi^2$	$\Delta\chi^2 <$ obs. p-value(H_0)	$\Delta\chi^2 <$ obs. p-value(H_1)	Sensitivity p-value$(H_0)\ \|H_1$	Sensitivity p-value$(H_1)\ \|H_0$
$1e\mathrm{N}p0\pi$	-3.89	0.285	0.021	0.957	0.061
$1e0p0\pi$	3.11	0.984	0.928	0.759	0.249
$1e\mathrm{N}p0\pi + 1e0p0\pi$	-0.58	0.748	0.145	0.968	0.049

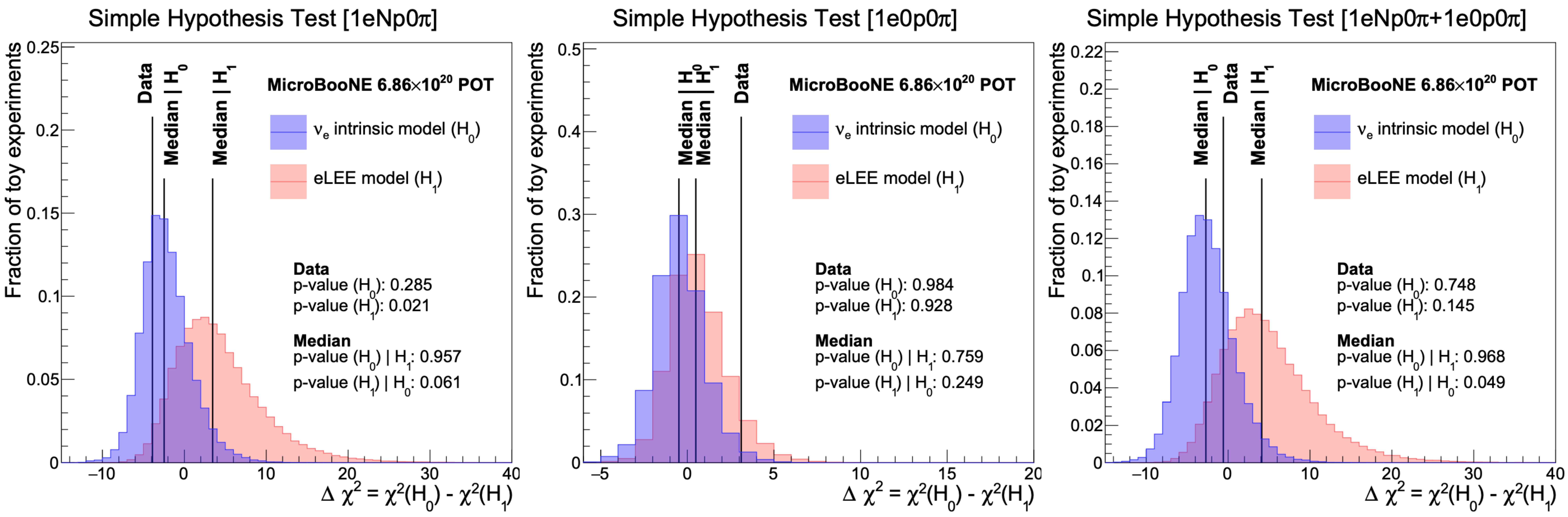

(a) $1e\mathrm{N}p0\pi$ (b) $1e0p0\pi$ (c) $1e\mathrm{N}p0\pi + 1e0p0\pi$

Signal Strength Fit

arXiv:2110.14065

Channel	Data μ_{BF}	Data 90% CL interval on μ	Sensitivity 90% upper limit on μ
$1eNp0\pi$	0.00	[0.00 , 0.82]	1.16
$1e0p0\pi$	4.00	[1.13 , 15.01]	3.41
$1eNp0\pi + 1e0p0\pi$	0.36	[0.00 , 1.57]	1.07

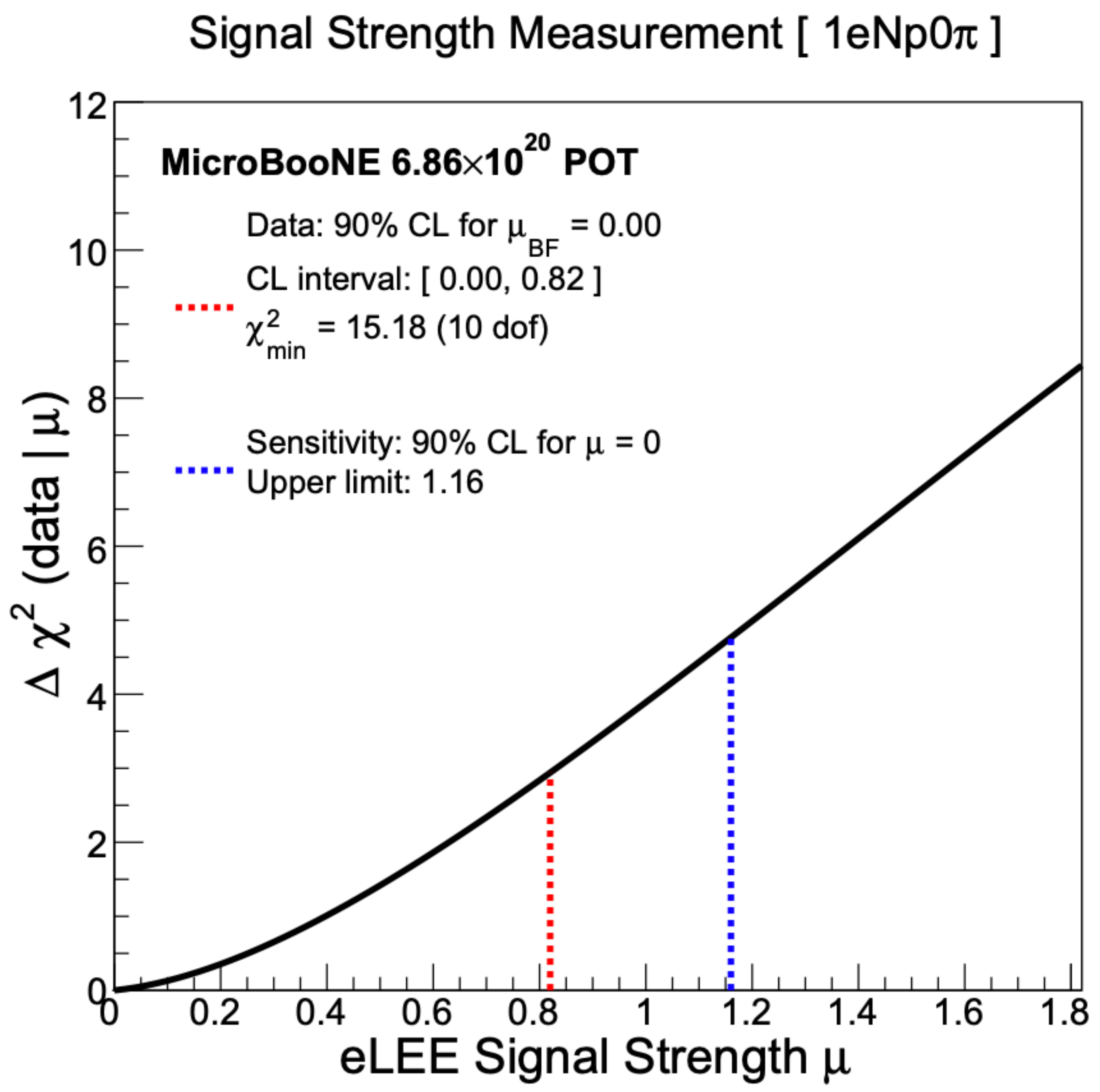

(a) $1eNp0\pi$

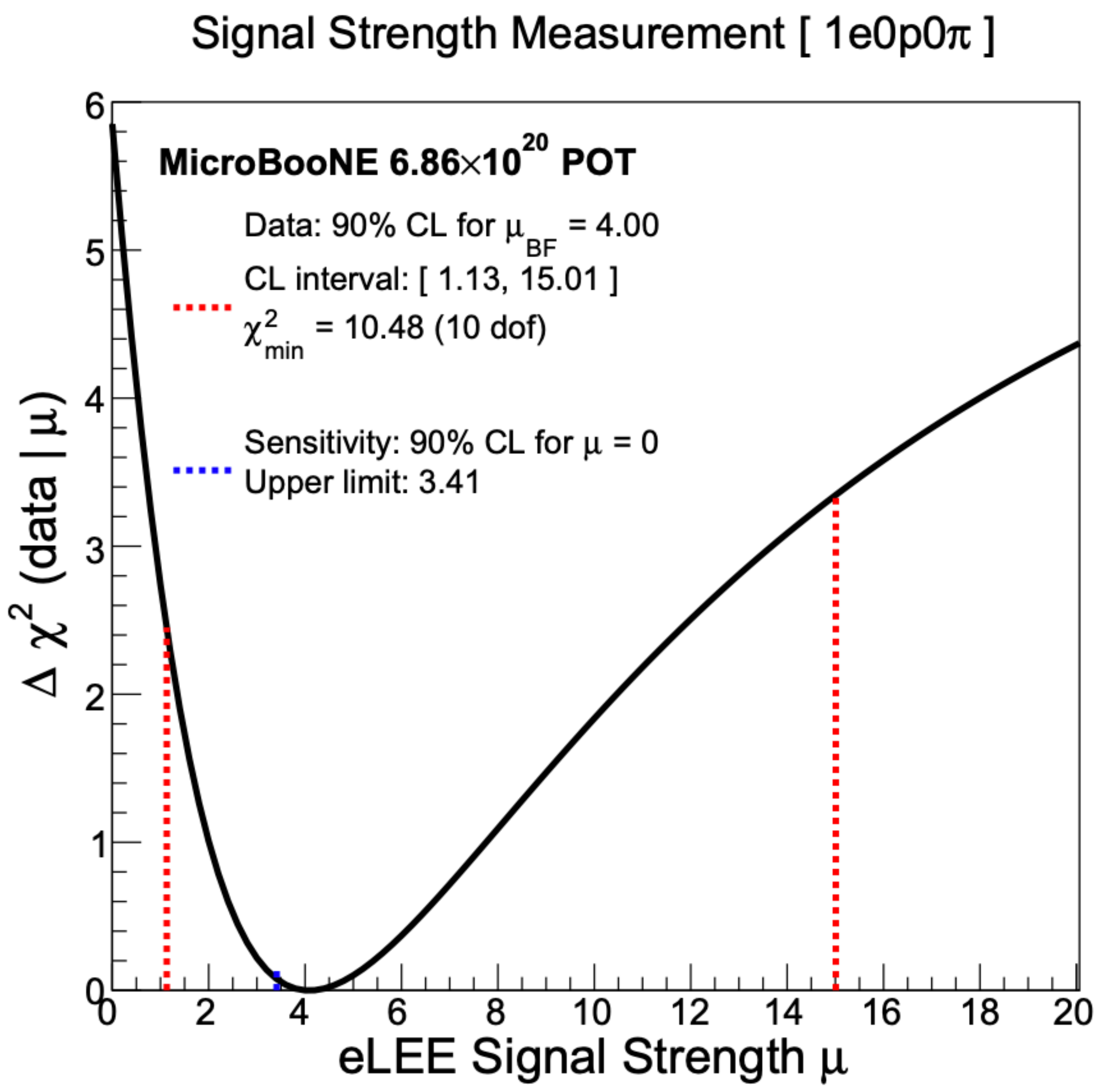

(b) $1e0p0\pi$

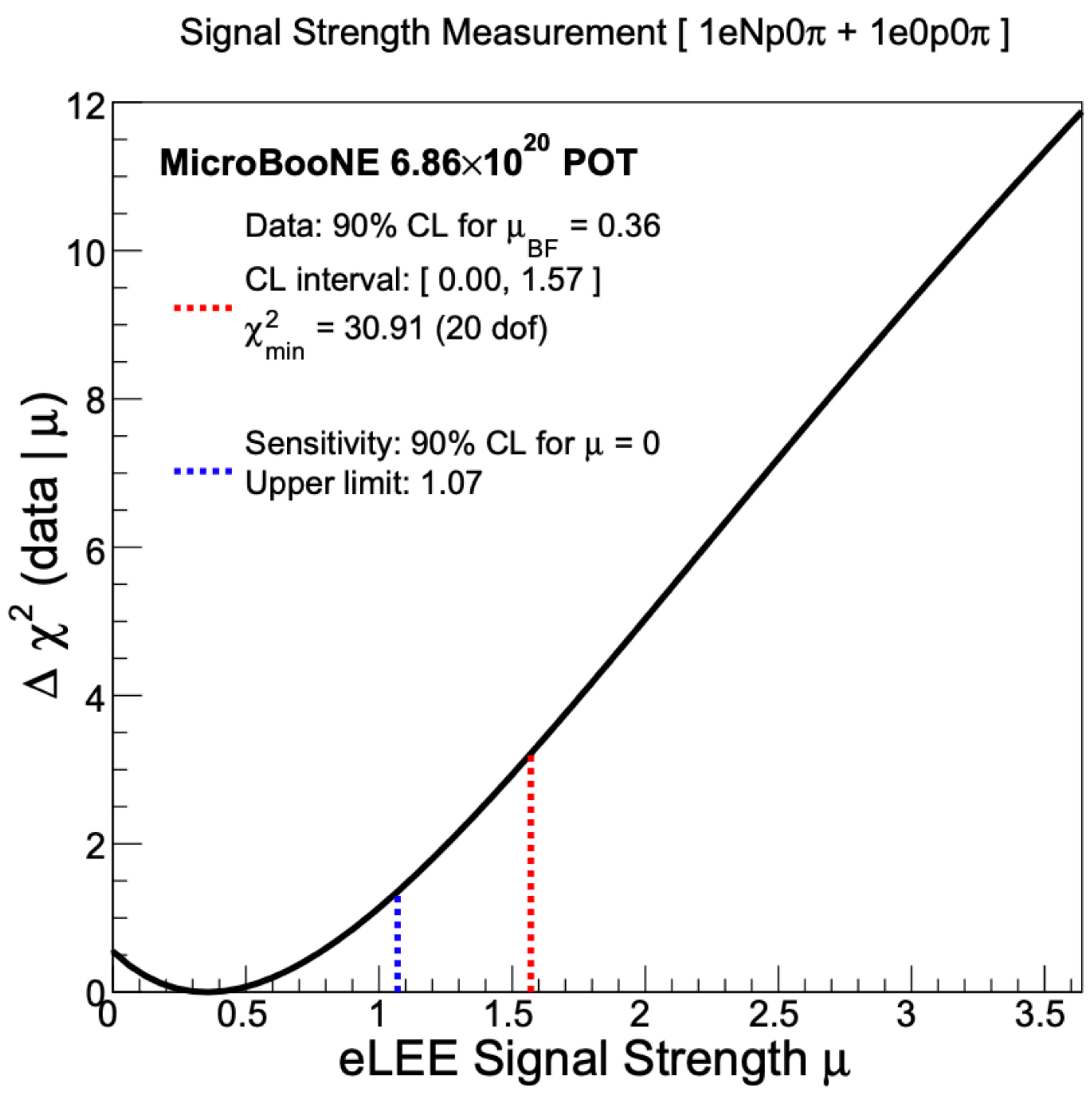

(c) $1eNp0\pi + 1e0p0\pi$

Reactor experiments

a	Experiment	f^a_{235}	f^a_{238}	f^a_{239}	f^a_{241}	$\sigma^{\text{exp}}_{f,a}$	$R^{\text{exp}}_{a,\text{HM}}$	$R^{\text{exp}}_{a,\text{EF}}$	$R^{\text{exp}}_{a,\text{HKSS}}$	$R^{\text{exp}}_{a,\text{KI}}$	δ^{exp}_a [%]	δ^{cor}_a [%]	L_a [m]
1	Bugey-4	0.538	0.078	0.328	0.056	5.75	0.927	0.962	0.916	0.962	1.4	1.4	15
2	Rovno91	0.614	0.074	0.274	0.038	5.85	0.924	0.965	0.914	0.962	2.8		18
3	Rovno88-1I	0.607	0.074	0.277	0.042	5.70	0.902	0.941	0.892	0.939	6.4	3.1	18
4	Rovno88-2I	0.603	0.076	0.276	0.045	5.89	0.931	0.971	0.920	0.969	6.4		17.96
5	Rovno88-1S	0.606	0.074	0.277	0.043	6.04	0.956	0.997	0.945	0.995	7.3	2.2	18.15
6	Rovno88-2S	0.557	0.076	0.313	0.054	5.96	0.956	0.994	0.945	0.993	7.3	3.1	25.17
7	Rovno88-3S	0.606	0.074	0.274	0.046	5.83	0.922	0.962	0.911	0.960	6.8		18.18
8	Bugey-3-15	0.538	0.078	0.328	0.056	5.77	0.930	0.966	0.920	0.966	4.2		15
9	Bugey-3-40	0.538	0.078	0.328	0.056	5.81	0.936	0.972	0.926	0.972	4.3	4.0	40
10	Bugey-3-95	0.538	0.078	0.328	0.056	5.35	0.861	0.895	0.852	0.894	15.2		95
11	Gosgen-38	0.619	0.067	0.272	0.042	5.99	0.949	0.992	0.939	0.988	5.4		37.9
12	Gosgen-46	0.584	0.068	0.298	0.050	6.09	0.975	1.016	0.964	1.014	5.4	2.0	45.9
13	Gosgen-65	0.543	0.070	0.329	0.058	5.62	0.909	0.945	0.899	0.944	6.7	3.8	64.7
14	ILL	1.000	0.000	0.000	0.000	5.30	0.787	0.843	0.777	0.827	9.1		8.76
15	Krasnoyarsk87-33	1	0	0	0	6.20	0.920	0.986	0.909	0.967	5.2	4.1	32.8
16	Krasnoyarsk87-92	1	0	0	0	6.30	0.935	1.002	0.924	0.983	20.5		92.3
17	Krasnoyarsk94-57	1	0	0	0	6.26	0.929	0.995	0.918	0.977	4.2	0	57
18	Krasnoyarsk99-34	1	0	0	0	6.39	0.948	1.016	0.937	0.997	3.0	0	34
19	SRP-18	1	0	0	0	6.29	0.934	1.000	0.923	0.982	2.8	0	18.2
20	SRP-24	1	0	0	0	6.73	0.998	1.070	0.987	1.050	2.9	0	23.8
21	Nucifer	0.926	0.008	0.061	0.005	6.67	1.007	1.074	0.995	1.056	10.8	0	7.2
22	Chooz	0.496	0.087	0.351	0.066	6.12	0.990	1.025	0.979	1.027	3.2	0	≈ 1000
23	Palo Verde	0.600	0.070	0.270	0.060	6.25	0.991	1.033	0.980	1.031	5.4	0	≈ 800
24	Daya Bay	0.564	0.076	0.304	0.056	5.94	0.950	0.988	0.939	0.987	1.5	0	≈ 550
25	RENO	0.571	0.073	0.300	0.056	5.85	0.936	0.974	0.925	0.973	2.1	0	≈ 411
26	Double Chooz	0.520	0.087	0.333	0.060	5.71	0.918	0.952	0.907	0.953	1.1	0	≈ 415
27	STEREO	1	0	0	0	6.34	0.941	1.008	0.930	0.989	2.5	0	$9-11$

Table 1: List of the experiments which measured the absolute reactor antineutrino flux [66]. For each experiment numbered with the index a: f^a_{235}, f^a_{238}, f^a_{239}, and f^a_{241} are the effective fission fractions of the four isotopes ^{235}U, ^{238}U, ^{239}Pu, and ^{241}Pu, respectively; $\sigma^{\text{exp}}_{f,a}$ is the experimental IBD yield in units of 10^{-43}cm^2/fission; $R^{\text{exp}}_{a,\text{HM}}$, $R^{\text{exp}}_{a,\text{EF}}$, $R^{\text{exp}}_{a,\text{HKSS}}$, and $R^{\text{exp}}_{a,\text{KI}}$, are the ratios of measured and predicted rates for the IBD yields of the models in Tab. 6; δ^{exp}_a is the total relative experimental statistical plus systematic uncertainty, δ^{cor}_a is the part of the relative experimental systematic uncertainty which is correlated in each group of experiments indicated by the braces; L_a is the source-detector distance.

arXiv:2203.07323

Fermilab

Alternative reactor flux models

arXiv:2203.07323

Model	Rates		Evolution		Rates + Evolution	
	$\overline{R}_{\text{mod}}$	RAA	$\overline{R}_{\text{mod}}$	RAA	$\overline{R}_{\text{mod}}$	RAA
HM	$0.936^{+0.024}_{-0.023}$	$2.5\,\sigma$	$0.933^{+0.025}_{-0.024}$	$2.6\,\sigma$	$0.930^{+0.024}_{-0.023}$	$2.8\,\sigma$
EF	$0.960^{+0.033}_{-0.031}$	$1.2\,\sigma$	$0.975^{+0.032}_{-0.030}$	$0.8\,\sigma$	$0.975^{+0.032}_{-0.030}$	$0.8\,\sigma$
HKSS	$0.925^{+0.025}_{-0.023}$	$2.9\,\sigma$	$0.925^{+0.026}_{-0.024}$	$2.8\,\sigma$	$0.922^{+0.024}_{-0.023}$	$3.0\,\sigma$
KI	$0.975^{+0.022}_{-0.021}$	$1.1\,\sigma$	$0.973^{+0.023}_{-0.022}$	$1.2\,\sigma$	0.970 ± 0.021	$1.4\,\sigma$

Table 7: Average ratio $\overline{R}_{\text{mod}}$ obtained in Ref. [66] from the least-squares analysis of the reactor rates in Tab. 1 and of the Daya Bay [251] and RENO [252] evolution data for the IBD yields of the models in Tab. 6. The RAA columns give the corresponding statistical significance of the reactor antineutrino anomaly. The descriptions of all the models are given in text.

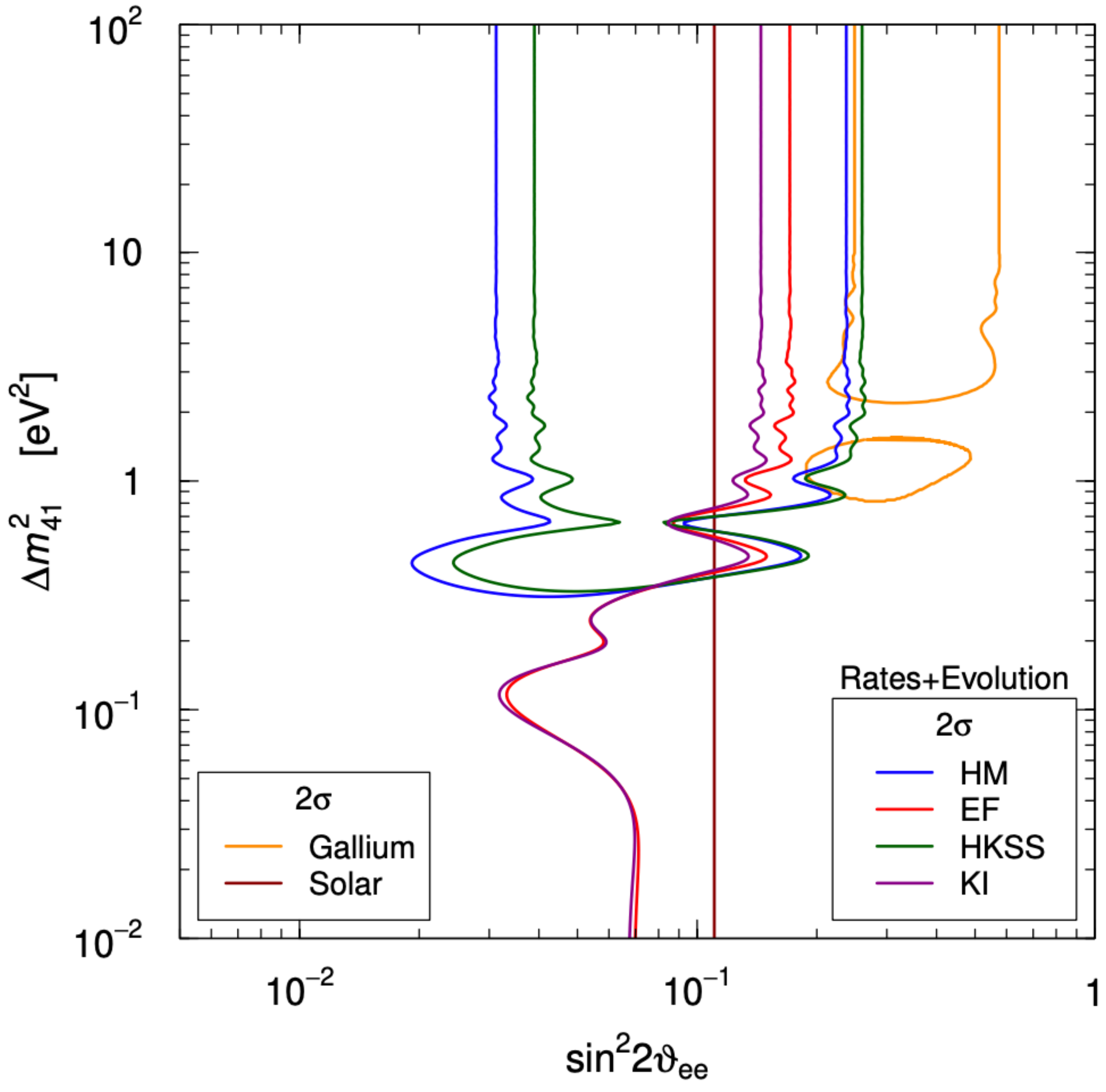

Figure 38: Contours of the 2σ allowed regions in the $(\sin^2 2\vartheta_{ee}, \Delta m^2_{41})$ plane obtained from the combined neutrino oscillation fit of the reactor rates in Tab. 7 and the Daya Bay [251] and RENO [252] evolution data. The blue, red, green, and magenta curves correspond, respectively, to the HM, EF, HKSS, and KI models in Tab. 6. Also shown are the contour of the 2σ allowed regions of the Gallium anomaly obtained in Ref. [137] from the combined analysis of the GALLEX, SAGE and BEST data (orange curve), and the 2σ bound obtained from the analysis of solar neutrino data in Ref. [258] (dark red vertical line).

Fermilab

Alternative reactor flux models

PLB 829 (2022) 137054

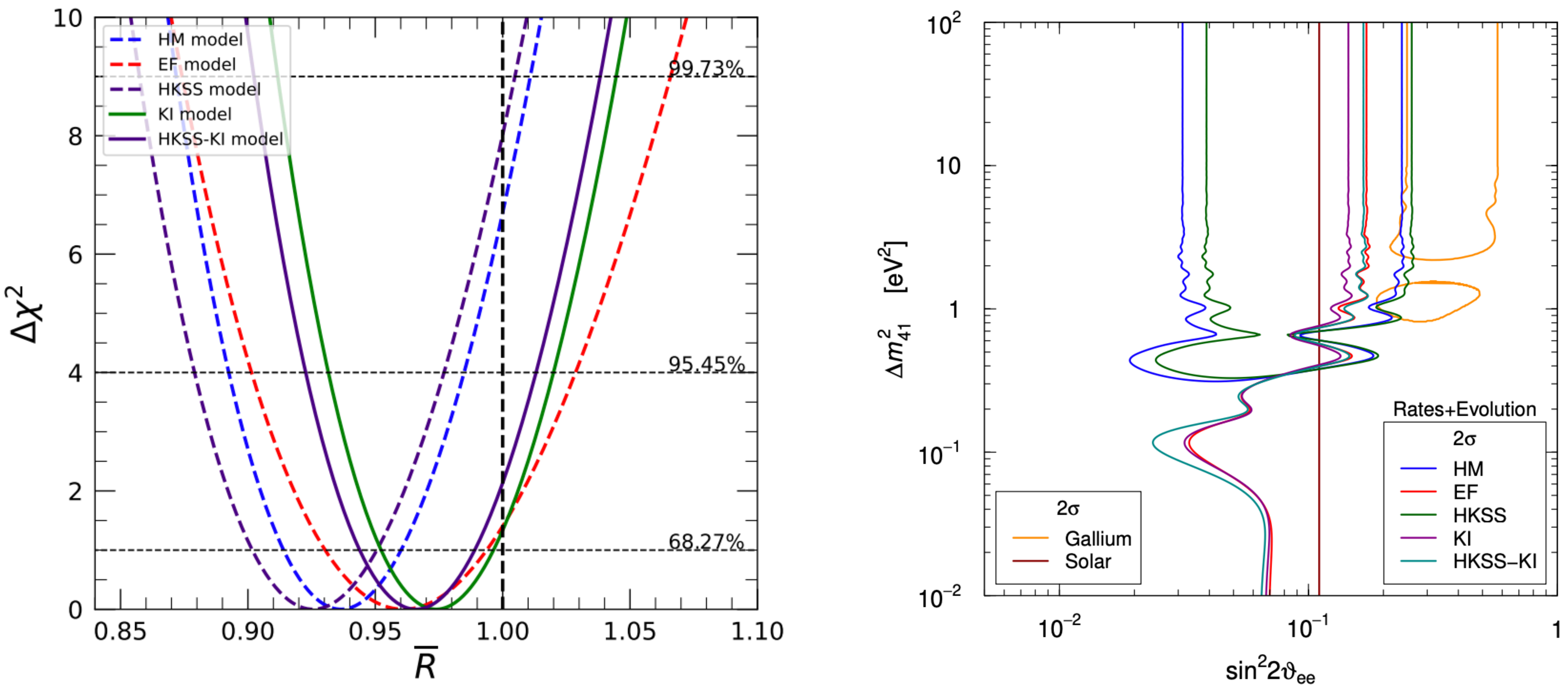

MiniBooNE 3+1 Oscillation Fit

PRD 103 (2021) 5, 052002

$$\Delta m^2 = 0.043\ \text{eV}^2,\ \text{and}\ \sin^2 2\theta = 0.807,$$

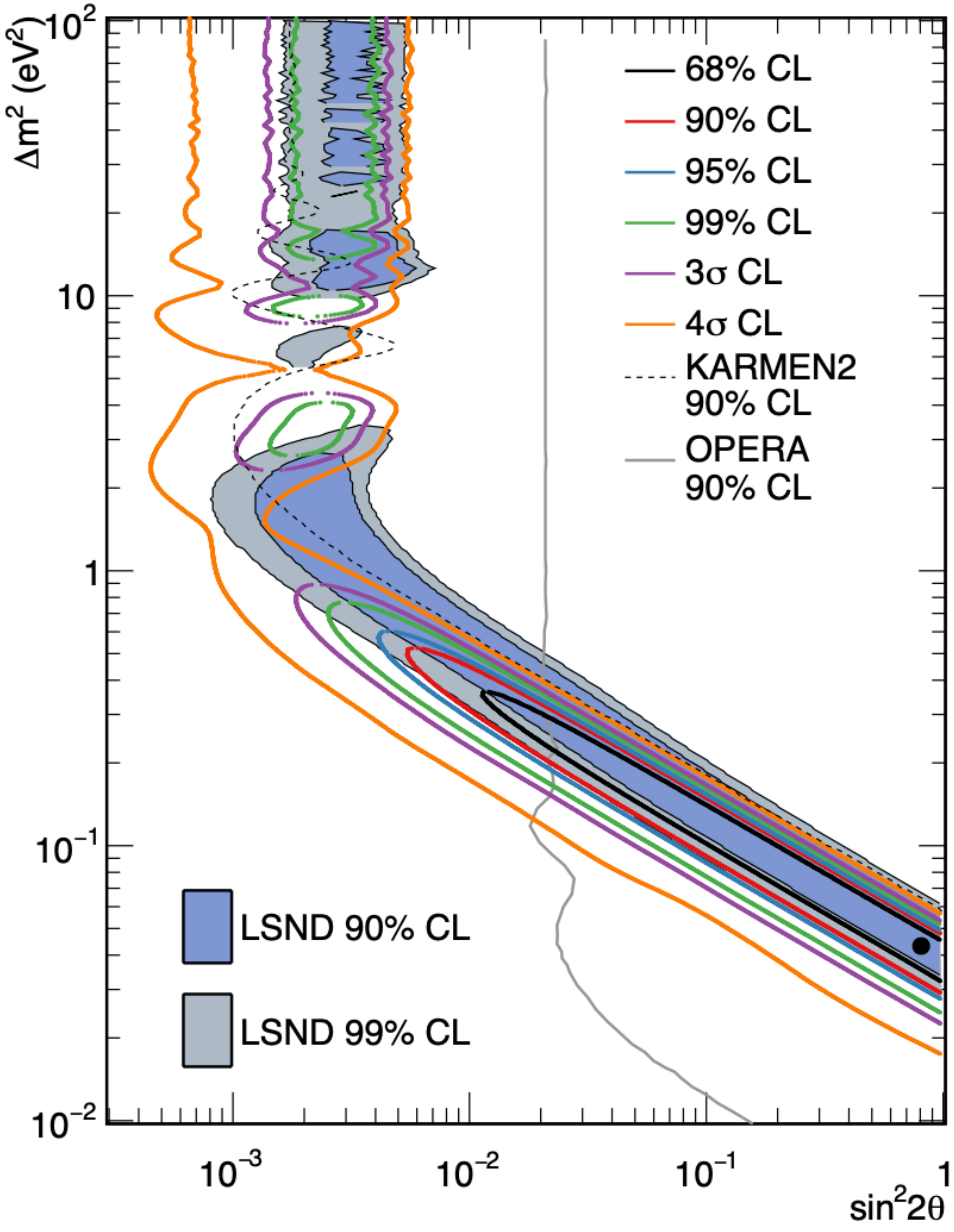

Fermilab

MB result

PRD 103 (2021) 5, 052002

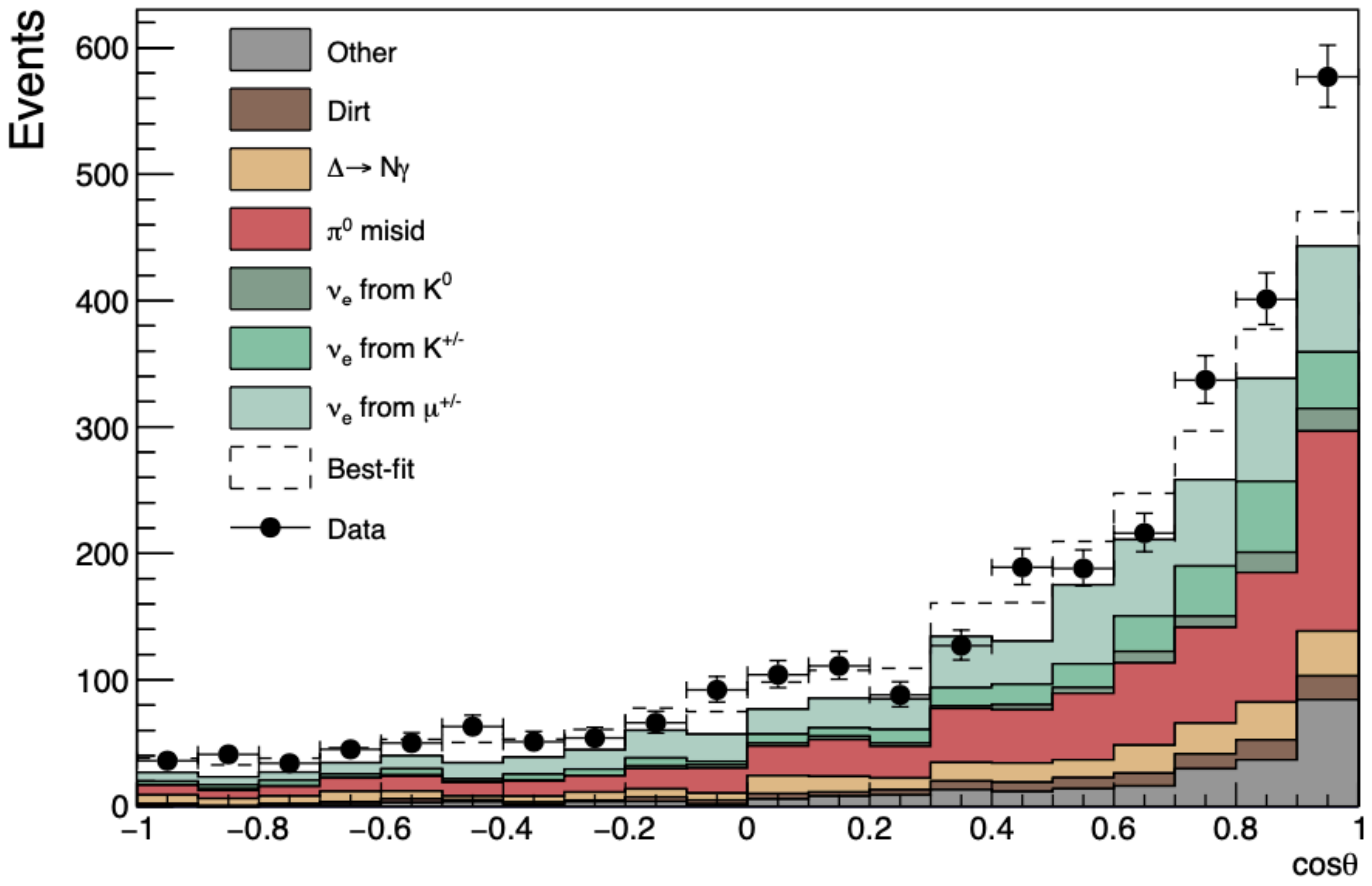

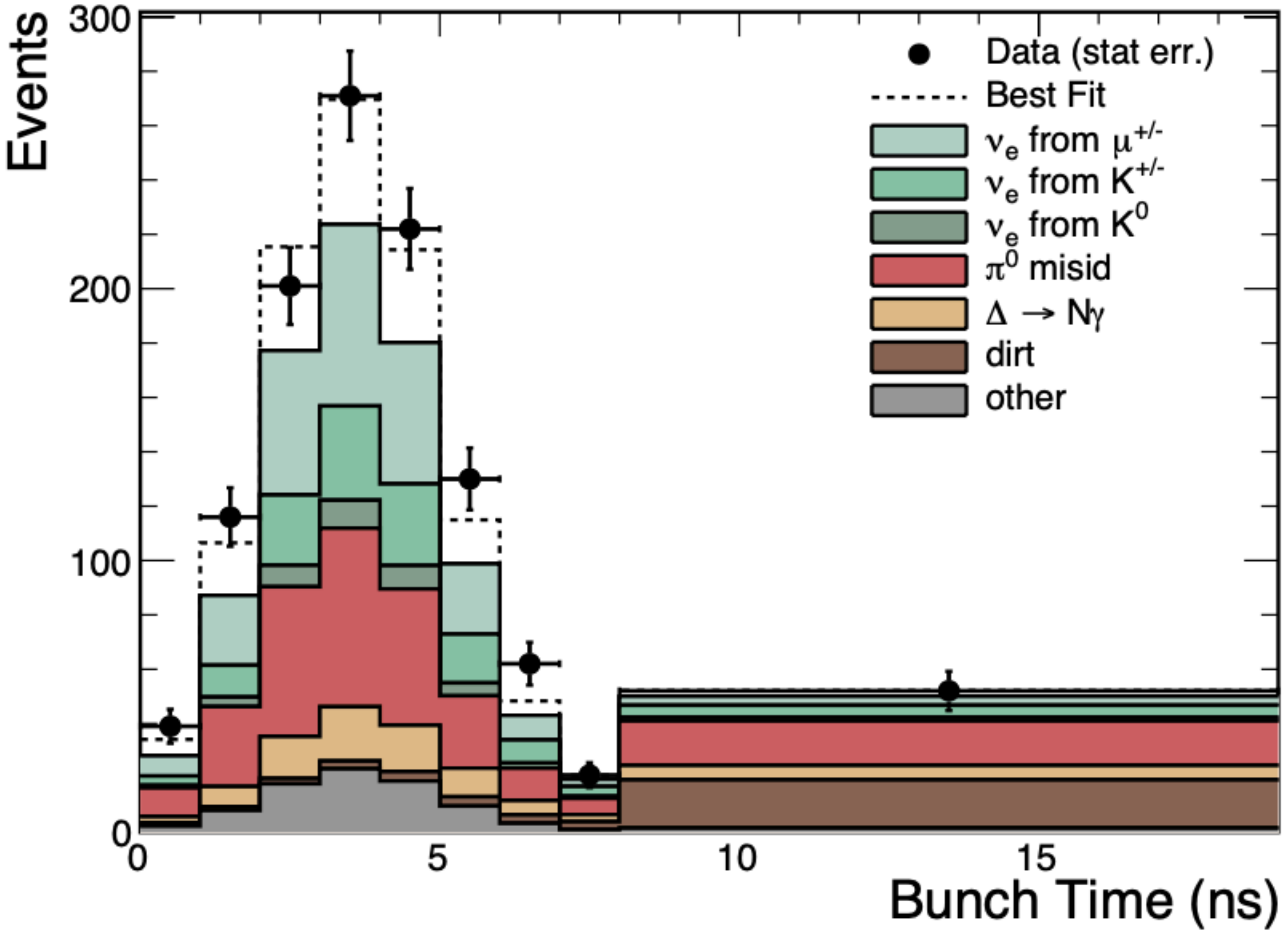

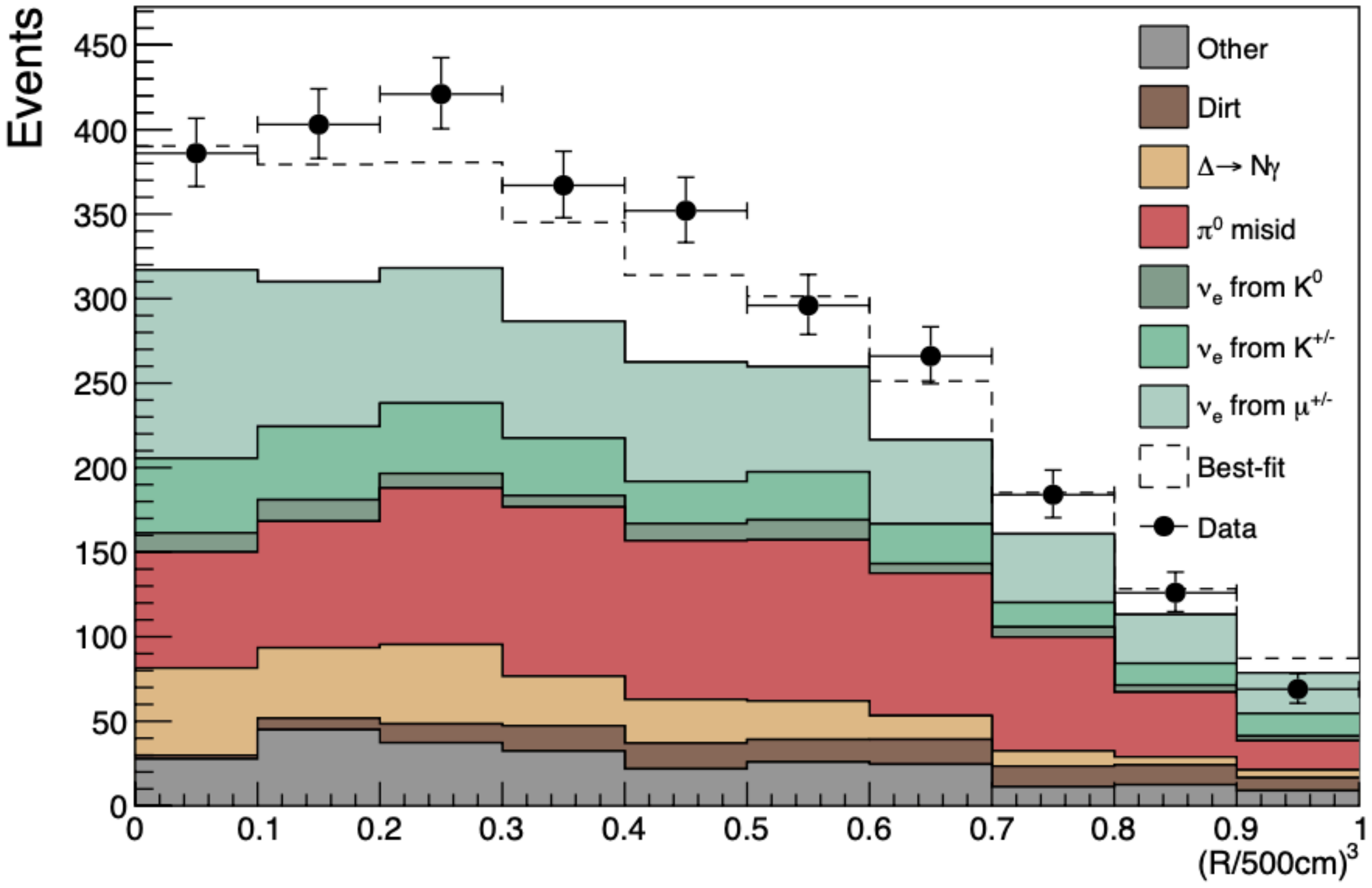

Appearance vs Disappearance

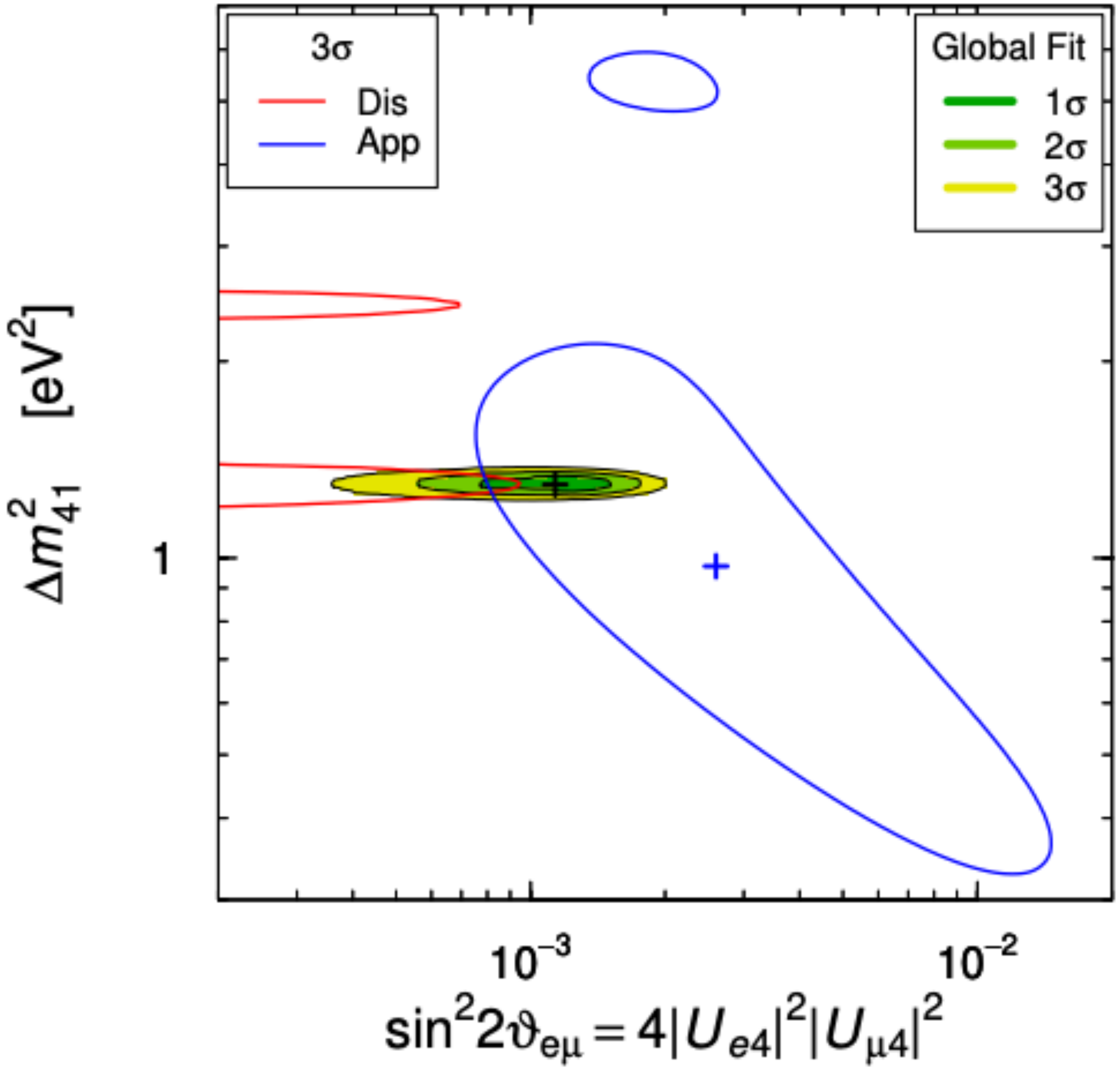

arXiv:1901.08330

Fermilab

Gallium cross sections

	$GALLEX_1$	$GALLEX_1$	$SAGE_{Cr}$	$SAGE_{Ar}$	Avg.
R_B	0.95 ± 0.11	$0.81^{+0.10}_{-0.11}$	0.95 ± 0.12	0.79 ± 0.08	0.86 ± 0.05
R_{HK}	0.85 ± 0.12	0.71 ± 0.11	$0.84^{+0.13}_{-0.12}$	0.71 ± 0.09	0.77 ± 0.08
R_{FF}	0.93 ± 0.11	$0.79^{+0.10}_{-0.11}$	$0.93^{+0.11}_{-0.12}$	$0.77^{+0.09}_{-0.07}$	0.84 ± 0.05
R_{HF}	$0.83^{+0.13}_{-0.11}$	0.71 ± 0.11	$0.83^{+0.13}_{-0.12}$	$0.69^{+0.10}_{-0.09}$	$0.75^{+0.09}_{-0.07}$
R_{JUN45}	0.97 ± 0.11	0.83 ± 0.11	0.97 ± 0.12	0.81 ± 0.08	0.88 ± 0.05

arXiv:2203.07323

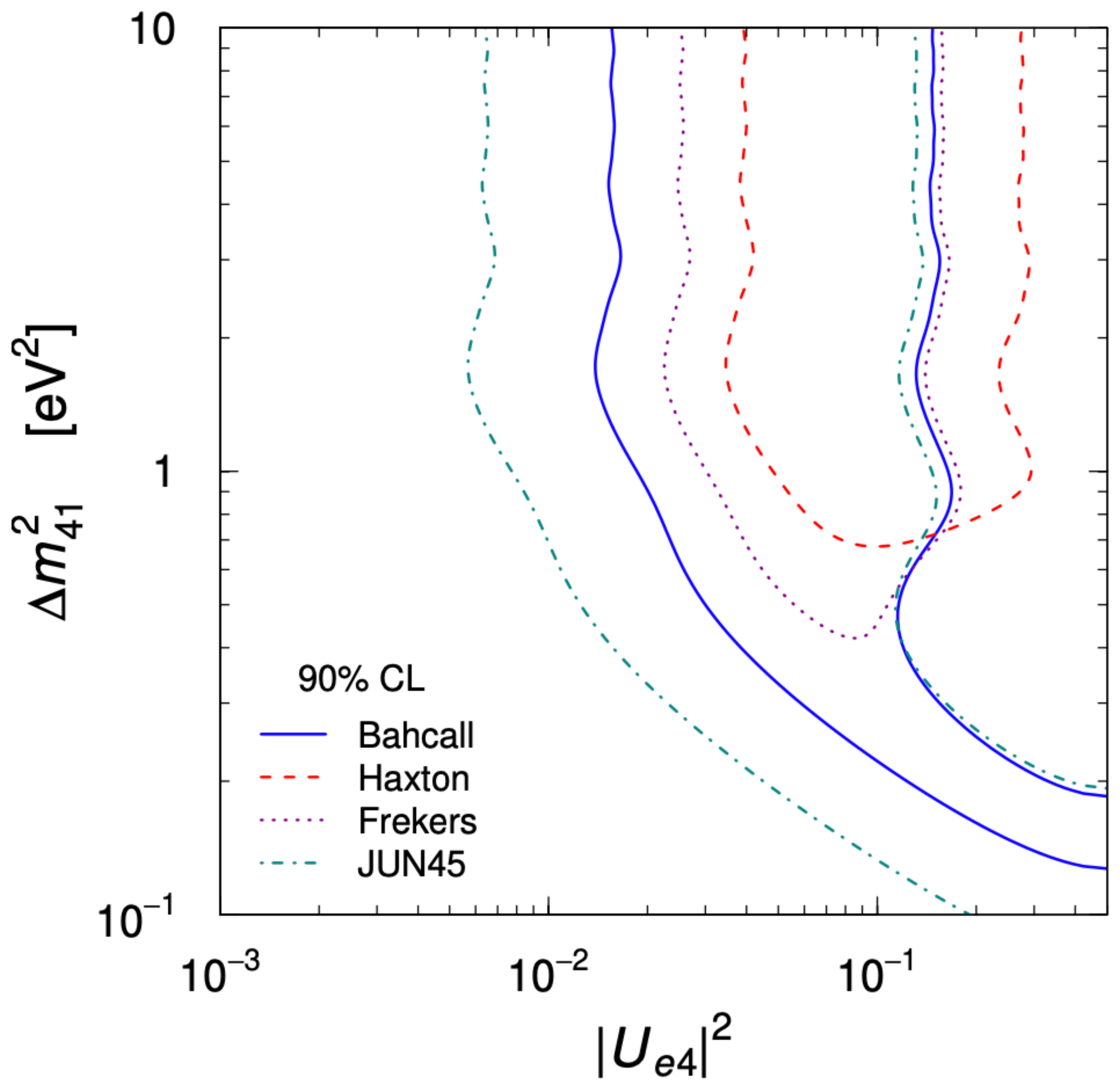

KARMEN limits

PRD 65 (2002) 112001

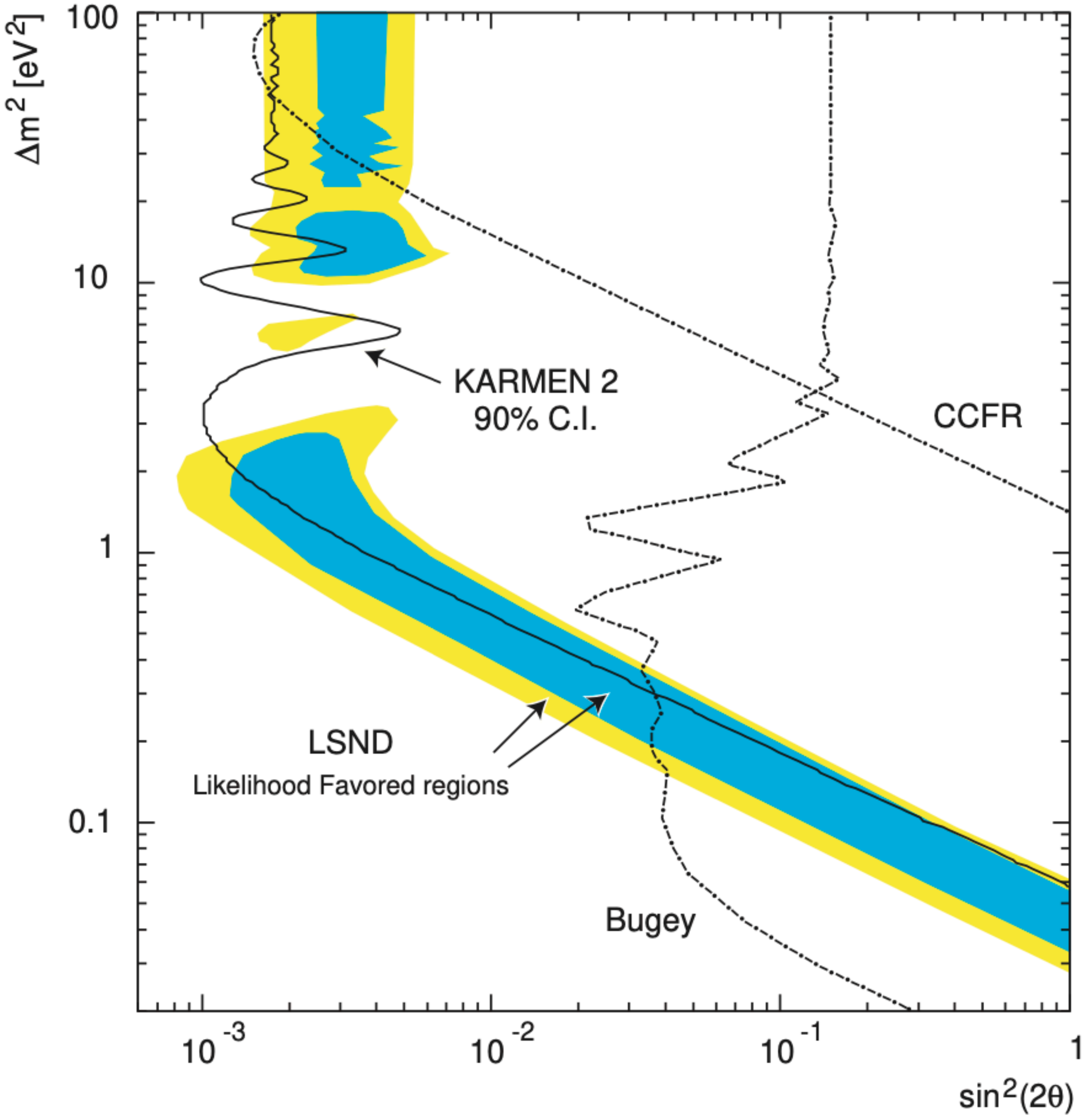

External 3+1 Fit of uB data

arXiv:2111.10359

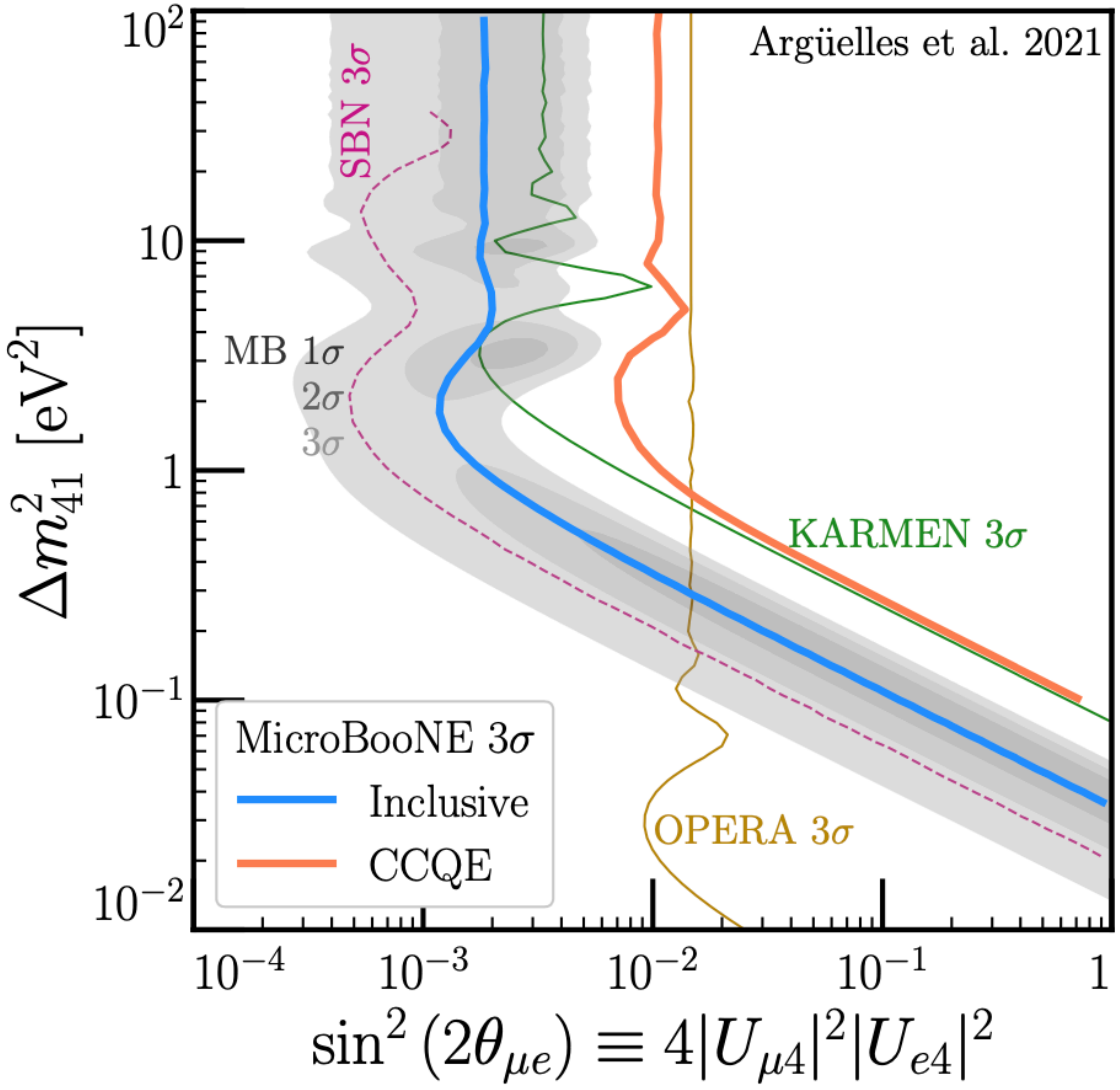

BEST Result

arXiv:2109.11482

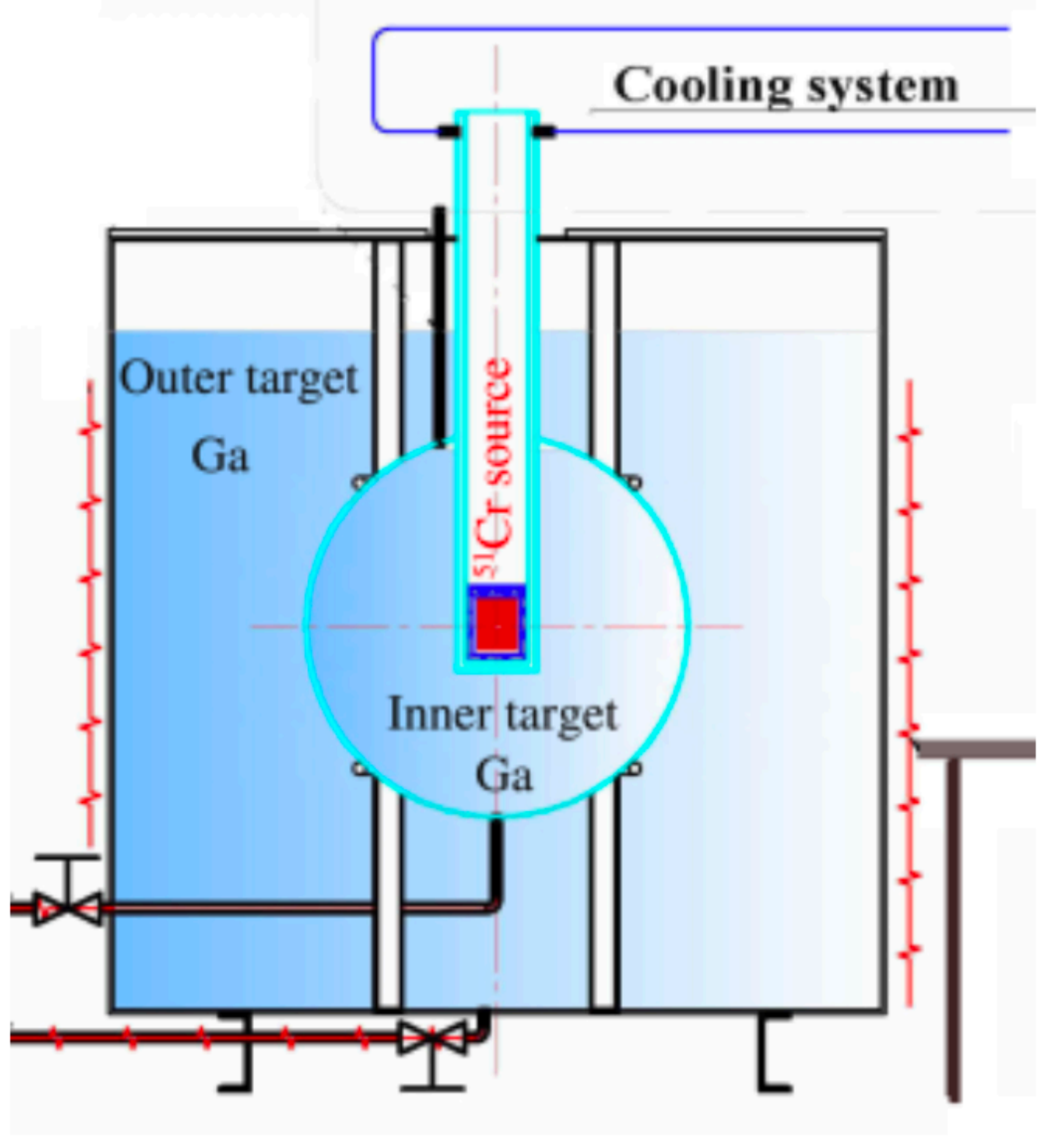

Figure 66: BEST detector configuration [137].

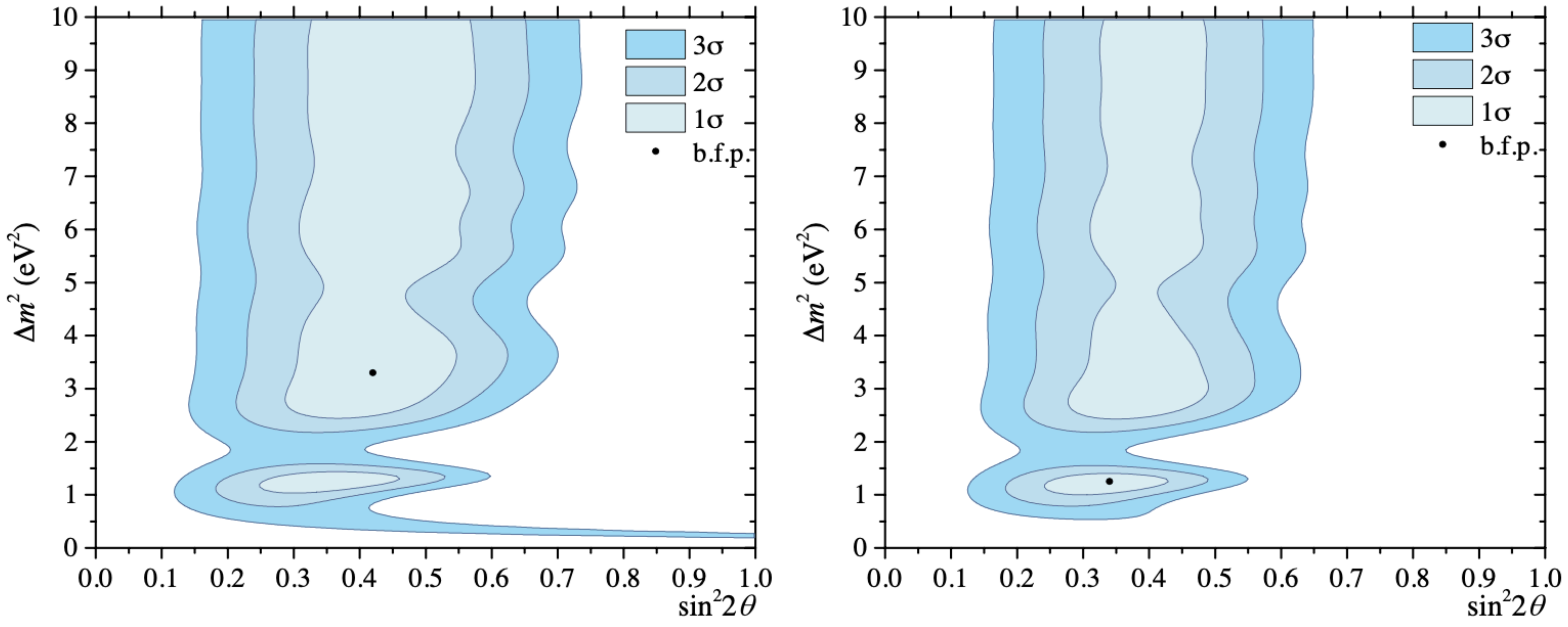

Figure 67: Allowed regions obtained in the $\sin^2 2\theta$–Δm^2_{41} parameter space from the analysis of the BEST results only (left) and from the BEST results combined with results from GALLEX and SAGE (right) [294]. Note that here $\sin^2 2\theta = 4\,|U_{e4}|^2 \left(1 - |U_{e4}|^2\right)$.